SPECTROSCOPY ON THE ASSEMBLY OF COWPEA CHLOROTIC MOTTLE VIRUS

Promotor: dr. C. Veeger, hoogleraar in de biochemie
Co-promotor: dr. ir. J.P.H. van der Want, hoogleraar in de virologie
Co-referent: dr. A.J.W.G. Visser, wetenschappelijk hoofdmedewerker

J. Krüse

SPECTROSCOPY ON THE ASSEMBLY OF COWPEA CHLOROTIC MOTTLE VIRUS

(with a summary in Dutch)

Proefschrift

ter verkrijging van de graad
van doctor in de landbouwwetenschappen,
op gezag van de rector magnificus,
dr. H.C. van der Plas,
hoogleraar in de organische scheikunde,
in het openbaar te verdedigen
op vrijdag 5 oktober 1979
des namiddags te vier uur in de aula
van de Landbouwhogeschool te Wageningen.

ISN 107 069

STELLINGEN

I. De door Angelides en Hammes gegeven fysische verklaring van de spectra van het met pyreenmaleïde gemodificeerde pyruvaat dehydrogenase complex is minder waarschijnlijk dan een chemisch alternatief zoals aangegeven door Wu et al.

Angelides, K.J. en Hammes, G.G. (1979) Biochemistry 18, 1223-1229.
Wu, C.W., Yarbrough, C.R. en Wu, F.Y.-H (1976) Biochemistry 15, 2863-2868.

II. De suggestie van Beddard et al. dat antennechlorofyll bestaat uit monomeren, is in strijd met het absorptiemaximum dat voor in vivo antennechlorofyll gevonden wordt. Tevens blijkt uit hun metingen dat chlorofyll in een zuiver lipide geen goed modelsysteem is voor het thylakoïdmembraan in de plant.

Beddard, G.S., Carlin, S.E. en Porter, G. (1976) Chem.Phys.Lett.43, 27-32.

III. Gelet op de lage gevoeligheid van NMR zeugmatografie is het onwaarschijnlijk dat deze techniek een concurrerend alternatief voor X-ray tomografie zal worden voor het verkrijgen van twee en drie dimensionale lichaamsdoorsneden van de mens.

Brunner, P. en Ernst, R.R. (1979) J.Magn.Res. 33, 83-106.

IV. De door Yagi et al. voor de D.vulgaris (Miyazaki) hydrogenase gemeten millimolaire absorptiecoëfficient van 47 bij 400 nm is niet in overeenstemming met de vermelde aanwezigheid van ongeveerd 8 atomen van zowel ijzer als zuurlabiel zwavel per molecuul, maar wijst op de aanwezigheid van drie 4Fe/4S clusters per enzymmolecuul.

Yagi, T., Kimura, K., Daidoji, H., Sakai, F., Tamura, S. en Inokuchi, H. (1976) J.Biochem. 79, 661-671.

V. De uitkomsten van de door Siler et al. uitgevoerde recombinatieproeven met cowpea-mozaïek virus mutant B sluiten niet uit dat de hogere specifieke infectiositeit van deze mutant overerft via de middencomponent en niet, zoals deze onderzoekers suggereren, via de bodemcomponent.

Siler, D.J., Babcock, J. en Bruening, G. (1976) Virology 71, 560-567.

VI. Het is juister gebruik te maken van de diffusiecoëfficient voor het bepalen van de gehydrateerde diameter van bolvormige deeltjes dan de door Juckes voorgestelde methode toe te passen, waarbij sedimentatiecoëfficient en zweefdichtheid gebruikt worden.

Juckes, I.R.M. (1979) J.Gen.Virol. 42, 89-94.

VII. Bij de verklaring van de gemeten polarisatiegraad van de tryptofaanemissie in alcohol dehydrogenase uit paardelever doet Iweibo enkele niet reële fysische aannamen.

Iweibo, I. (1976) Biochim.Biophys.Acta 446, 192-205.

VIII. Het inmengen van hoger aangeslagen triplettoestanden in de laagste triplettoestand leidt niet noodzakelijkerwijs tot een afname van de waarde van de nulveldsplitsingsparameter $|D|$. Bovendien moet de term diffuus bij het bespreken van golffuncties vermeden worden.

Ugurbil, K., Maki, A.H. en Bersohn, R. (1977) Biochemistry 16, 901-907.
Kooter, J.A. (1978). The lowest triplet state of some metal porphins: A study by ESR and Zeeman spectroscopy. Proefschrift, Rijksuniversiteit te Leiden.

IX. De mate waarin resultaten van spectroscopische waarnemingen aan een eiwit kunnen worden geïntepreteerd hangt ten nauwste samen met de kennis omtrent de drie dimensionale structuur van het eiwit.

X. Het onderbrengen van kunstwerken zou kunnen worden vereenvoudigd door ook voor werkloze bouwvakkers een contraprestatieregeling te ontwerpen.

Proefschrift van J. Krüse 5 oktober 1979.

Aan mijn vader en moeder

Aan Margreet

VOORWOORD

Bij het voltooien van dit proefschrift gaat mijn dank uit naar alle mensen, die hun medewerking in welke vorm dan ook daaraan geleverd hebben.

Voor diverse bijdragen aan het experimentele werk en discussies daarover dank ik Daniëlle Breedveld, Claudi Dortland-Dazert, Hans Grande, Joop Groenewegen, Marcus Hemminga, Henk Hilhorst, Arie van Hoek, Adrie de Jager, Peter Kampmeyer, Dick Lohuis, Maarten Noort, Lia Pieper, Roelof Platenkamp en Cees van Schagen.

Ton Visser ben ik zeer erkentelijk voor de intensieve begeleiding van dit onderzoek. Dick Verduin dank ik voor het leveren van grote hoeveelheden gezuiverd virusmateriaal, geïsoleerd eiwit, RNA en opbouwende kritiek.

Prof. dr. C. Veeger verleende mij tijdens mijn onderzoek aan de Landbouwhogeschool gastvrijheid op de afdeling Biochemie. Zijn kritische opmerkingen bij het schrijven van dit proefschrift en de besprekingen met hem en de hoogleraren dr. A. van Kammen, dr. J. Lyklema en dr. ir. J.P.H. van der Want in het kader van de werkgroep "Assemblage van bolvormige plantevirussen" werden als zeer nuttig ervaren.

Een deel van het onderzoek werd uitgevoerd bij de vakgroep Moleculaire Fysica van de Landbouwhogeschool en op het Huygens Laboratorium van de Rijksuniversiteit te Leiden. De daar genoten gastvrijheid werd zeer op prijs gesteld.

Bij het drukklaar maken van dit proefschrift werd veel steun ondervonden van de tekenaars K. Boekhorst en B.J. Sachteleben. Dr. J.W. Davies corrigeerde van enkele hoofdstukken de Engelse tekst. Het vele typewerk werd nauwgezet uitgevoerd door Jenny Toppenberg-Fang van de vakgroep Biochemie, Wil Landeweerd van de vakgroep Moleculaire Biologie en de dames Neijenhuis en Laoh van de afdeling tekstverwerking.

Margreet, jou wil ik bedanken voor je optreden in alle hiervoor genoemde categorieën, maar vooral voor je morele steun in moeilijke tijden.

CONTENTS

LIST OF ABBREVIATIONS

ANS	8-anilino-1-naphtalene sulphonic acid
BBMV	broad bean mottle virus
BMV	brome mosaic virus
CCMV	cowpea chlorotic mottle virus
CD	circular dichroism
CMV	cucumber mosaic virus
D	zero-field splitting parameter
DNA	deoxyribonucleic acid
DTNB	5,5'-dithiobis(2-nitrobenzoic acid)
E	zero-field splitting parameter
$E^{1\%}_{260\ nm}$	extinction of a 1% solution at 260 nm and an optical pathlength of 1 cm
EDTA	ethylene diaminetetra-acetic acid
EPR	electron paramagnetic resonance
Eqn	equation
ESR	electron spin resonantie
fwhm	full width at half maximum
HLAD	horse liver alcohol dehydrogenase
NMR	nuclear magnetic resonance
ODMR	optical detection of magnetic resonance
ORD	optical rotatory dispersion
P	degree of polarization
PLP	pyridoxal-5'-phosphate
Poly-A	polyadenylic acid
PPO	2,5-diphenyloxazole
PT	pseudo top component
PVX	potato virus X
Q	quantum yield
RNA	ribonucleic acid
RNase	ribonuclease
S	Svedberg unit, order parameter
SL	spin labelled
ST-EPR	saturation transfer electron paramagnetic resonance

T	triangulation number
TMV	tobacco mosaic virus
TNS	2-p-toluidinyl naphtalene-6-sulphonate
Tris	tris(hydroxymethyl)-aminomethane
TYMV	turnip yellow mosaic virus
$\bar{v}$	partial specific volume
λ_{max}	radiation wavelength with maximum intensity
τ_c	correlation time
τ_m	fluorescence lifetime determined with phase fluorometry from depth of modulation
τ_p	fluorescence lifetime determined with phase fluorometry from phase shift

1. INTRODUCTION

Many small viruses are composed of nucleic acid, encapsulated in a coat, which is built from a large number of relatively small protein subunits. Since the information on the genome of the virus is limited, it is more efficient to build up the viral protein coat from a large number of small identical protein subunits rather than from one large protein molecule.

The protein coat can protect the nucleic acid from the damaging external influences in the organism, like nucleases. On the other hand the nucleic acid has to be released from the nucleoprotein particles to express the genetic information, contained in the nucleic acid. This is believed to take place during or shortly after the penetration of the virus into the cell by a dissociation of the nucleoprotein particles into protein oligomers and free nucleic acid. After this process the genetic information is transcribed, the metabolism of the cell is changed and viral coat protein is made for the encapsulation of newly synthetized RNA. The protected nucleic acid can leave the cell to be transported to other parts of the organism. The reconstitution of the virus particles from its components is often referred to as the assembly of the virus.

The structure of viruses and mechanism of dissociation and assembly has been reviewed extensively [1,2]. Recently progress has been made in understanding the structure and assembly of tobacco mosaic virus (TMV), which is a rod shaped virus [3,4]. In this thesis special attention is paid to cowpea chlorotic mottle virus, which belongs to the bromovirus group [5,6]. This is a group of spherical, RNA containing, plant viruses, in which the 180 identical protein subunits are arranged in an icosahedral symmetry. This type of packing allows only a discrete number of subunits per nucleoprotein particle. It can be deduced that in the case of more than 60 subunits per particle such a packing results in more than one type of environment of the subunits leading to a so-called quasi-symmetrical arrangement. This is in contrast with the arrangement in the rod of a virus like TMV, where all subunits are in equivalent positions, except for those on the outer ends of the rod [7].

The assembly and dissociation behaviour of the group of bromoviruses has been studied in several ways. Most of the attention was directed to the confor-

mational changes in the macroscopic structure of the nucleoprotein particles. A recent review of literature and some work on this subject is given in the thesis of Verduin [8].

In the study presented here, we tried to use spectroscopic techniques to characterize the protein subunits in the nucleoprotein particles of CCMV. In addition the spectral properties were monitored as a function of conformational changes in the complex. The aim was to characterize in this way the different conformational states and to determine the factors in the protein structure involved in the process of dissociation and assembly. It was supposed, that the use of spectral techniques could yield information on the protein-protein and protein-RNA interactions, that determine the conformation of the stable virus particles. Changes in spectral properties could elucidate the process of dissociation and assembly in an indirect, but fast and sensitive way.

In chapter two, a review is given of the properties of and of investigations with the bromoviruses. Also some results are given of the application of spectroscopic techniques used to investigate the structural properties and conformational transitions in viruses. Special attention in this context is given to tobacco mosaic virus.

The next two chapters deal with the intrinsic spectroscopic properties of CCMV. In chapter three, a study of the fluorescence properties of the coat protein is presented. Chapter four is a study of the photo-excited metastable triplet states of the tryptophanyl residues in the protein at 77 K and at 1.2 K. The triplet states are characterized to obtain additional information about the nature of the tryptophanyl residues in the protein subunits and their involvement in the protein-RNA interaction. The techniques used in these studies are phosphorescence spectroscopy and optical detection of magnetic resonance.

Chapters five and six give the results of experiments in which probes are bound to the protein and information is obtained by determination of the spectral characteristics of the modified protein. In chapter five, the spectral properties are given of CCMV protein to which a fluorescent probe had been attached. The mobility and the orientation of this probe, pyridoxal-5'-phosphate, appeared to be influenced by the quarternary structure of the nucleoprotein particles. The changes were monitored by fluorescence lifetime and fluorescence polarization measurements. In this way, information was obtained about the role of mono- and divalent cations. Chapter six is a preliminary study on the mobility of a spin label, which was covalently attached to the virus by a reaction with the SH-groups in the coat protein. The mobility was followed by electron paramagnetic resonance (EPR) which is sensitive for relatively fast motions, corresponding

to segmential flexibility in the protein or mobility of the subunits in the nucleoprotein particles. Also the recently developed technique of saturation transfer EPR was applied. This is more appropriate for the detection of the overall tumbling of the virus particles.

In chapter seven, studies on the binding of mono- and divalent cations to nucleoprotein, protein and RNA are described. In the binding experiments Mn^{2+} was used as a paramagnetic probe and EPR was utilized to follow the degree of binding. The binding of other cations was studied by performing competition experiments with Mn^{2+}.

The results of these studies are summarized and discussed in chapter eight.

REFERENCES

1. Kaper, J.M. (1975) The Chemical Basis of Virus Structure, Dissociation and Reassembly. Amsterdam, Oxford, New York: North-Holland/American Elsevier.
2. Casjens, S. and King, J. (1975) Ann.Rev.Biochem. 44, 555-611.
3. Butler, P.J.G. and Durham, A.C.H. (1977) Adv.Prot.Chem. 31, 187-251.
4. Bloomer, A.C., Champness, J.N., Bricogne, G., Staden, R. and Klug, A. (1978) Nature (Lond.) 276, 362-368.
5. Bancroft, J.B. (1970) Adv.Vir.Res. 16, 99-134.
6. Lane, L.C. (1974) Adv.Vir.Res. 19, 151-220.
7. Caspar, D.L.D. and Klug, A. (1962) Cold Spring Harbor Symp. Quant. Biol. 27, 1-24.
8. Verduin, B.J.M. (1978) Characterization of Cowpea Chlorotic Mottle Virus and its Assembly, PhD Thesis, Agricultural University, Wageningen, The Netherlands.

2. LITERATURE REVIEW ON COWPEA CHLOROTIC MOTTLE VIRUS AND THE SPECTROSCOPY OF VIRUSES

2.1. COWPEA CHLOROTIC MOTTLE VIRUS

Cowpea chlorotic mottle virus is a small spherical plant virus, belonging to the bromovirus group. The properties of these viruses were extensively reviewed by Bancroft [1] in 1970 and by Lane [2] in 1974. Since then, detailed studies on the association of virus coat protein and on the assembly of protein and RNA have been performed by Adolph and Butler [3,4] and Jacrot [5] in Cambridge. Verduin characterized cowpea chlorotic mottle virus and its assembly [6,7,8]. Several studies were performed on the related brome mosaic virus (BMV) especially by Hirth *et al.* in Strasbourg [9-17].

The spherical nucleoprotein particles of CCMV are composed of RNA, which is encapsulated in a coat of 180 identical protein subunits. The subunits are arranged in an icosahedral symmetry, resulting in a triangulation number (T) of three [18]. The diameter of the particles is approximately 28 nm.

CCMV consists of three types of nucleoprotein particles, which is manifested in differences in buoyant density. The heavy (H) and light (L) particles each contain one RNA molecule with a M_r of 1.20 and 1.07 x 10^6 respectively, while in the medium (M) particle two smaller strands with M_r's of 0.81 and 0.25 x 10^6 are encapsulated (Fig. 1) [19,20]. The protein subunits of the particles are identical, with a molecular weight of 19,400 [21].

Kaper suggested a classification of the viruses based on the relative importance of the two types of interaction, which are responsible for the stability of the nucleoprotein particles [22]. One class of viruses with cucumber mosaic virus (CMV) as a characteristic representative, is mainly stabilized by protein-RNA interactions, while in another class the protein-protein interactions determine the stability of the viruses. An example of the last group is turnip yellow mosaic virus (TYMV). The group of bromoviruses may be placed between these two extremes. Here the two types of interactions are equally important.

From the investigations on the stability and conformation of CCMV nucleoprotein and its protein [1,3] one can arrive at the following scheme. The nucleoprotein particles are stable at pH 5.0 and low ionic strength ($I \approx 0.1$). A raise in pH to 7.5 enlarges the diameter of the particles [23,24]. This swelling is

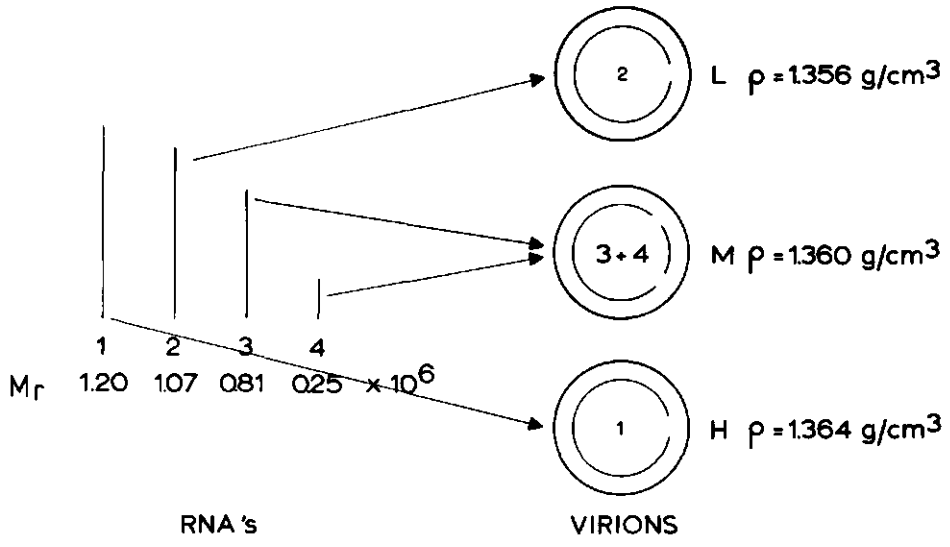

Fig. 1. The distribution of RNA molecules over the three different CCMV nucleoprotein particles. The buoyant densities of the light (L), medium (M) and heavy (H) particles were determined by Bancroft and Flack [19].

due to ionization of some abnormally titrating carboxyl groups in the protein, which causes a repulsion between the subunits [5]. In BMV small concentrations of divalent cations (5 mM) or higher concentrations of monovalent cations (0.1 M) can bind to the negatively charged groups on the protein and the RNA and in this way the swelling due to repulsion is reduced [13]. A similar effect is probably occuring in CCMV [5]. At higher ionic strength ($I > 0.2$) the salt bridges between the RNA and the protein in the spherical particles are broken, and the virus will dissociate into protein dimers [4] and RNA [1,2]. The formation of dimers instead of monomers is probably due to the lower stability of the latter molecules in solution. Here several types of interaction may play a role, such as hydrophobic and electrostatic interaction.

Protein can be prepared by precipitating the RNA from a solution of dissociated particles [6]. Dialysis of the protein solution against buffer pH 5.0 and 1.0 M NaCl results in the association into spherical protein particles, called pseudo-top component (PT). These particles have a structure which is very simi-

lar to the nucleoprotein particles [25]. The preparation of PT is possible for CCMV and BMV but not for BBMV.

Extensive schemes of the different aggregation states found for CCMV at various pH and ionic strength values were given by Bancroft [1] and Adolph and Butler [3]. Verduin [6] observed, that the pH-dependent dissociation and association of the isolated protein shows a hysteresis of about 0.5 pH unit. This means that the association of protein dimers into PT starts at lower pH values than the dissociation of empty protein particles into dimers. A similar hysteresis was observed in the proton titration studies and the swelling behaviour of CCMV [5] and BMV [13,26].

The role of lysine in the stabilization of CCMV nucleoprotein particles was shown in a study of Bancroft *et al.*[27], who compared the properties of CCMV with those of a mutant with a lysyl to arginyl replacement. In contrast to wild type CCMV, the mutant does not disassemble in 1 M NaCl, pH 7.5. Also differences occur in the swelling behaviour between CCMV and the mutant. Tremaine *et al.*[28] showed the importance of the N-terminal region of the protein subunits in the maintenance of the virus structure at pH 7.4. The digestion of 25 amino acid residues from the N-terminus by the action of trypsin broke the virus into smaller components. Similar observations were made for BMV [11].

The aromatic amino acid residues may also play an important role in the stabilization of the viruses by an interaction of these residues with RNA. For instance, spectroscopic observations led to the conclusion that base stacking interactions between tryptophan and nucleotides were involved in the binding of DNA to T4 phage gene 32 protein [29]. In the protein subunit of CCMV, three tryptophanyl, four phenylalanyl and five tyrosyl residues were found [21].

2.2. SPECTROSCOPY OF VIRUSES

2.2.1. Tobacco Mosaic Virus

Many spectroscopic studies have been performed on tobacco mosaic virus. Most attention has been paid to the aromatic amino acid residues tryptophan and, to a smaller extent, tyrosine. The interpretation of the spectroscopic properties was facilitated by the availability of mutants in which one or more of the three tryptophanyl residues per protein subunit were substituted by other amino acids.

The first example of application of fluorescence in the investigation of viruses is formed by the experiments of Guttenplan and Calvin [30]. They determined the fluorescence properties of TMV and its protein as a function of pH. In addition to this the fluorescence upon binding of the probe 2-p-toluidinyl-6-sulphonate (TNS) to TMV was determined at different pH values. The changes in the fluorescence properties of TMV and TNS were correlated with structural transitions in virus and protein upon variation of the pH. The virus seems to be more stable than the protein without RNA. Considerable differences between the quantum yield of the disaggregated and aggregated protein could be observed, which were ascribed to conformational changes or quenching caused by intersubunit contacts, when aggregation took place. From the studies of Guttenplan and Calvin it was further concluded that the fluorescence of the protein is mainly determined by buried tryptophanyl residues.

The fluorescence properties of TMV were also investigated by Taniguchi and Taniguchi [31], but by a slightly different approach. Conformational changes in the virus and the protein assemblies were induced by variation of the temperature. They used the ordinary strain and two other strains. One of the mutants lacks two tryptophanyl residues. This difference is manifested in the absence of the temperature dependent transition, which occurred in the other strains. It was concluded that the two tryptophanyl residues at position 17 and 52 are involved in a structural transition, while the residue at position 152 remains unaffected. Further it was shown that differences exist in the fluorescence polarization of the three tryptophanyl residues.

Using different strains of TMV the quantum yield of each of the three tryptophanyl residues was established by Magne *et al.* [32]. They estimated a very efficient energy transfer from tyrosyl to tryptophanyl residues. This is in good agreement with the location of these aromatic amino acid residues in the protein subunit, which was obtained from X-ray diffraction analysis of TMV protein at a resolution of 0.28 nm [33].

The interaction of tobacco mosaic virus protein with synthetic polynucleotides was studied using polynucleotides labelled with fluorescent groups [34]. From energy transfer measurements between the modified nucleotides and tryptophan a distance of 1.7 to 2.0 nm between Trp 52 and the RNA binding region was estimated. A similar value was obtained in the X-ray studies on TMV [33,35].

Another type of spectroscopic study performed on TMV involves the application of circular dichroism (CD), optical rotatory disperion (ORD) and light absorption. The spectra obtained by these methods, yield in the wavelength area

between 250 and 300 nm information about the nature of the aromatic amino acid residues.

Vogel and Jaenicke [36] compared the CD and absorption spectra of TMV protein of wild type strain with those of a mutant in which Tyr 139 was replaced by a cysteine residue. They found interaction between Trp 17 and Trp 52, which was sensitive towards changes in the quarternary structure of TMV protein. Tyr 70 and Tyr 72 were thought to be located in a hydrophobic environment, where they form hydrogen bonds. The suggestion of Vogel and Jaenicke, based on CD data, that Tyr 70, 72 and 139 are located close to each other, was afterwards confirmed by the X-ray structure of TMV protein.

In an ORD and CD study of five strains of TMV Dobrov *et al.* [37] investigated the interaction between RNA and TMV protein. It was concluded that differences in the protein-RNA interaction exist among the various strains. However the possible involvement of tryptophanyl residues in this interaction was rejected.

In another study by Shie, Dobrov and Tikchonenko [38], the Raman spectra of TMV and cucumber virus 4 (a strain of TMV) were compared. According to these results significant differences in the protein folding of the two strains are present. The special nature of the tyrosyl residues in TMV revealed by CD [36], was confirmed in this study. Two tyrosines are buried and hydrogen bonded, while the other two tyrosines are exposed to the solvent. The free RNA shows a much higher degree of base stacking than the RNA in the virus particles. Also the presence of two different conformations of the phosphodiester bonds and the ribose residues in the intraviral RNA can be concluded from these laser Raman studies.

For the investigation of the dynamic properties the application of magnetic resonance seems to be very useful. Two types of experiments can be distinguished here: nuclear magnetic resonance (NMR) of native TMV and TMV enriched with ^{13}C-isotopes and electron paramagnetic resonance (EPR) on spin labelled TMV protein and nucleic acid. De Wit *et al.* [39,40,41] used NMR to monitor the internal flexibility in the protein oligomers and nucleoproten particles. The motion within the subunits in the oligomers is used in a thermodynamical model which describes the entropy-driven association process. Similar NMR experiments were performed by Jardetzky *et al.* [42]. They showed that the lack of a well defined electron density of residues 88-114 in the X-ray map of the protein [33] was caused by a thermal motional disorder and not by an irregular packing of the segment in the crystal. The flexible region, which is thought to act as a trap for the RNA in the assembly process, disappears after assembly has taken place.

By the attachment of a nitroxide spin label to the single SH-group of a TMV protein subunit, it was possible to study the association process of TMV protein

by EPR and saturation-transfer EPR (ST-EPR) [43,44]. The association of spin labelled (SL) TMV protein was disturbed by the presence of the spin label. From ST-EPR studies it was concluded that the association products formed are much larger than those obtained for unlabelled TMV protein.

By EPR and ST-EPR Powell *et al.* [45] were able to follow the assembly of spin labelled poly-A and TMV protein. In this way they showed that SL-poly-A is encapsulated in a similar way to TMV-RNA.

2.2.2. Other viruses

In TMV, the interpretation of the spectral properties is facilitated by the knowledge of the X-ray structure and by the availability of several mutants, especially those differing in tryptophan content. For other viruses similar spectral studies were performed. In this way it was found for BMV that some of the tryptophanyl residues are buried in an apolar environment and others have a strongly quenched fluorescence. It appeared that the fluorescence is slightly influenced by protein-protein interaction, while no effect of RNA could be observed [12].

Potato virus X was studied with spèctral techniques like CD and fluorescence. These methods yielded some information on the nature of the tryptophanyl residues. It was concluded that the tryptophan environment may be influenced by the presence of RNA [46]. By the use of the fluorescent "polarity" probe 8-anilino-naphtalene sulphonate (ANS) the changes in hydrophobicity could be monitored during the reconstitution of the dissociated virus [47]. By employing the same techniques, the pH dependence of the conformation of PVX coat-protein was also investigated. Only the isolated coat protein subunits exhibit a strong dependence of fluorescence and CD on the pH. This was correlated with a conformational change that may determine the reconstitution of PVX from its components [48].

Laser Raman studies have also been performed on spherical viruses. Extensive studies were performed on MS2 phage, its capsid and its RNA [49]. In this way, information was obtained about the folding of the protein chain, the conformation of the RNA and the temperature stability of the virus particle. Similar experiments were done for TYMV [50].

In the following chapters studies are described, in which some of the techniques mentioned here were applied to CCMV.

2.3. REFERENCES

1. Bancroft, J.B. (1970) Adv.Vir.Res. 16, 99-134.
2. Lane, L.C. (1974) Adv.Vir.Res. 19, 151-220.
3. Adolph, K.W. and Butler, P.J.G. (1974) J.Mol.Biol. 88, 327-341.
4. Adolph, K.W. and Butler, P.J.G. (1977) J.Mol.Biol. 109, 345-357.
5. Jacrot, B. (1975) J.Mol.Biol. 95, 433-446.
6. Verduin, B.J.M. (1974) FEBS Lett. 45, 50-54.
7. Verduin, B.J.M. (1978) J.Gen.Virol. 39, 131-147.
8. Verduin, B.J.M. (1978). Characterization of Cowpea Chlorotic Mottle Virus and its Assembly. PhD Thesis, Agricultural University, Wageningen, The Netherlands.
9. Pfeiffer, P. and Hirth, L. (1974) Virology 58, 362-368.
10. Pfeiffer, P. and Hirth, L. (1974) Virology 61, 160-167.
11. Pfeiffer, P. and Hirth, L. (1975) FEBS Lett. 56, 144-148.
12. Herzog, M., Pfeiffer, P. and Hirth, L. (1976) Virology 69, 394-407.
13. Pfeiffer, P. and Durham, A.C.H. (1977) Virology 81, 419-432.
14. Herzog, M., Gerard, D., Hirth, L. and Laustriat, G. (1977) Biochim.Biophys. Acta 493, 167-177.
15. Herzog, M. and Hirth, L. (1978) Virology 86, 48-56.
16. Chauvin, C., Pfeiffer, P., Witz, J. and Jacrot, B. (1978) Virology 88, 138-148.
17. Cuillet, M., Herzog, M. and Hirth, L. (1979) Virology, 95, 146-153.
18. Caspar, D.L.D. and Klug, A. (1962) Cold Sprin Harbor Symp. Quant. Biol. 27, 1-24.
19. Bancroft, J.B. and Flack, I.H. (1972) J.Gen.Virol. 15, 247-251.
20. Reijnders, L., Aalbers, A.M.J., Van Kammen, A. and Thuring, R.J.W. (1974) Virology 60, 515-521.
21. Bancroft, J.B., McLean, G.D., Rees, M.W. and Short, M.N. (1971) Virology 45, 707-715.
22. Kaper, J.M. (1975) The Chemical Basis of Virus Structure, Dissociation and Reassembly. Amsterdam, Oxford, New York: North-Holland/American Elsevier pp. 382-386.
23. Bancroft, J.B., Hills, G.T. and Markham, R. (1967) Virology, 34 224-239.
24. Adolph, K.W. (1975) J.Gen.Virol. 28, 147-154.
25. Finch, J.T. and Bancroft, J.B. (1968) Nature (Lond.) 220, 815-816.
26. Zulauf, M. (1977) J.Mol.Biol. 114, 259-266.

27. Bancroft, J.B., Rees, M.W., Johnson, M.W. and Dawson, J.R.O. (1973) J.Gen. Virol. 21, 507-513.
28. Tremaine, J.H., Agrawal, H.O. and Chidlow, J. (1972) 48, 245-254.
29. Hélène, C., Toulme, F., Charlier, M. and Yaniv, M. (1976) Biochem.Biophys. Res.Commun. 71, 91-98.
30. Guttenplan, J.B. and Calvin, M. (1973) Biochim.Biophys.Acta 322, 294-300 and 301-320.
31. Taniguchi, M. and Taniguchi, T. (1975) Biochim.Biophys.Acta 386, 1-17.
32. Magne, A., Gerard, D., Hirth, L. and Laustriat, G. (1977) Biochim.Biophys. Acta 495, 189-194.
33. Bloomer, A.C., Champness, J.N., Bricogne, G., Staden, R. and Klug, A. (1978) Nature (Lond.) 276, 362-368.
34. Ledneva, R.K., Razjivin, A.P., Kost, A.A. and Bogdanov, A.A. (1978) Nucleic Acid Res. 5, 4225-4243.
35. Stubbs, G., Warren, S., and Holmes, K. (1977) Nature (Lond.) 267, 216-221.
36. Vogel, D. and Jaenicke, R. (1976) Eur.J.Biochem. 61, 423-431.
37. Dobrov, E.N., Kust, S.V., Yakovleva, O.A. and Tikchonenko, T.I. (1977) Biochim.Biophys.Acta 475, 623-637.
38. Shie, M., Dobrov, E.N. and Tikchonenko, T.I. (1978) Biochem.Biophys.Res. Commun. 81, 907-914.
39. De Wit, J.L. (1978). Nuclear Magnetic Resonance of Tobacco Mosaic Virus PhD Thesis, Agricultural University, Wageningen, The Netherlands.
40. De Wit, J.L., Hemminga, M.A. and Schaafsma, T.J. (1978) J.Magn.Res. 31, 97-107.
41. De Wit, J.L. and Schaafsma, T.J. (1978) FEBS Lett. 92, 273-277.
42. Jardetzky, O., Akasaka, K., Vogel, D., Morris, S. and Holmes, K.C. (1978) Nature (Lond.) 273, 564-566.
43. Hemminga, M.A., De Jager, P.A. and De Wit, J.L. (1977) Biochem.Biophys. Res.Commun. 79, 635-639.
44. Hemminga, M.A., Van den Boomgaard, T. and De Wit, J.L. (1978) FEBS Lett. 85, 171-174.
45. Powell, A.T., Gordon, M.P., Caspary, W.J., Greene, J.J. and Ts'O, P.O. (1978) Nucleic Acid Res. 5, 3977-3992.
46. Homer, R.B. and Goodman, R.M. (1975) Biochim.Biophys.Acta 378, 296-304.
47. Goodman, R.M. (1977) Virology 76, 72-78.
48. Homer, R.B. and Dalton, D.I. (1976) Biochim.Biophys.Acta 446, 542-546.
49. Thomas, G.J., Jr., Prescott, B., McDonald-Ordzie, P.E. and Hartman, K.A. (1976) J.Mol.Biol. 102, 103-124.

50. Hartman, K.A., McDonald-Ordzie, P.E., Kaper, J.M., Prescott, B. and Thomas, G.J., Jr. (1978) Biochemistry 17, 2118-2123.

Eur. J. Biochem. 95, 21–29 (1979)

3. INTRINSIC FLUORESCENCE OF COWPEA-CHLOROTIC-MOTTLE-VIRUS PROTEIN

Jacob KRÜSE, Benedictus J. M. VERDUIN, and Antonie J. W. G. VISSER

Departments of Biochemistry and Virology, Agricultural University, Wageningen

(Received September 4 / December 1, 1978)

Changes in the environment of the aromatic amino acid residues in the protein subunits of cowpea chlorotic mottle virus were studied with fluorescence techniques. The fluorescence properties of the protein in nucleoprotein particles, empty protein shells and dimers of the coat protein subunit were determined.

According to fluorescence spectra (excitation at 295 nm, emission maxima at 342 – 346 nm depending on pH and ionic strength) the tryptophan residues are located in a polar environment. With excitation at 235 nm a strong shoulder at about 300 nm in the total emission spectrum can be observed. This emission must be attributed to the tyrosine residues in the protein and can also be observed as a fast component in the fluorescence decay curve. The lifetimes were compared with those of the other bromoviruses which are different in amino acid composition. From excitation spectra of cowpea chlorotic mottle virus it can be concluded that energy is transferred from tyrosine to tryptophan residues.

Increase in the quantum yield of the tryptophan emission of the nucleoprotein particles upon raising the ionic strength and pH are attributed to a diminishing interaction between the protein and the RNA. The fluorescence properties of the protein hardly change when the empty protein shells are dissociated into protein dimers.

Quenching studies with potassium iodide and acrylamide indicate that the tryptophan residues in the protein are attainable more easily at low ionic strength than at high ionic strength.

Cowpea chlorotic mottle virus (CCMV) is a multicomponent spherical plant virus, which belongs, together with brome mosaic virus (BMV) and broad bean mottle virus (BBMV), to the group of bromoviruses [1,2]. Their purified preparations consist of almost equal proportions of three different nucleoprotein particles. Two of them contain one RNA strand of M_r about 1.1×10^6 and the third has two smaller RNA components with molecular weights of about 0.8×10^6 and 0.3×10^6. The protein coat of these particles is similar and consists of 180 identical polypeptides with a molecular weight of 19400, arranged on the surface of an icosahedron.

The nucleoprotein particles, which are stable at pH 5.0, increase in hydrodynamic volume when the pH is raised to 7.5. The resulting decrease in sedimentation coefficient from 88 S to 78 S has been explained by radial expansion of protein and nucleic acid due to electrostatic repulsion [2]. Increasing the ionic strength to 1.0 M at pH 7.5 dissociates the swollen virus into coat protein dimers [3] and RNA [1,2]. When the RNA is removed, the proteins dimers can reversibly associate into empty spherical protein shells called pseudo-top component. The arrangement of the polypeptides in these shells is similar to that in the nucleoprotein coat [4].

In each CCMV protein subunit three tryptophan, five tyrosines and four phenylalanines are present. For BMV and BBMV proteins the number of aromatic amino acid residues are, respectively, two and zero tryptophans, five and four tyrosines and five and seven phenylalanines [5]. By observing the fluorescence properties of the aromatic amino residues, information can be obtained about the direct environment and the localization of these residues in the protein particles [6,7].

This paper reports on fluorescence of CCMV protein. The fluorescence properties studied were peak location and band width of emission spectra, excitation spectra, lifetimes and degree of polarization. In particular, the changes in these parameters induced upon passing through the different states of aggregation of the virus have been measured and correlated with structural features of the virus particles.

Abbreviations. CCMV, cowpea chlorotic mottle virus; BBMV, broad bean mottle virus; BMV, brome mosaic virus; fwhm, full width at half maximum.

MATERIALS AND METHODS

Virus

CCMV was isolated from 7-day-infected cowpea leaves as described before [8]. The coat protein was prepared according to the $CaCl_2$ method and pseudotop component was obtained by dialysing against 1 M NaCl, pH 5.0 [9]. BMV and BBMV were grown in barley and horse bean respectively. Virus and coat protein were isolated by the same procedures as described for CCMV. The nucleoprotein and protein preparations were dialyzed against 0.02 M cacodylic acid buffer of the desired pH and ionic strength. All measurements were done in this buffer. Preparations of each bromovirus contained the three different nucleoprotein particles in the same ratio as the isolates from the plants. Both protein and nucleoprotein were used in a concentration of about 0.1 mg/ml.

Absorption Spectra

Absorption spectra were recorded with a Cary 14 spectrophotometer.

Fluorescence Spectra

Fluorescence spectra were measured with a Hitachi-Perkin Elmer MPF 2A spectrofluorimeter equipped with a thermostated cell holder and with a home-built apparatus. It was composed of a 450-W xenon lamp and an M4QIII Zeiss monochromator for excitation and a Jarrell-Ash 0.25-m Ebert monochromator (model 82.410) with a cooled EMI 9659 QB S20 photomultiplier for detection. The light beam was chopped at 124 Hz. The photomultiplier signal was amplified by a PAR 128A lock-in amplifier, supplied with a reference signal from the light chopper. The cell holder could be thermostated between − 180 C and room temperature, using either liquid nitrogen or circulating methanol as coolant. The fluorescence spectra were recorded at 4 C.

The sensitivity of the detection system was calibrated with a standard tungsten lamp [10]. The quantum yield was determined by comparing an integrated and corrected spectrum with that of a tryptophan solution of known concentration ($Q = 0.14$) [11].

Fluorescence lifetimes were determined with a phase fluorometer [12, 13]. Fluorescence decay curves were obtained with a single-photon counting apparatus consisting of a gated flash lamp unit (Applied Photophysics Ltd), a 56 DUVP/03 Philips photomultiplier, operated at 2400 V, NIM modules of the Ortec 9200 system and a Laben multichannel analyzer. A flash in deuterium (1 atm) passing through a Jarrell Ash 0.25-m monochromator (model 82.410) was used for excitation. The emission from the thermostated sample cuvette was observed through a set of filters consisting of a Schott WG 305, a Chance Pilkington 0X7 and a

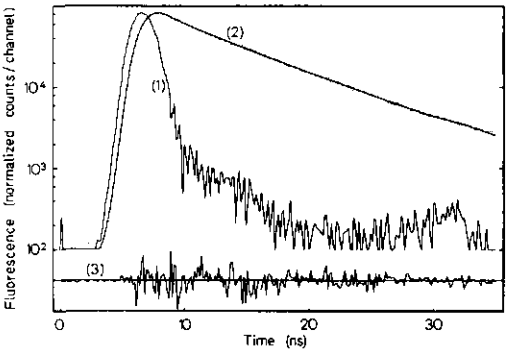

Fig. 1. *Example of the analysis of a fluorescence decay curve measured by means of single photon counting.* (1) Excitation profile, calculated by deconvoluting the decay curve of the quantum counter with a known lifetime. (2) The dots represent experimental data, the drawn line is the calculated decay curve. (3) The deviation function $DV(i) = [F_c(i) - F(i)]/\sqrt{F(i)}$ where $F(i)$ is the content of the ith channel and $F_c(i)$ is the calculated value of this content. The scale is linear

$NiSO_4/CoSO_4$ liquid filter with a maximum transmission at 317 nm and a full width at half maximum (fwhm) of 42 nm [14] or through a Balzer K 36 band filter ($\lambda_{max} = 366$ nm, fwhm = 47 nm). The filters used were chosen in such a way that a glycogen solution with a turbidity comparable to that of the virus solutions resulted in a negligeable number of counts. Because of its wavelength dependence the response function of the apparatus was determined with a reference compound by a method described elsewhere [15]. This reference compound was a degassed solution of *p*-diphenylbenzene (BDH) in cyclohexane (Merck, Uvasole). The life-time of this compound was determined as 0.95 ns with the phase fluorimeter operating at 60 MHz. The lifetime was homogeneous with respect to measurements of phase shift and modulation [12]. The decay experiments were performed at 9 °C. Analysis of the data was performed using a non-linear regression algorithm for the deconvolution of the fluorescence decay [16] described by:

$$F_c(t) = \int_0^t g(T) \cdot I(t-T)\mathrm{d}T \qquad (1)$$

where $g(T)$ is the instrumental response function and $I(t)$ is the decay law assumed to be: $\sum_{j=1}^{n} \alpha_j e^{-t/\tau_j}$, with $n = 1$ (mono-exponential), $n = 2$ (bi-exponential) or $n = 3$ (tri-exponential). After adjustment of the parameters α_j and τ_j the fit was checked by calculating the convolution product of $I(t)$ and $g(t)$ [Eqn (1)] and by visual comparison of the experimental $F(t)$ and the calculated curves $F_c(t)$ (Fig. 1). The criterion of best fit was attained after a search for the minimum value of χ^2:

$$\chi^2 = \sum_{i=1}^{N} W_i [F(i) - F_c(i)]^2 \qquad (2)$$

in which the summation is made over N channels.

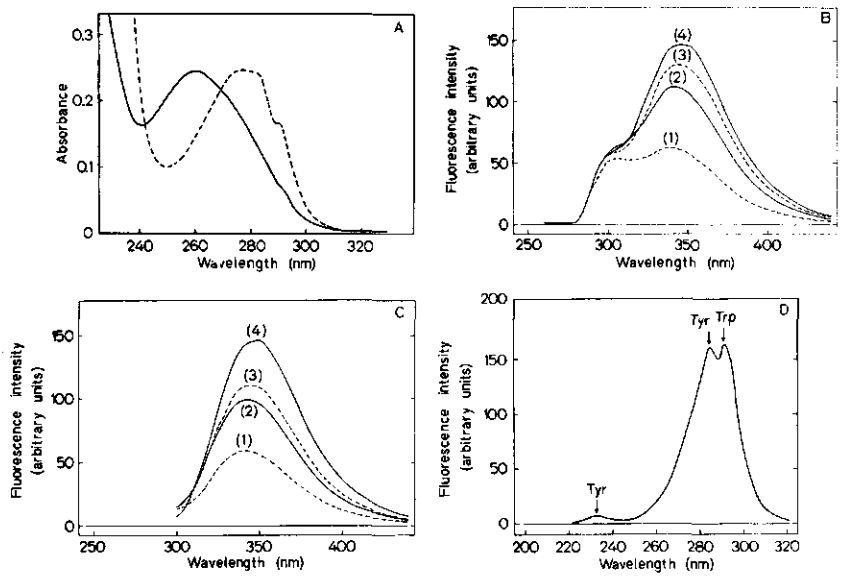

Fig. 2. *Absorption and fluorescence spectra of CCMV protein and nucleoprotein.* (A) Absorption spectra of CCMV protein at pH 7.5 + 1 M NaCl (----), and CCMV nucleoprotein at pH 5 (——). (B) Corrected fluorescence spectra of CCMV nucleoprotein excited at 235 nm: (1) pH 5.0, (2) pH 5.0 + 1.0 M NaCl, (3) pH 7.5, (4) pH 7.5 + 1.0 M NaCl. (C) As for B with excitation at 295 nm. (D) Characteristic excitation spectrum of CCMV nucleoprotein. This spectrum is not corrected for lamp intensity at different wavelengths. The detection wavelength is at 350 nm

$$W_i = \frac{1}{(N-f)F(i)} \qquad (3)$$

where f is a number related to the number of lifetime components in which deconvolution takes place: 2, 4 or 6 for a mono, di, or tri-exponential fit respectively. The factor $(N-f)$ denotes the degrees of freedom.

Also plotted is a diviation function of the residuals defined as:

$$DV(i) = \frac{F_c(i) - F(i)}{\sqrt{F(i)}} \qquad (4)$$

for each channel i.

Fluorescence Polarization

Fluorescence polarization values were determined on an apparatus built according to the idea of Weber and Bablouzian [17]. Excitation was at 292 nm (fwhm = 10 nm) and the emission was detected with a combination of the Schott filters WG 320 + UG1 (λ_{max} = 365 nm, fwhm = 52 nm).

RESULTS

Absorption Spectra

The virus exhibited an absorption maximum at 260 nm, mainly originating from the RNA. The contribution of the protein appeared as a shoulder in the absorption spectrum of the nucleoprotein. The spectrum of the protein showed a maximum at 277 nm and a shoulder at 290 nm originating from the tyrosine and the tryptophan residues respectively (Fig. 2A). The tryptophan shoulder was shifted as compared to the shoulder at 288 nm in the absorption spectrum of a solution of free tryptophan. The differences between free tryptophan and tryptophan in the protein might reflect a less polar environment of the tryptophans in the protein [6, 7].

Fluorescence Spectra

The fluorescence was observed with a band width of 3.3 nm. Excitation was at 285 and 295 nm. Pseudotop component and the protein dimers exhibited similar fluorescence spectra that were independent of their aggregation states as influenced by pH and ionic strength. On the other hand, a change in pH and ionic strength had a remarkable effect on the protein fluorescence of the nucleoprotein particles (Fig. 2B). At pH 5.0 and low ionic strength, where the virus is stable, the emission spectrum showed a maximum at 342 nm when excited in the tryptophan absorption band at 295 nm. No RNA fluorescence could be detected. An increase of the ionic strength at pH 5.0

Table 1. *Emission parameters of CCMV protein fluorescence*
Excitation was at 295 nm (fwhm = 2.2 nm). Measurement were at 4 °C unless indicated otherwise. The accuracy of the emission wavelength maximum (λ_{max}) was ± 1 nm and of the quantum yield (Q) about 5% of the value. fwhm is the width of the emission curve at half intensity of the maximum

Component	Solution conditions	Q	fwhm	λ_{max}
			nm	
Nucleoprotein	pH 5.0	0.075	60	342
	pH 5.0 + 1 M NaCl	0.13	59	346
	pH 7.5	0.16	59	345
	pH 7.5 + 1 M NaCl	0.19	59	346
Protein		0.19	60	346
Protein and nucleoprotein at room temperature	pH 7.5 + 1 M NaCl	0.13		346

to 1 M NaCl resulted in a higher quantum yield and a shift of the emission maximum to 346 nm. Under these conditions no changes in hydrodynamic properties have been observed (Verduin, unpublished results). At low ionic strength ($I < 0.1$ M) and pH 7.5, where the virus is swollen and assumed to be stabilized mainly by electrostatic protein – nucleic-acid interactions, a further increase in the quantum yield was observed. The quantum yield was slightly higher than at 1 M NaCl pH 5.0 and the maximum shifts to 345 nm. Increasing the ionic strength at pH 7.5, thereby causing dissociation of the virus into protein dimers and RNA, enhanced the quantum yield even more. Characteristics of the fluorescence spectra of CCMV protein are collected in Table 1.

The presence of 0.01 M $MgCl_2$ in a solution of low ionic strength at pH 7.5, that partly prevents the swelling of the nucleoprotein particles, had too small an effect on the fluorescence intensity to be expressed in a value of the quantum yield. In all cases the full width at half maximum (fwhm) of the tryptophan emission band was 60 ± 1 nm. The fluorescence quantum yield of the undissociated nucleoprotein was always lower than that of the RNA-free protein solutions (cf. Table 1). The fact that the fluorescence spectra of the RNA-free protein showed no observable dependence on the pH and ionic strength was in sharp contrast to the sensitivity towards NaCl concentration of the nucleoprotein emission. This suggests that an RNA-protein interaction might be responsible for the changes observed within the virus.

In excitation spectra of a diluted tyrosine solution (detection at 300 nm) a peak at 235 nm can be located. This maximum is absent in excitation spectra of either tryptophan solutions or diluted tryptophan and tyrosine solutions mixed in a ratio, identical to that found in the coat protein, when detection is at 350 nm. However, in an excitation spectrum of CCMV nucleoprotein (Fig. 2D) a band at 235 nm is also present when detection is at 350 nm. This is probably due to energy transfer from tyrosine to tryptophan residues within the protein.

Excitation at 235 nm of the virus solutions (fwhm of excitation is 4 nm) resulted in a dependence of the tryptophan emission intensity at 350 nm on pH and ionic strength, comparable to the observations upon excitation at 295 nm. When exciting the nucleoprotein at 235 nm, a strong shoulder is observed at 300 nm in the emission spectrum. This shoulder can be attributed to the presence of tyrosine residues, since free tyrosine exhibits an emission maximum in this region whereas a free tryptophan solution hardly shows any contribution at this wavelength. The intensity at 300 nm does not depend on the different conformations of the virus (Fig. 2B and C).

Excitation Spectra and Energy Transfer

Uncorrected fluorescence excitation spectra with a detection wavelength at 350 nm (fwhm = 4 nm) showed three peaks: at 235 nm, mainly from the tyrosine residues, at 285 nm, and at 292 nm (Fig. 2D). The shape of the excitation spectrum did not change when the detection wavelength was varied between 350 and 400 nm. The peak at 285 nm is partly due to the tyrosine residues. This was confirmed by measuring the excitation spectrum with 300 nm as detection wavelength, in which case only bands with maxima at 235 and 285 nm could be observed. Studies on solutions of tryptophan, tyrosine and a mixture of these amino acids also indicated that this conclusion was justified (results not shown). The detection of the band at 235 nm was possible because of the low absorbance of the cacodylic acid solution at this wavelength. With the diluted protein and nucleoprotein solutions (approximately 0.1 mg/ml), where no corrections for screening effects due to high absorbance were necessary, no changes in the relative intensities of the peaks at 285 and 292 nm in the excitation spectra were observed, when pH and ionic strength were varied. This demonstrated that the energy transfer from tyrosines to tryptophans was not very dependent on the structure of the virus particles. The amount of energy transfer could be estimated from absorption and from lamp-intensity-corrected excitation spectra of the protein [18 – 20]. Upon comparing these spectra with the absorption spectra of aqueous solutions of tryptophan and of a mixture of tryptophan and tyrosine (3:5), it was shown that the efficiency of energy transfer from tyrosine to tryptophan was about 30%.

For a donor-acceptor pair the efficiency E is defined as:

$$E = \frac{1}{1 + \left(\frac{r}{R_0}\right)^6} \quad [19] \qquad (5)$$

Table 2. *Fluorescence lifetimes of tryptophan and tyrosine residues in bromovirus proteins*
The fluorescence lifetimes were measured by the single photon counting technique. A_i is the amplitude of the exponential function e^{-t/τ_i}, multiplied with the fluorescence lifetime τ_i. Deconvolution with three time constants gave the best fit. $\langle\tau\rangle$ is the averaged lifetime $(\Sigma_i A_i\tau_i)/(\Sigma A_i)$. χ^2 is a function of the deviation between the measured and the calculated decay curve (see Methods). In all experiments the temperature was 9 °C. The aggregation state is characterized by pH and molarity of NaCl in the solution

Virus	Wavelength of		Component	Aggregation state		A_1	τ_1	A_2	τ_2	A_3	τ_3	$\langle\tau\rangle$	χ^2
	excitation	detection		pH	[NaCl]								
	nm				M		ns		ns		ns		
CCMV	235	317	nucleoprotein	5	0	0.12	0.39	0.48	2.1	0.40	6.3	3.6	1.1
				5	1.0	0.12	0.42	0.39	2.3	0.49	6.9	4.3	1.2
				7.5	0	0.12	0.40	0.37	2.4	0.51	7.1	4.6	0.85
				7.5	1.0	0.03	0.11	0.38	2.4	0.59	7.0	5.1	1.3
			protein	5	1.0	0.07	0.26	0.37	2.1	0.57	6.8	4.7	1.1
				7.5	1.0	0.04	0.53	0.41	2.4	0.55	7.2	5.0	1.3
	235	366	nucleoprotein	5	0	0.07	0.57	0.16	2.3	0.77	7.2	6.0	1.3
				5	1.0	0.03	0.26	0.12	2.1	0.85	7.2	6.4	1.3
				7.5	0	0.05	0.89	0.15	3.5	0.80	7.7	6.7	1.1
				7.5	1.0	0.01	0.12	0.07	1.9	0.92	7.3	6.9	1.1
			protein	5	1.0	0.04	0.92	0.08	2.7	0.88	7.3	6.7	1.6
				7.5	1.0	0.02	0.15	0.08	2.6	0.90	7.5	7.0	1.4
	295	366	nucleoprotein	5	0	0.15	0.41	0.18	2.7	0.67	7.4	5.5	1.3
				5	1.0	0.06	0.37	0.14	1.9	0.80	7.3	6.1	1.4
				7.5	0	0.07	0.63	0.14	2.9	0.79	7.6	6.5	1.3
				7.5	1.0	0.04	0.31	0.09	2.3	0.87	7.5	6.7	1.2
			protein	5	1.0	0.07	0.51	0.10	2.8	0.83	7.5	6.5	1.5
				7.5	1.0	0.04	0.28	0.09	3.1	0.87	7.7	7.0	1.1
BMV	235	317	nucleoprotein	5	0	0.07	0.21	0.49	1.08	0.44	3.0	1.9	1.4
				5	1.0	0.15	0.21	0.54	1.52	0.31	3.8	2.0	1.1
				7.5	1.0	0.23	0.38	0.55	1.87	0.22	4.0	2.0	1.1
BBMV	235	317	nucleoprotein	5	0	0.05	0.10	0.11	1.68	0.84	3.8	3.4	1.4
				5	1.0	0.04	0.15	0.15	1.50	0.81	3.8	3.4	1.2
				7.5	1.0	0.04	0.14	0.12	1.58	0.84	3.9	3.5	1.2

where r = distance between donor and acceptor and R_0 = the Förster critical distance where E is 50%. For the donor-acceptor pair Tyr-Trp, a R_0 of 1.31–1.5 nm is assumed [19, 20].

Since there are five tyrosine and three tryptophan residues per protein subunit, multiple pathways of energy transfer can exist, making it difficult to draw conclusions about relative distances and orientations from the value of the efficiency. The observed increase in the fluorescence quantum yield of the virus particles, when ionic strength or pH were raised, was not accompanied by a change in the shape of the excitation spectra monitoring tryptophan emission at 350 nm. The efficiency of energy transfer from tyrosine to tryptophan residues thus appeared to be independent of this increase in quantum yield. This must be explained by assuming that the originally non-fluorescent tryptophan residues are equally effective as an acceptor of the tyrosine excitation energy.

Fluorescence Lifetimes

CCMV protein and nucleoprotein solutions were excited at 235 and 295 nm. The time-resolved emission was observed through filters having transmission maxima at 317 and 366 nm. A typical example of such a fluorescence decay experiment is shown in Fig. 1. At 317 nm both tyrosine and the blue side of tryptophan emissions could be observed, while at 366 nm only tryptophan emission is transmitted. The results are collected in Table 2. It should be noted that in all solutions studied the decay function could not be assumed to be mono-exponential. On the other hand the decay profiles measured with a standard compound like *N*-acetyl-tryptophanamide in buffer pH 7.0 [21] could be fitted with a single lifetime. For comparison, the results obtained with other bromoviruses are also included. In order to emphasize the relative importance of the different lifetime com-

ponents, the amplitudes of the exponential functions are multiplied with their lifetimes. This product is directly comparable to the contributions of the different chromophores to the time-independent emission intensity at a particular wavelength region. It is to be noted that the relatively large differences in quantum yield, induced when the nucleoprotein particles were subjected to changes in pH and ionic strength, are not reflected similarly in the fluorescence lifetimes detected at 366 nm. The averaged lifetimes, $\langle\tau\rangle = (\sum_i \alpha_i\tau_i^2)/(\sum_i \alpha_i\tau_i)$, do not show these large differences either.

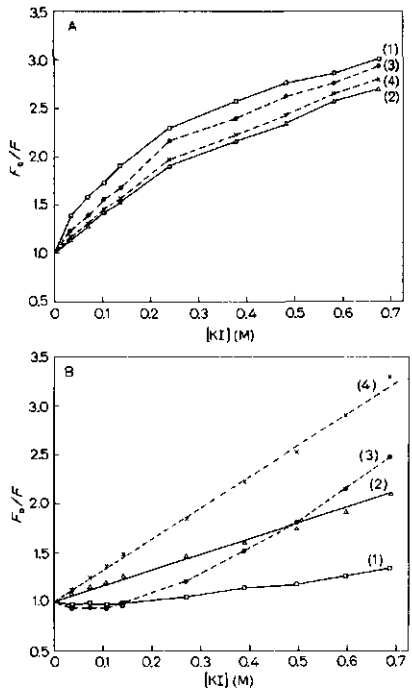

Fig. 3. *Stern-Volmer plots for the KI quenching of the fluorescence of CCMV protein.* (A) Free coat protein: (1) pH 5.0 + 0.2 M NaCl; (2) pH 5.0 + 1.0 M NaCl; (3) pH 7.5 + 0.2 M NaCl; (4) pH 7.5 + 1.0 M NaCl. (B) Nucleoproteins: (1) pH 5.0; (2) pH 5.0 + 1.0 M NaCl; (3) pH 7.5; (4) pH 7.5 + 1.0 M NaCl

The discrepancy between lifetimes and quantum yields can be interpreted by assuming that a static rather than a dynamic quenching mechanism is involved for a fraction of the tryptophans without affecting the corresponding lifetimes.

When excitation was at 235 nm, emission at 317 nm showed, in addition to the decay characteristics observed at 366 nm, a contribution of a lifetime component of 2–3 ns (see Table 2). This can be attributed to the tyrosine residues and is in agreement with the results obtained from BBMV protein, in which no tryptophan residues are present. The values of the lifetimes of the pseudotop conformation of the protein at pH 5.0 + 1 M NaCl and the dissociated protein at pH 7.5 + 1 M NaCl are comparable to those found for the nucleoproteins under the same conditions (Table 2).

Fluorescence Quenching

The protein fluorescence can be quenched dynamically by addition of potassium iodide or acrylamide to the solution [22, 23]. In the case of more than one emitter the fraction of chromophores to be quenched by I^- ions can be estimated [22]. The quenching data are shown in Fig. 3A for the protein and Fig. 3B for the nucleoprotein. The relevant parameters are collected in Table 3. Investigation with protein solutions indicated that at least 2–2.5 tryptophan residues per subunit could be quenched easily. Interpretation of the results obtained with nucleoprotein solutions at low ionic strength was difficult because of interference with the salt effect. The fluorescence quantum yield increases rapidly upon raising the ionic

Table 3. *Fluorescence quenching by KI*
The quenching constant, K_{sv}, and the fraction of tryptophans that can be quenched, $(fa)_{eff}$, were obtained according to Lehrer [22]

Component	Aggregation state		K_{sv} (M^{-1})	$(fa)_{eff}$	Shift in emission maximum
	pH	[NaCl]			
		M	M^{-1}		nm
Virus	5				342 → 340
	5	1.0	2.6 ± 0.2	0.8	346 → 339
	7.5				345 → 343
	7.5	1.0	4.1 ± 0.2	0.85	346 → 340
Protein	5	0.2	18.3 ± 0.8	0.7	345 → 339
	5	1.0	5.1 ± 0.2	0.8	346 → 339
	7.5	0.2	9.4 ± 0.7	0.75	346 → 339
	7.5	1.0	6.75 ± 0.5	0.8	346 → 340

strength and then decreases with addition of I^- ions. Acrylamide does not show this effect. The proteins at high ionic strength were quenched less easily than at lower ionic strength (Fig. 3A). This indicates that at high salt concentrations the chromophores are more shielded than at low ionic strength. In all cases the emission maximum is shifted to lower wavelengths after addition of quencher, indicating the presence of more buried tryptophan residues.

Polarization

The degree of polarization of the tryptophan emission in the intact nucleoprotein particles has a value of 0.22 when excited at 292 nm. This value slightly decreases to 0.19 when the particles dissociate. The decrease can be explained in terms of decrease of the rotational correlation time of the protein. This is apparent from the Perrin equation [24]:

$$\left(\frac{1}{P} - \frac{1}{3}\right) = \left(\frac{1}{P_0} - \frac{1}{3}\right)\left(1 + \frac{RT\tau}{\eta V_m}\right) \qquad (6)$$

Since the volume of the particles decreases upon dissociation and the averaged lifetime remains constant, the last term in the equation, $RT\tau/\eta V_m$ where V_m is the molar volume, thus increases, assuming all other quantities to be invariant. From the observed depolarization, we can roughly estimate the dimension of the protein dimers, when the polarization of the non-dissociated particles is adopted as the limiting polarization P_0. Assuming the dimers to be spherical particles, we obtain a diameter of about 5.5 nm. When we estimate the dimension of the dimers using neutron scattering data from Jacrot et al. [25], we obtain a comparable magnitude. The degree of polarization of the pseudo-top component has the same value as the nucleoprotein solutions and also decreases upon dissociation.

DISCUSSION

The changes in the fluorescence quantum yield observed when ionic strength or pH are raised, can be explained in terms of weakening of interaction between the protein subunits and the RNA strand. A direct interaction between RNA and some tryptophan residues might play a role or, alternatively, the influence of RNA exerted on the protein subunits causes changes in the internal structure of the protein. The phenomena observed at low ionic strength ($I < 0.1$ M) in the nucleoprotein particles cannot be compared with the effects in empty protein shells at low ionic strength, because in the latter case the protein precipitates. The interpretation of the changes in the fluorescence quantum yield is supported by the following arguments.

First, the changes occur within the nucleoprotein particles and not within the protein in the pseudo-top component or dimer. (The emission from nucleoprotein particles increases upon raising ionic strength from 0.2 M to 1.0 M, but the emission from the RNA-free particles remains constant under these conditions.)

Second, an increase of salt concentration, known to disrupt ionic linkages, causes an enhancement of fluorescence quantum yield even at pH 5.0.

Third, weakening and disappearance of interaction between protein and RNA was also observed in BMV by Pfeiffer and Hirth [26,27]. By increasing the ionic strength at pH 5.5 they were able to remove RNA from the nucleoprotein particles. Also, from our own observations with CCMV, we know that it is possible to make nucleic-acid-free protein particles by increasing the ionic strength of the solutions at pH 6.5 (Verduin, unpublished results). Probably no complete dissociation is needed in this process.

Last, Chauvin et al. [28] observed a decrease in the radial extension of BMV RNA when virus at pH 5.5 was moved from 0.2 M KCl to 1.5 M KCl. No change in the radial position of the coat protein was noticed upon this increase of ionic strength.

The influence of RNA on the fluorescence of CCMV protein was not observed with BMV [29]. From comparison of the latter observations on BMV [29] with our own experiments on BMV and CCMV, it is obvious that the tryptophan residues in BMV protein have completely different fluorescence characteristics (lifetimes, quantum yields, emission maxima) to those in CCMV protein. These differences cannot be explained exclusively by the difference in the number of tryptophan residues in CCMV (3) and BMV (2). In contrast with the situation in CCMV, the environment of the tryptophan residues in BMV probably does not change when ionic strength and pH are raised.

The shift in emission maximum that accompanies the increase in quantum yield must be attributed to the fact that the tryptophans that become more fluorescent upon weakening of the interaction between RNA and the protein, are now located in a slightly more polar environment (the outer regions of the protein subunits).

The increase in fluorescence quantum yield of CCMV protein, mentioned before, is not manifested in a proportional change in the lifetimes of the tryptophan fluorescence. This can be explained by assuming that a static quenching process dominates, which means that the quenching group or residue is in interaction with the quenched tryptophan during a time interval that is at least equal or longer than the fluorescence lifetime. This is in contrast to a dynamic quenching process as is caused by addition of KI. Here the quenching is caused by a collision between an I^- ion and a chromophore that exists in an excited

state. In this process a decrease in lifetime roughly proportional to the change in quantum yield is observed.

Since the fluorescence decay curves of the tryptophan fluorescence (excitation at 295 nm, detection at 366 nm) cannot be fitted with one single time constant, we must conclude that a heterogeneity exists in the tryptophan residues of the protein. Excitation at 235 nm and detection at 317 nm shows, in addition to a lifetime component of about 2 ns (mainly due to the tyrosine emission), a component of about 7.0 ns (due to tryptophan emission). The contribution of this last component increases when the quantum yield of the tryptophan emission increases. Comparing the results of the lifetime measurements on CCMV with those of BMV (our averaged lifetimes are in good agreement with the results of Herzog et al. [29]) one sees that the fluorescence in BMV is dominated by the tyrosines and tryptophans with short lifetimes. According to Burstein et al. [7], the short tryptophan lifetimes indicate that these residues are shielded from the solution. This interpretation might explain the lack of interaction between the tryptophans and the RNA in BMV.

The heterogeneity in the tryptophan residues of CCMV is also observed in the KI quenching experiment. The different tryptophan emissions cannot be quenched equally well and the quenching causes a shift of the emission maximum to a lower wavelength. This suggests that the tryptophan residues with an emission maximum at relatively short wavelength (335–340 nm) are shielded more effectively from the solvent than the 'red-shifted' tryptophans (340–350 nm). The classification that Burstein gave of the tryptophan residues in different environments can be applied to CCMV in a satisfactory way. From the observed lifetimes, quantum yields and widths of the emission band (Table 2) we may conclude that the tryptophan residues are in a more or less polar environment [7].

Polarization of the tryptophan fluorescence in CCMV and of free tryptophan in a rigid solution [6] shows that the tryptophan residues are rigidly attached to the protein frame work. Also the intact virus particles and pseudo-top component must have a rather rigid structure. This can be concluded from the values of the fluorescence polarization and from the calculated values of the rotational correlation times.

The observed energy transfer from tryptophan to tyrosine seems independent of the conformation state of the protein and nucleoprotein particles. The insensitivity can be partly due to averaging of the energy transfer from each of the five tyrosines to each of the three tryptophans. On the other hand, large changes in the tertiary structure of the protein should be reflected in a pronounced change of efficiency of energy transfer from tyrosine to tryptophan.

From this study we can learn that the major effects are caused by a change on the outside of the protein particles. No evidence has been found that the internal structure of the protein particles is changed. The internal probes used here have the advantage over external probes that they do not disturb the structure of the particles.

Excitation at 235 nm appears to be a fast and accurate method in characterising the different conformations of CCMV and its isolated protein.

In conclusion, the fluorescence parameters both of products of reassembly experiments and of native virus may provide useful information in the investigation of the assembly mechanism. Since the effects mentioned here are absent in BBMV and BMV, attempts will also be made to use external fluorescent probes as a tool in further characterization of the association-dissociation mechanism of the bromoviruses.

We thank Drs A. van Kammen, J. Lyklema, C. Veeger and J. P. H. van der Want for regular discussions and Dr P. Pfeiffer for sending us a manuscript prior to publication. We are indebted to Mrs K. M. Krüse-Wolters for preparing virus and protein, Mr B. J. Sachteleben for drawing the figures and Mrs J. C. Toppenberg-Fang for typing the manuscript. This research was in part supported by the Netherlands Foundation for Chemical Research (SON) with financial aid from the Netherlands Organization for the Advancement of Pure Research (ZWO).

REFERENCES

1. Bancroft, J. B. (1970) *Adv. Virus Res. 16*, 99–134.
2. Lane, L. C. (1974) *Adv. Virus Res. 19*, 151–220.
3. Adolph, K. W. & Butler, P. J. G. (1977) *J. Mol. Biol. 109*, 345–357.
4. Finch, J. T. & Bancroft, J. B. (1968) *Nature (Lond.) 220*, 815–816.
5. Bancroft, J. B., Rees, M. W. & Short, M. N. (1971) *Virology, 45*, 707.
6. Konev, S. V. (1967) *Fluorescence and Phosphorescence of Proteins and Nucleic Acids*, Plenum Press, New York.
7. Burstein, E. A., Vedenkind, N. S. & Ivkova, M. N. (1973) *Photochem. Photobiol. 18*, 263–279.
8. Verduin, B. J. M. (1978) *J. Gen. Virol. 39*, 131–147.
9. Verduin, B. J. M. (1974) *FEBS Lett. 45*, 50–54.
10. Parker, C. A. & Rees, W. T. (1960) *Analyst, 85*, 587–600.
11. Eisinger, J. (1969) *Photochem. Photobiol. 9*, 247–258.
12. Spencer, R. D. & Weber, G. (1969) *Ann. N.Y. Acad. Sci. 158*, 361–376.
13. Schürer, K., Ploegaert, P. G. F. & Wennekes, P. G. M. (1976) *J. Sci. Instrum. 9*, 8121–8124.
14. Passner, A., McCall, S. L. & Leventhal, M. (1976) *Rev. Sci. Instrum. 47*, 1221–1222.
15. Wahl, Ph., Auchet, J. C. & Donzel, B. (1974) *Rev. Sci. Instrum. 46*, 28–32.
16. Grinvald, A. & Steinberg, I. Z. (1974) *Anal. Biochem. 59*, 583–598.
17. Visser, A. J. W. G., Grande, H. J., Müller, F. & Veeger, C. (1974) *Eur. J. Biochem. 45*, 99–107.
18. Förster, Th. (1965) in *Modern Quantum Chemistry* (Sinanoglu, O., ed.) vol. 3, pp. 93–137, Academic Press, New York.

19. Eisinger, J., Feuer, B. & Lamola, A. A. (1969) *Biochemistry*, *8*, 3908–3915.
20. Steinberg, I. Z. (1971) *Annu. Rev. Biochem. 40*, 83–114.
21. Grinvald, A. (1976) *Anal. Biochem. 75*, 260–280.
22. Lehrer, S. S. (1971) *Biochemistry*, *10*, 3254–3263.
23. Eftink, M. R. & Ghiron, C. A. (1976) *Biochemistry*, *15*, 672–680.
24. Perrin, F. (1929) *Ann. Phys. (Paris) 12*, 169–275.
25. Jacrot, G., Pfeiffer, P. & Witz, J. (1976) *Phil. Trans. R. Soc. Lond. B276*, 108–112.
26. Pfeiffer, P. & Hirth, L. (1974) *Virology*, *58*, 362–368.
27. Herzog, M., Pfeiffer, P. & Hirth, L. (1976) *Virology*, *69*, 394–407.
28. Chauvain, C., Pfeiffer, P., Witz, J. & Jacrot, B. (1978) *Virology*, in the press.
29. Herzog, M., Gerard, D., Hirth, L. & Laustriat, G. (1977) *Biochim. Biophys. Acta*, *493*, 167–177.

J. Krüse, B. J. M. Verduin, and A. J. W. G. Visser, Laboratoria voor Biochemie en voor Virologie, Landbouwhogeschool, De Dreijen 11, NL-6703 BC Wageningen, The Netherlands

4. PHOSPHORESCENCE AND ODMR OF COWPEA CHLOROTIC MOTTLE VIRUS

4.1. SUMMARY

Phosphorescence spectra of the tryptophanyl residues in cowpea chlorotic mottle virus were recorded at 77 K and the influence of the quarternary structure on the emission characteristics was investigated. The position of the phosphorescence maxima appeared to be invariant under changes in the aggregation state of the virus particle. In contrast to the results of fluorescence experiments, the phosphorescence probably originates from tryptophanyl residues, buried in the hydrophobic interior of the virus.

Optical detection of magnetic resonance on the triplet state of the tryptophanyl residues, shows a slight shift in the zero field transitions, when the interaction between the protein and the RNA is abolished. This shift is discussed in terms of changes in polarity and in polarizability of the environment of the phosphorescing tryptophanyl residues when the interaction between RNA and the protein subunits decreased. The zero field transitions in the virus are further characterized by a great line width, when comparisons are made with similar transitions observed in other proteins. This shows the great heterogeneity in environment of the tryptophanyl residues, and makes the recognition and interpretation of changes in the transitions very complicated.

4.2. INTRODUCTION

Cowpea chlorotic mottle virus, a spherical, RNA containing virus, belongs together with brome mosaic virus and broad bean mottle virus to the group of bromoviruses [1, 2] . The RNA is encapsulated in a protein coat in an icosahedral symmetry. The coat is composed of 180 identical protein subunits [3]. The nucleoprotein particles are stable at low ionic strength below neutral pH. At pH 7.5 the particles are swollen and an increase in ionic strength at this pH results in dissociation of the virus into protein dimers and free RNA [2, 4]. Also at low pH (below neutrality) the conformation of the RNA in the virus particles can be changed by an increase in ionic strength [5,6,7].

Each protein subunit contains 3 tryptophanyl and 5 tyrosyl residues [8]. From fluorescence experiments we have already concluded, that the environment

of part of the tryptophanyl residues is changed, when the particles are swelling or dissociating or when the RNA configuration within the virus particles is changed at low pH. In the empty protein core (without RNA) the fluorescence properties are similar to those of the dissociated nucleoprotein particles [7].

In addition to the fluorescence of aromatic amino acid residues [9] phosphorescence [10, 11, 12] and optical detection of magnetic resonance (ODMR) [13] can give independent information about the environment and location of these residues in the protein. In the work presented here these techniques were used in order to characterize the environment of the phosphorescing tryptophanyl residues. Furthermore, the interaction between the protein and the RNA was investigated by employing delayed emission properties of this system.

4.3. MATERIALS AND METHODS

4.3.1. Virus

CCMV was isolated according to the procedure described by Verduin [14]. Protein was prepared by the $CaCl_2$ precipitation method [15]. The virus was dialyzed against 0.02 M cacodylic acid buffer of desired pH. For the low temperature measurements equal amounts of virus solution and ethylene-glycol (Merck) were mixed. The virus concentration in the phosphorescence experiments at 77 K was approximately 0.2 mg/ml. In the ODMR experiments concentrations of 5 mg/ml were used. Here buffers containing 0.1 M sodium acetate and 0.1 M sodium phosphate were used at pH 5.0 and 7.5 respectively. To these buffers 0.2 M NaCl (low ionic strength) or 1.0 M NaCl (high ionic strength) was added.

4.3.2. Phosphorescence

Phosphorescence spectra were recorded on a home built apparatus, described before [7]. In the phosphorescense experiments choppers, both in excitation and detection light paths were used. The choppers were rotating synchronously, π radians out of phase, at a frequency of 124 Hz. The 0.25 m Jarrell-Ash monochromator was used with the high blaze grating and slits of 1 mm, resulting in a bandwidth of 3.3 nm. The scanning was performed by a stepping motor. In order to obtain larger sensitivity photon counting was used in part of the experiments.

The single photoelectron pulses of the EMI 9659 QB photomultiplier were fed into a pulse shaping system, consisting of an Ortec 113 scintillation preamplifier, an Ortec 451 spectroscopy amplifier and an Ortec 436 discriminator. The output (counts/second) was stored in a Laben Multi Channel Analyzer Model 8001, operating in the multiscaling mode. The stepping through the channels and the synchronization with the stepping motor was accomplished with a home-built trigger and timing control unit. The digital data were stored on cassette tapes for further processing by a DEC 10 computer system.

4.3.3. Optical detection of magnetic resonance

The ODMR experiments were performed on an experimental setup, described by Schmidt [16] and Schmidt *et al.* [17] . For excitation a 900 Watt Xenon lamp (Oriel) was used and a Kasha filter [18] was placed in the excitation light path to remove the radiation with wavelengths above approximately 350 nm. The excitation light was selected with a Fociflex monochromator. The sample was placed in a four window helium cryosat, that could reach a temperature of 1.2 K by pumping the helium.

The detection system consisted of a 0.5 m Spex-monochromator with 3 mm slits (bandwidth = 3.2 nm) and an EMI 9659 QB photomultiplier, cooled down to -25^{o}C. The photomultiplier signal was amplified by a PAR 5101 lock-in amplifier and this signal was fed into a Nicolet signal averager (Model 527).

The microwaves were obtained from a Hewlett Packard HP 8690 sweep oscillator, equipped with a 1-2 GHz or a 2-4 GHZ Backward Wave Oscillator as a plug-in. In some experiments the microwave signal was amplified by means of a travelling wave tube. The microwaves were fed through a coaxial cable into a helix containing the sample. The microwave was swept slowly through the zero field transitions.

In a second series of experiments two helium cryostats were used and the zero field transitions of the viral coat protein in two different conformational states, were recorded simultaneously. By using one sweep oscillator, the effects of fluctuations in the microwave source were eliminated in the direct comparison of the two samples. The microwaves were split in a circulator and fed into the two helium cryostats. The excitation light sources were high pressure mercury lamps (HBO 200 Watt) followed by Kasha filters. The emission light was selected by narrow band pass filters (Balzer, series A and B) selecting the light around 410 and 440 nm. In one of the setups an EMI 9558 QB photomultiplier and a PAR 5101 amplifier were used for detection, whereas the other

detection unit consisted of a RCA 1P28 and a PAR 220 lock-in amplifier. Both signals were sampled in a Hewlett-Packard 5485A/5486A two channel averager.

In the ODMR experiments the microwave frequency was swept at a rate of 25 MHz/sec through the transitions. The power was in the order of 10 mW. The sweep range was 1.4 - 1.9 GHz to detect the (|D|-|E|) transition and 2.4 - 2.9 GHz to observe the 2|E| transition [19].

4.4. RESULTS

4.4.1. Phosphorescence spectra and lifetimes

The phosphorescence spectrum of cowpea chlorotic mottle virus is independent of its conformational state. Next to a contribution of tyrosine, which becomes apparent upon excitation below 290 nm, the spectrum shows tryptophan phosphorescence emission maxima at 413 and 440 nm. No contribution of the RNA to the phosphorescence could be detected (Fig. 1). The conclusion, that the emission between 360 and 400 nm is originating from the tyrosine and not from the RNA, is supported by the following observations: The emission is present both in protein and nucleoprotein solutions; it only appears upon excitation at wavelengths, where also tyrosine absorbs; the phosphorescence of broad bean mottle virus, with a protein coat containing tyrosyl but no tryptophanyl residues, and of free tyrosine shows between 360 and 400 nm an emission similar to the emission of CCMV detected in this spectral area.

When the widths of the emission peaks at 413 and 440 nm are compared with the bandwidths in an emission spectrum of tryptophan methyl ester [19] it can be observed that in the case of CCMV the peaks are about 50% broadened.

Fig. 1. Phosphorescence of CCMV and BMV at pH 5.0

Excitation was at 235 nm and 295 nm. The spectra were recorded in the absence and presence of 1.0 M NaCl in the buffer solution. Photocounting was used for detection, T = 77 K and fwhm of detection 3.2 nm.

A	CCMV pH 5.0	excitation 235 nm
B	CCMV pH 5.0	excitation 295 nm
C	CCMV pH 5.0 + 1.0 M NaCl	excitation 235 nm
D	CCMV pH 5.0 + 1.0 M NaCl	excitation 295 nm
E	BMV pH 5.0	excitation 235 nm
F	BMV pH 5.0	excitation 295 nm
G	BMV pH 5.0 + 1.0 M NaCl	excitation 235 nm
H	BMV pH 5.0 + 1.0 M NaCl	excitation 295 nm

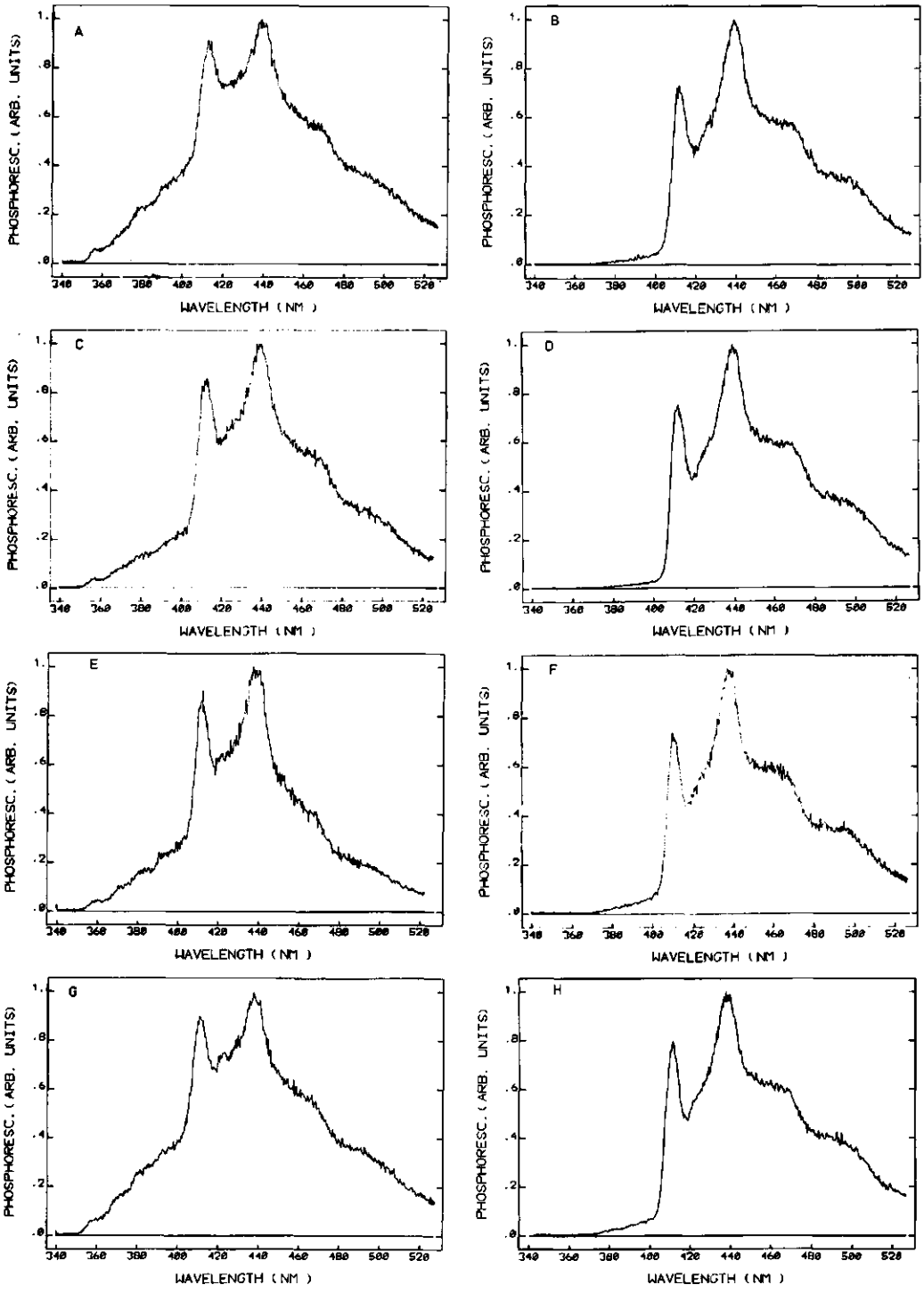
A
B
C
D
E
F
G
H
PHOSPHORESC. (ARB. UNITS)
WAVELENGTH (NM)
340 360 380 400 420 440 460 480 500 520
0 .2 .4 .6 .8 1.

This must be explained by a distinct heterogeneity in the environment of the tryptophanyl residues in the protein.

From the fluorescence emission and lifetime measurements it was already concluded, that the fluorescent tryptophanyl residues are more or less exposed to the solvent [7]. The results of Longworth [11], obtained for several proteins and of Purkey and Galley [19] for the structured phosphorescence of HLAD, show that the phosphorescence of the buried tryptophanyl residues is generally shifted to higher wavelength. In contrast with the fluorescence results of CCMV, the position of the phosphorescence maxima (413, 440 nm) should also be explained in terms of emission originating from buried residues.

In the excitation spectra (not shown), with detection at 440 nm, maxima at about 286 and 293 nm were observed. The slight red shifts in excitation maxima, compared with the maxima from fluorescence excitation spectra is due to a slow decay of the triplet during the scanning of the spectra. From the presence of both bands in the excitation spectra the energy transfer, already observed in the fluorescence spectra, is confirmed here. The similarity between the excitation spectra of the protein and nucleoprotein solutions excludes the possibility of energy transfer from the RNA to the tryptophanyl and tyrosyl residues in the protein.

The phosphorescence spectra of CCMV were compared with those of TMV, BMV and BBMV. The results are summarized in Table I. In the case of TMV and BMV the emission maxima are shifted to lower wavelengths compared with CCMV. This suggests a more exposed environment of the tryptophanyl residues in these viral proteins. The fluorescence of these proteins [20, 21, 22] however suggests also the similar opposite behaviour as is evident in CCMV.

Table I. Spectral characteristics of phosphorescence of viral proteins. The phosphorescence spectra were recorded in 0.02 M cacodylic acid buffer pH 5.0 at 77 K. The excitation was at 285 nm (fwhm 3 nm) and the band width of detection was with a fwhm of 3 nm.

	λ max fluorescence	λ max phosphorescence	
CCMV	342 nm [7]	413 nm	440 nm
BMV	327 nm [20]	411 nm	438 nm
BBMV	305 nm	393 nm	no tryptophan
TMV	330 nm [21, 22]	407.5 nm	437 nm

The phosphorescence decay of the tryptophanyl residues in CCMV-protein shows only a minor variation, when the aggregation state is varied. Lifetime values of 6.1 ± 0.2 sec were measured by closing a mechanical shutter. From the relatively long phosphorescence lifetimes, it can be concluded, that either the phosphorescence is dominated by tryptophans with a long phosphorescence lifetime or that the phosphorescence is not partially quenched by e.g. complex formation in the excited state.

4.4.2. Optical detection of magnetic resonance

Because of the relative insensivity of the phosphorescence spectra to conformational changes, we decided to obtain a more detailed characterization of the triplet states of tryptophan in the viral coat protein, by determining the zero field splitting parameters of the triplet state. Maki [23] has pointed out that in the case of coinciding origins of the phosphorescence additional information on the different triplet states can be obtained from ODMR experiments.

In a series of experiments the positions of the zero field transitions of CCMV in stable and dissociated form were measured. Also the zero field transitions of the empty protein shell (pseudo top component) were determined. The results are summarized in Table II.

Table II. Zero field splitting parameters of CCMV protein in different conformational states.
Excitation was at 290 nm through a Fociflex monochrometer, using a 1000 Watt Oriel Xenon lamp and a Kasha prefilter.
T = 1.2 K. The sweep rate was 25 MHz/sec.

	detection	$\|D\|-\|E\|$ (GHz)	fwhm (MHz)	$2\|E\|$ (GHz)	fwhm (MHz)
virus pH 5.0	410 nm	1.68	(230)		
	413 nm	1.67	(200)	2.70	(275) ⊛
	440 nm	1.68	(245)	2.70	(300)
protein pH 5.0	410 nm	1.71	(150)		
+ 1.0 M NaCl	413 nm	1.68	(150)	2.71	(260)
	440 nm	1.68	(165)	2.70	(250) ⊛⊛⊛
	reverse sweep	1.64	(160)	2.68	(240)
virus pH 7.5	410 nm	1.70	(265) ⊛⊛	2.70	(300)
+ 1.0 M NaCl	423 nm	1.68	(180)		
	440 nm	1.68	(185)	2.69	(260)

⊛ a shoulder at 2.60 GHz was present
⊛⊛ a shoulder at 1.57 GHz was present
⊛⊛⊛ the $|D|/hc$ and $|E|/hc$ values, calculated from the average of the two sweeps are: $|D|/hc = 0.1002\ cm^{-1}$
$|E|/hc = 0.0449\ cm^{-1}$

Because of the weakness of the ODMR signal a long sampling time was needed to collect data with a reasonable signal to noise ratio. On the other hand the sweep of the microwave frequency through the transition cannot be too fast. The spin lattice relaxation is not negligable at the temperatures of the ODMR experiments (1.2 K). These temperatures are needed to cause population differences between the three triplet substates. After a microwave transition, the response of the system (followed by means of a change in phosphorescence intensity) depends strongly on the lifetime of the emitting sublevel [24] . For a more exact determination of the microwave transition we used the average from the sweep from low to high frequency and the sweep from high to low frequency (Table II).

In order to avoid errors, resulting from fluctuations in the microwave frequency of the source and to compare the microwave transitions of two different conformational states of the viral coat protein simultaneously, we used in another series of experiments two idential helium cryostates. The presence of systematic differences between the two setups was checked by interchanging the two different samples. From this we conclude that the observed changes in the zero field transitions were not due to systematic differences in the dual experimental arrangement.

In the simultaneous comparison of the two different conformational states of the viral protein, we were only interested in the relative positions of the transition maxima. Therefore no corrections were applied for the shift in the position of these maxima, due to a long response to changes in the phosphorescence. The results of the experiments, in which two different conformational states were compared simultaneously, are given in Table III and Fig. 2.

From the simultaneous comparison of on one hand the virus at low pH and low ionic strength (stable virus) and on the other hand the virus at high pH and high ionic strength (dissociated virus) (Table IIId) or the empty protein particles (Table IIIa-c), it is seen that a shift occurs in the ($|D|-|E|$) and ($2|E|$) transitions. A comparison of the $|D|$ and $|E|$ values with the observations of other authors [24, 25, 26, 27] and a correlation with the emission maxima [11] shows that the increase of $|D|$ and the decrease of $|E|$ might point into the direction of a slight spectral shift to lower wavelength, when the RNA-protein interaction disappears. The microwave transitions, observed here for the protein of CCMV, exhibit in all cases a large width of the resonance line, while no clear structure can be observed. Apart from the fact, that there are at least three different tryptophan environments, this broad resonance can also

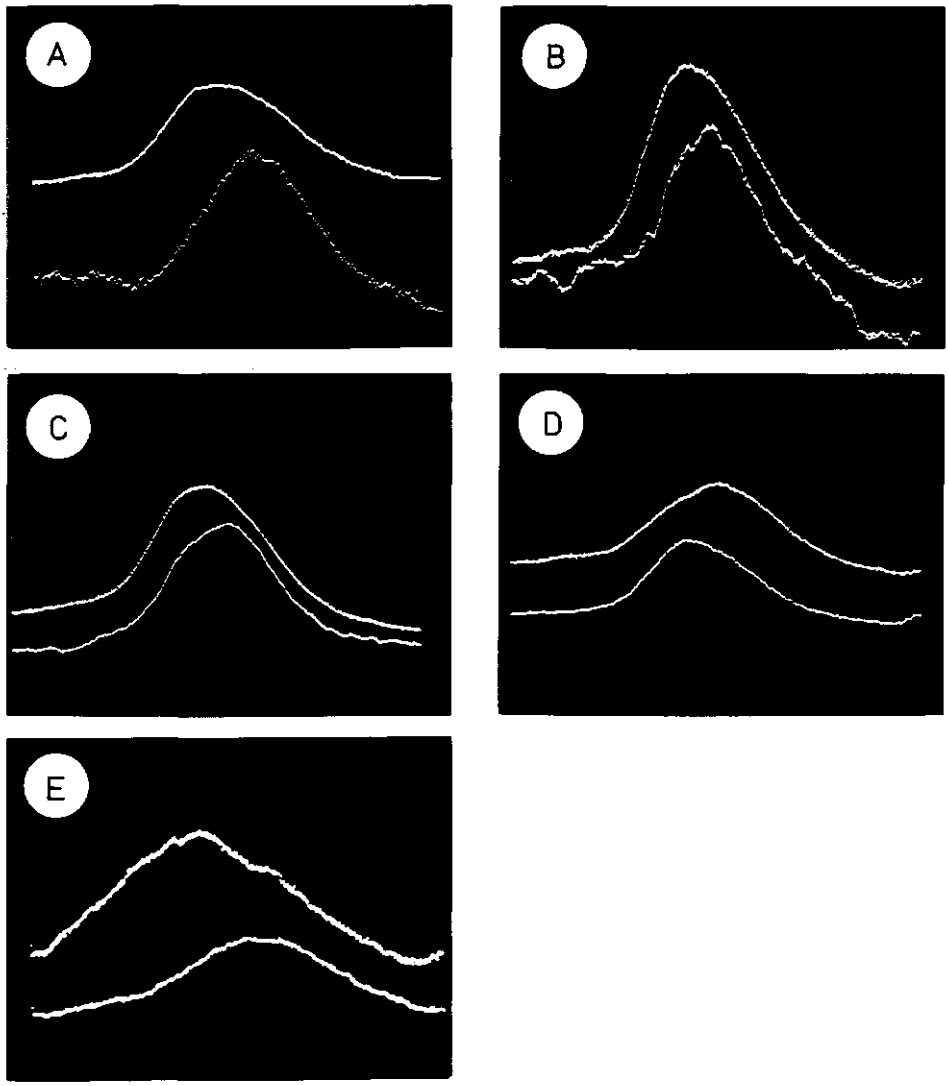

Fig. 2. Spectra of the zero field transitions of CCMV
The different pictures correlate with the experiments summarized in Table III. The traces are from approximately 1.4 - 1.9 GHz ($|D|-|E|$) and 2.4 - 2.9 GHz ($2|E|$)

A) $|D|-|E|$ transitions of virus (top) and protein (bottom) (Table IIIa)
B) $|D|-|E|$ transitions of virus (top) and protein (bottom) (Table IIIb)
C) $|D|-|E|$ transitions of virus (top) and protein (bottom) (Table IIIc)
D) $|D|-|E|$ transitions of virus (bottom) and protein (top) (Table IIId)
E) $2|E|$ transitions of virus (bottom) and protein (top) (Table IIId)

Table III. Position of zero field transitions of different sets of CCMV preparations. Excitation was with high pressure mercury lamps (150 Watt) through Kasha filters. The sweep rate was 25 MHz/sec and T = 1.2 K. In the experiments summarized here sets of two conformational states of the virus coat protein were compared simultaneously by sweeping through the microwave transition and using one sweep generator.

		detection	$\|D\|-\|E\|$ (GHz)	fwhm(MHz)	$2\|E\|$ (GHz)	fwhm(MHz)
a. virus	pH 5.0 + 0.2 M NaCl	410 nm	1.64	210		
protein	pH 5.0 + 1.0 M NaCl	410 nm	1.69	190		
b. virus	pH 5.0 + 0.2 M NaCl	410 nm	1.62	190		
protein	pH 5.0 + 1.0 M NaCl	410 nm	1.65	175		
c. virus	pH 5.0 + 0.2 M NaCl	440 nm	1.64	200		
protein	pH 5.0 + 1.0 M NaCl	440 nm	1.68	170		
d. virus	pH 5.0 + 0.2 M NaCl	440 nm	1.62	185	2.69	250
protein	pH 5.0 + 1.0 M NaCl	440 nm	1.67	215	2.61	280

be caused by statistical fluctuations in the environment of each of the tryptophanyl residues [19] . This large width severely complicates the observation and interpretation of changes in the environment of the tryptophanyl residues, which are caused by a change in protein-RNA interaction.

4.5. DISCUSSION

The spectroscopic properties of the tryptophan residues in CCMV were investigated at low temperatures, 77 and 1.2 K. The results yield both additional and contradicting information upon comparison with the fluorescence experiments on CCMV [7]. From the fluorescence properties of CCMV at $4^{\circ}C$ it was concluded that the emitting tryptophanyl residues are located in a rather polar environment. It was also observed that at least two of the three tryptophanyl residues are exposed to the aqueous solvent. A decrease in interaction between RNA and the protein results in an enhancement of the fluorescence and a shift of the emission maximum to higher wavelengths. These results are explained by assuming that some of the tryptophanyl residues, originally quenched by the presence of the RNA, become fluorescent and exposed to the solvent, when the protein-RNA interaction decreases.

The fluorescence results seem to contradict with the phosphorescence spectra of the coat protein of CCMV. The maxima of the phosphorescence spectra show no observable shifts upon swelling and dissociation of the virus. The position of these maxima (413 and 440 nm) should be attributed to tryptophanyl residues

buried in a apolar environment [11, 19]. However, the polarity of the environment itself has only a minor influence on the phosphorescence characteristics of the tryptophanyl residues at 77 K. The solvent molecules around the chromophoric group cannot reorientate in a rigid matrix after excitation. A more important factor determining the phosphorescence is the possibility of hydrogen bond formation between the proton on the imino group of the indole ring and groups in the protein or of the solvent molecules. Konev [10] pointed out that this H-bond may decrease the intensity of the phosphorescence of tryptophan relative to the fluorescence. Thus it might be expected that because of hydrogen bond formation the phosphorescence of the exposed residues is quenched relative to the emission of the residues unable to form hydrogen bonds. This may explain the red shift of the phosphorescence, since delayed emission is dominated by the buried residues [11, 19].

Another factor to be considered, is the electrical polarizability of the environment of the tryptophanyl residues. A large polarizability may cause a red shift in the phosphorescence maximum [19]. Especially the aromatic amino acid residues and the nucleotides, having high mobile π electron densities, may show a large polarizability.

A possibility that cannot be excluded as an explanation of the unexpected phosphorescence results is a conformational change that is caused by a lowering of the temperature in order to obtain a rigid solution. A decrease of the entropy contributions to the interaction energies in the protein may be responsible for these changes.

The ODMR results show, in contrast to the phosphorescence emission, some differences in the zero field transitions of the virus and the protein in different conformations. The $|D|-|E|$ transition of the stable virus is characterized by a large resonance line width (Fig. 2, Table II and III). The transition seems to be composed of two contributions. A decrease of interaction between protein and RNA reduces the low frequency contribution in the signal, relative to the high frequency part. In the $2|E|$ transition the contribution at the high frequency side is reduced upon dissociation of the virus. These results may be understood, assuming that the removal of the RNA lowers the polarizability of the environment of the tryptophanyl residues, which become more exposed to the solvent.

A decrease in $|D|$ may be explained by an increase in the distance between the two unpaired electrons of the triplet wavefunction. This can be caused by a

contact between the excited chromophores and molecules in the environment. The admixing of triplet wavefunctions of the surrounding molecules results in a slight delocalization of the electrons in the excited triplet state. The red shift in the phosphorescence maxima, which is caused by the resulting stabilization of the triplet states, can thus be accompanied by a decrease in $|D|$. From a comparison of the phosphorescence maxima and the observed $|E|$ value it can be concluded that the red shift in phosphorescence generally results in larger $|E|$ values [24, 25, 26, 27].

In some experiments on virus solution, a zero field transition was observed at approximately 1.55 GHz, upon detection at 388 nm. Since the zero field transitions of tyrosine are all above 2 GHz, the origin of this transition must be looked for elsewhere. A comparison with the studies of Co and Maki [28] learns that nucleotides such as adenine may be responsible for this resonance. At high microwave powers (50 mW) a shoulder at 1.37 GHz appeared in the virus solutions at pH 5.0 and low ionic strength. The situation was not investigated for other conformational states of the virus. This observation can be explained by assuming that the tryptophan zero field transitions become saturated at high microwave powers, while another species with a different relaxation behaviour and a weak phosphorescence becomes visible. The possibility that this resonance is originating from a tryptophan-nucleotide interaction has to be investigated further, although the position of this resonance seems to exclude a tryptophan-adenine complex [28].

The simultaneous occurrence of the different effects may interfere and complicate the interpretation of the final effects on fluorescence and phosphorescence spectral data and on the zero field splitting parameters $|D|$ and $|E|$. The comparison of the results of the different techniques may be helpful in the elucidation of the structural properties of the protein in the environment of tryptophan. At this moment only a few of such studies were carried out on model compounds and well characterized proteins. The seemingly contradicting observations, made with CCMV, also occur in other proteins. Bovine serum albumine for instance has characteristics, that are very much the same as found for CCMV with the techniques mentioned here [10, 11, 29]. Comparison of the tryptophan environments in these two proteins may be helpful means in the understanding of the spectral properties of CCMV.

4.6. REFERENCES

1. Bancroft, J.B. (1970) Adv. Vir. Res. 16, 99-134.
2. Lane, L.C. (1974) Adv. Vir. Res. 19, 151-220.
3. Finch, J.T. and Bancroft, J.B. (1968) Nature 220, 815-816.
4. Adolph, K.W. and Butler, P.J.G. (1977) J. Mol. Biol. 109, 345-357.
5. Chauvin, C., Pfeiffer, P., Witz, J. and Jacrot, B. (1978) Virology 88, 138-148.
6. Pfeiffer, P. and Hirth, L. (1974) Virology 58, 362-368.
7. Krüse, J., Verduin, B.J.M. and Visserm A.J.W.G. (1979) Eur. J. Biochem. 95, 21-29.
8. Bancroft, J.B., Rees, M.W. and Short, M.N. (1971) Virology 45, 707-715.
9. Burstein, E.A., Vedenkind, N.S. and Ivkova, M.N. (1973) Photochem. Photobiol. 18, 263-279.
10. Konev, S.V. (1969) Fluorescence and Phosphorescence of Proteins and Nucleic Acids, Plenum Press, New York.
11. Longworth, J.W. (1971) in: Excited states of Proteins and Nucleic Acids, (Steiner, R.F. and Weinryb, I. eds.), Plenum Press, New York.
12. Galley, W.C. in: Biochemical Fluorescence, Concepts, (Chen, R.F. and Edelhoch, H. eds.), Vol. 2, pp 409-439, Marcel Dekker, Inc., New York.
13. Maki, A.H. and Zuclich, J.A. (1975) Topics in Current Chemistry 54, 115-163.
14. Verduin, B.J.M. (1978) J. Gen. Virol. 39, 131-147.
15. Verduin, B.J.M. (1974) FEBS Lett. 45, 50-54.
16. Schmidt, J. (1971) Modulation of Phosphorescence by Microwaves, thesis University of Leiden.
17. Schmidt, J., Antheunis, D.A. and Van der Waals, J.H. (1971) Molecular Physics 22, 1-17.
18. Passner, A., McCall, S.L. and Leventhal, M. (1976) Rev. Sci. Instr. 9, 8121-8124.
19. Purkey, R.M. and Galley, W.C. (1970) Biochemistry 9, 3569-3575.
20. Herzog, M., Gerard, D., Hirth, L. and Laustriat, G. (1977) Biochim. Biophys. Acta 493, 167-177.
21. Guttenplan, J.B. and Calvin, M. (1973) Biochim. Biophys. Acta 322, 294-300.
22. Magne, A., Gerard, D., Hirth, L. and Laustriat, G. (1977) Biochim. Biophys. Acta 495, 189-194.

23. Maki, A.H. (1977) Biophys. J. 19, 78-80.
24. Zuclich, J., Schweitzer, D., and Maki, A.H. (1973) Photochem. Photobiol. 18, 161-168.
25. Ugurbil, K., Maki, A.H. and Bersohn, R. (1977) Biochemistry 16, 901-907.
26. Maki, A.H. and Co, T. (1976) Biochemistry 15, 1229-1235.
27. Ross, J.B.A., Rousslang, K.W., Deranleau, D.A. and Kwiram, A.L. (1977) Biochemistry 16, 5398-5402.
28. Co, T. and Maki, A.H. (1978) Biochemistry 17, 182-186.
29. Zuclich, J., Schweitzer, D. and Maki, A.H. (1972) Biochem. Biophys. Res. Commun. 46, 1764-1768.

5. FLUORESCENCE OF COWPEA CHLOROTIC MOTTLE VIRUS MODIFIED WITH PYRIDOXAL-5'-PHOSPHATE

5.1. SUMMARY

Cowpea chlorotic mottle virus (CCMV), which is stable at pH 5.0, has been modified at this pH with 0.5-0.7 pyridoxal-5'-phosphate (PLP) molecules per protein subunit. The fluorescence properties of the labelled CCMV-protein in different aggregation states of the virus provide information about the labelled part of the protein and the changes induced in its environment, when the nucleoprotein particles are swollen or dissociated. Fluorescence excitation- and emission spectra indicate the presence of radiationless energy transfer from the aromatic amino acid residues to the label. Comparison of the fluorescence lifetimes of the labelled and the unlabelled protein confirms the existence of energy transfer.

The mobility of the labelled part, which can be estimated from the fluorescence polarization of PLP, is higher than expected from the dimensions of the virus and the protein subunits. Polarization values and the fluorescence lifetimes depend on the presence of small amounts of NaCl or $MgCl_2$ in the buffer solution at pH 7.5. This is due to structural changes in the vicinity of the PLP-label of the RNA and of the protein part.

5.2. INTRODUCTION

Cowpea chlorotic mottle virus, a spherical plant virus, belongs to the group of bromoviruses [1,2]. The viruses have a divided genome [3]. The nucleoprotein particles have a diameter of about 28 nm and are built from 180 identical protein subunits, arranged in an icosahedral shell [4]. M_r of a protein subunit of CCMV is 19,400. Two nucleoprotein particles contain one RNA strand with M_r of approximately 1.2 and 1.1 million respectively. The third particle has two smaller RNA molecules of M_r 0.8 and 0.3 million.

The virus particles are stable at pH 5.0 and low ionic strength ($I < 0.1$). An increase of the ionic strength at this pH reduces the radial extension of the RNA in the nucleoprotein [5] and the interaction between the protein subunits and

the RNA [6,7]. At pH 7.5 and low ionic strength the nucleoprotein particles swell. This swelling can be partly prevented by the addition of divalent cations [8] or higher amounts of monovalent cations [5]. These ions may bind to the RNA, to the protein or between those compounds. In this way charged groups are neutralized and the swelling due to repulsion between equally charged groups is reduced [9]. An increase of ionic strength at pH 7.5 to 1.0 M NaCl leads to a dissociation of the virus particles into RNA [2] and protein dimers [10]. Empty protein particles (pseudo top) can be made by dialysis of a solution of protein dimers against buffer of pH 5.0 and 1.0 M NaCl [11]. The architecture of the shell is similar to the nucleoprotein coat [4], but the particles have a different surface charge [12].

The N-terminal region of the protein subunits of the bromoviruses is important in the stabilization of the virus particles at pH 7.5. The swollen particles at pH 7.5 are sensitive to a treatment with trypsin [13]. At the N-terminus 25 amino acid residues are cleaved off by trypsin and this causes a collapse of the virus particles. Similar observations were made for BMV [14].

In CCMV there are 12 lysyl residues per protein subunit [12,18] and three of them are located in the N-terminal part that is cleaved off by trypsin digestion.

Pyridoxal-5'-phosphate is a compound frequently used in the investigation of the role of lysyl residues in proteins [15]. From fluorescence properties of the protein labelled with PLP, information can be obtained about the position and the environment of the label [16] and about the internal and overall mobility of the labelled protein [17].

In this paper we describe the fluorescence properties of cowpea chlorotic mottle virus that has been labelled with pyridoxal-5'-phosphate. The PLP was covalently attached to CCMV in the compact conformation at pH 5.0. The changes in the fluorescence of the labelled virus (PLP-CCMV), when this is brought into different states of aggregation may provide additional information about the structural changes, that play a role in the mechanism of dissociation and assembly.

5.3. MATERIALS AND METHODS

5.3.1. Virus

CCMV was isolated from 7-day-infected cowpea leaves as described by Verduin [19]. The coat protein was prepared according to the $CaCl_2$-method [11].

5.3.2. Reaction of CCMV with PLP

CCMV was labelled with PLP following the procedure of Schnackerz and Noltman [20]. Virus (6.5 mg/ml) was incubated at $4^{o}C$ in the dark in the presence of 50 mM sodium acetate, pH 5.0, 10 mM $MgCl_2$ and 1 mM EDTA and a 35-fold molar excess of PLP as compared with the protein subunit concentration. After one hour the reaction mixture was diluted 25 times with the same buffer (without PLP) and subsequently a freshly prepared solution of 0.6 M sodiumborohydride (BDH) was added in portions of 10 µl until the yellow colour of the reaction mixture had disappeared completely. In this procedure the pH of the virus solution was never above pH 5.5. Labelled virus was separated from the reaction products by dialysis against several changes of 50 mM sodium acetate buffer containing 1 mM EDTA and 10 mM $MgCl_2$ and the complete removal of unbound PLP was checked by monitoring the fluorescence of the dialysis buffer. For the fluorescence experiments the virus solution was dialyzed against 20 mM sodium cacodylate and 1 mM EDTA, pH 5.0 and pH 7.5, in the presence of various concentrations of NaCl or $MgCl_2$.

The number of the PLP molecules per coat protein subunit was estimated from the extinction of the labelled virus at 260 and 325 nm, assuming for CCMV: $E^{1\%}_{260\ nm} = 58.5$ [2] and a molar extinction coefficient of PLP at 325 nm of 10,000 [21-24].

5.3.3. Absorption

Absorption spectra were measured with a Cary 14 spectrophotometer, equipped with a thermostated cuvette holder.

5.3.4. Fluorescence

Fluorescence emission and excitation spectra were recorded on a MPF 2A Hitachi Perkin Elmer spectrofluorometer, in which the cuvettes can be thermostated.

The spectra were not corrected for variations in detection and excitation wavelengths.

Polarization values were determined with an apparatus, built according to the design of Weber and Bablouzian [25]. The polarization values were corrected according to a method described by Azumi and McGlyn [26], using the equation

$$P = \frac{V_v - H_v\ (V_h/H_h)}{V_v + H_v\ (V_h/H_h)}$$

where V denotes the vertical and H the horizontal plane of polarization upon detection. The subscripts refer to the direction of polarization of the excitation. The excitation was at 330 nm (fwhm 10 nm) and detection was through a set of Schott Filters: GG385 + BG1 (λmax 425 nm, fwhm 85 nm), to remove the first and second order light of the excitation source. The accuracy of the determined polarization values was better than 0.005. The lifetimes of the PLP-fluorescence and the protein emission were obtained with a phase-fluorometer [27,28] operating at 60 Mc. Excitation light was selected with a Jarrell-Ash 0.25 m Ebert monochromator (Model 82.410) with slits of 2 mm (fwhm = 3.2 nm). In the detection light path a GG385 + BG1 filter combination was used for PLP fluorescence (see polarization) and a WG320 + UG1 (Schott, λmax = 365 nm, fwhm = 52 nm) for the protein fluorescence.

The lifetime of the PLP fluorescence was also determined with single photon counting at 10°C. The fluorescence decay curves were obtained with an apparatus as described previously [7]. A flash in air (1 atm) was used from which most of the strong 337 nm N_2-emission was isolated by an Eppendorf 334 interference filter. For detection the bandwidth of the 0.25 m Applied Photophysics monochromator was set on 10 nm. The detection was at 395 nm. To determine the response function of the apparatus a degassed solution of 2,5-diphenyloxazole (PPO, Eastman Kodak) in cyclohexane (Merck, Uvasol) was used as a reference compound. The lifetime of this compound, determined with the phase-fluorometer operating at 60 MHz, was 1.36 ns. The data were analyzed using a method described elsewhere [7]. In the experiments described here the decay law is assumed to be

$$I\ (t) = \sum_{j=1}^{n} \alpha_j\ e^{-\ t/\tau_j} \qquad \text{with n = 2 (bi-exponential).}$$

All fluorescence experiments were performed at 4°C unless indicated otherwise with a nucleoprotein concentration of approximately 0.25 mg/ml.

5.3.5. General properties of CCMV labelled with PLP

Labelled CCMV was characterized by electron microscopy, gel electrophoresis, sedimentation analysis and infectivity tests following the procedures as described by Verduin [19].

5.4. RESULTS

5.4.1. Reactivity of CCMV towards PLP and general properties of PLP-CCMV

CCMV was incubated at pH 5.0 with increasing concentrations of PLP, varying the molar ratio of PLP to protein subunits from 10 to 200. Under these conditions a maximum number of 1.2 ± 0.1 PLP molecules per protein subunit could be introduced. For the fluorescence experiments CCMV containing 0.5 to 0.7 PLP molecules per protein subunit, was used. This compound is designated as PLP-CCMV. The modification of CCMV with PLP neither did change the sedimentation coefficient, the infectivity and the appearance in the electron microscope nor the electrophoresis of RNA and protein in SDS polyacrylamide gels.

5.4.2. Fluorescence properties of PLP-CCMV

Excitation and emission of PLP-CCMV were determined for the virus in different conformational states. In Fig. 1 these spectra are shown for PLP-CCMV at pH 5.0 (stable virus) and in 1.0 M NaCl at pH 7.5 (dissociated virus). There is an increase in fluorescence of the protein upon dissociation and this is partly caused by weakening of interaction between RNA and some tryptophanyl residues [7]. With stable virus preparations next to the protein emission at about 315 and 340 nm a shoulder at 390 nm can be observed. This emission must be attributed to the PLP label. As judged from excitation spectra of pyridoxaminephosphate (not shown) and labelled nucleoprotein, selective excitation of the aromatic amino acid residues in the protein without excitation of PLP, is difficult to realize. To get at least a qualitative picture of changes in energy transfer from the tryptophanyl and tyrosyl residues to PLP, it is more useful to extract information from the lifetimes of the protein fluorescence.

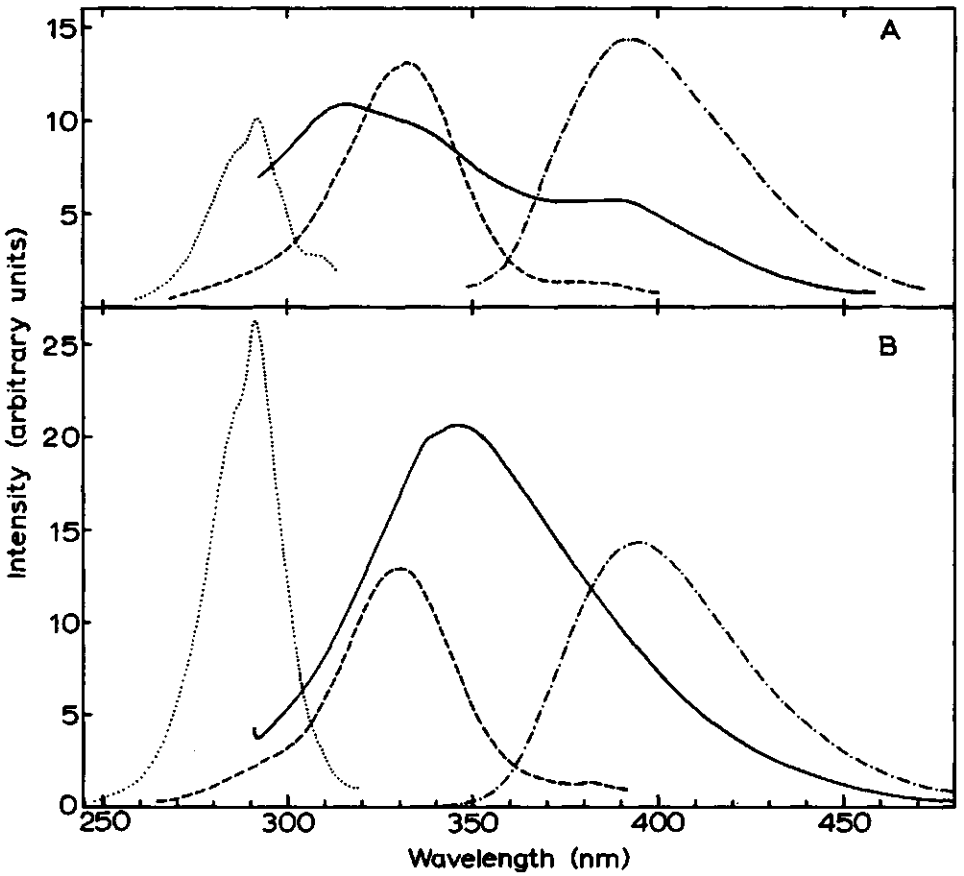

Fig. 1. Excitation and emission spectra of CCMV labelled with PLP.
The bandwidth was for detection 4 nm and for excitation 3 nm.
A) pH 5.0, stable virus particles; detection at 345 nm (.....), excitation at 285 nm (———), detection at 440 nm (-----) and excitation at 330 nm (-.-.-.-.).
B) idem for pH 7.5 + 1.0 M NaCl, dissociated virus.

5.4.3. Energy transfer

From excitation spectra of the PLP emission and from protein emission spectra (Figs. 1 A and B and Ref. 7) the existence of a considerable overlap between absorption of PLP and emission of CCMV-protein is observed. The efficiency of electronic energy transfer is defined by Förster [29] as:

$$E = \frac{1}{1 + (\frac{r}{R_o})^6} \qquad \text{where}$$

r = distance between donor and acceptor and R_o = the Förster critical distance, where E is 0.5. R_o depends among other things on spectral overlap of donor emission and acceptor absorption and on relative orientation of donor and acceptor. Churchich [16,30] estimated the R_o for energy transfer from tryptophan to PLP for five different proteins to be in the range of 1.6 to 2.4 nm. Since the quantum yield of the protein fluorescence depends on the conformation of the nucleoprotein particles [7], the critical distance R_o is slightly affected (to about 16% increase in the case of complete dissociation). The amount of energy transfer can be estimated from the quantum yield or the lifetime of the donor fluorescence in the absence (Q_o, τ_o) and in the presence (Q, τ) of the energy acceptor. The efficiency can be written as:

$$E = 1 - \frac{\tau}{\tau_o} = 1 - \frac{Q}{Q_o} \qquad [31]$$

Using 292 nm excitation the lifetime of the PLP-CCMV protein fluorescence is under all circumstances shorter than that of the unlabelled nucleoprotein (Fig. 2). At pH 5.0 no large changes in lifetime occur upon increasing the NaCl concentration to 1.0 M or addition of 0.01 M $MgCl_2$. At pH 7.5 the presence of various amounts of NaCl or $MgCl_2$ in the buffer strongly influences the fluorescence lifetimes of the labelled protein. At low ionic strength addition of 0.01 M $MgCl_2$ reduces this lifetime, probably because of a more efficient energy transfer from the aromatic residues to PLP, when the swelling of the particles is reduced. The same effect, although less pronounced, is observed upon addition of 0.2 M NaCl. A further increase in ionic strength, causing dissociation of the virus into coat protein dimers and RNA, results in longer lifetimes.

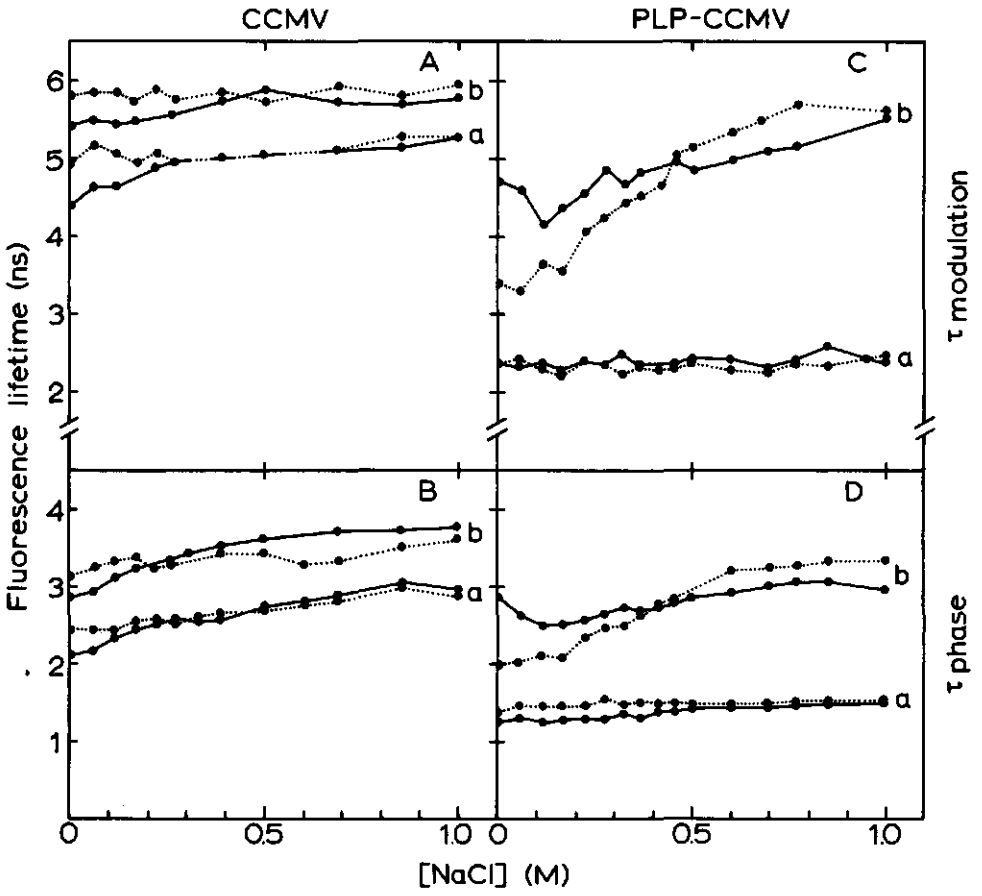

Fig. 2. Dependence of the protein lifetime fluorescence on ionic strength and the presence of divalent cations.
A and B refer to the situation for unlabelled CCMV and C and D to CCMV labelled with PLP (PLP-CCMV). The lifetimes are determined with phase fluorometry from changes in modulation (A and C) and phase shifts (B and D).
The solid lines are measured in the absence and the dotted lines in the presenece of 0.01 M $MgCl_2$.
a) CCMV at pH 5.0 and b) at pH 7.5. See M & M for experimental details.

Titration of a nucleoprotein solution (PLP-CCMV) at pH 7.5 with $MgCl_2$ caused a decrease of the fluorescence lifetime, indicating that at pH 7.5 the change in fluorescence lifetime is reversible (Fig. 3).

At pH 7.5 the differences between the fluorescence lifetimes of unlabelled (Fig. 2 A and B) and labelled protein solutions (Fig. 2 C and D) are relatively smaller than at pH 5.0.

Since an increase in transfer efficiency results in shorter lifetimes, the last observation must be explained by a more efficient energy transfer at pH 5.0.

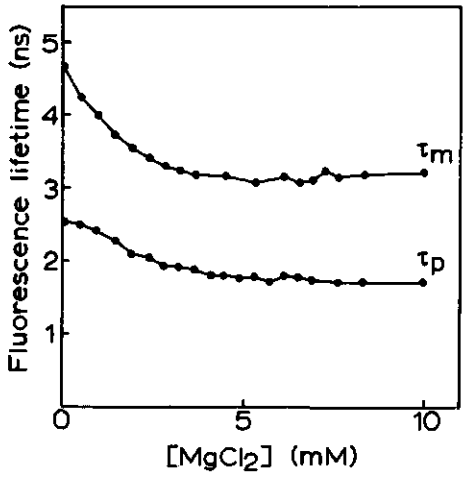

Fig. 3. Variation of fluorescence lifetimes with varying concentrations of $MgCl_2$.
The lifetimes, τ_m (modulation) and τ_p (phase), measured with a phase fluorometer, were determined for PLP-CCMV at pH 7.5 and low ionic strength ($I < 0.1$).

5.4.4. PLP fluorescence lifetimes

The fluorescence lifetimes of PLP have been determined in two ways: from single photon counting (Table I) and from phase fluorometry (Table II). We have to conclude that under all circumstances the decay is composed of more than one lifetime. Apart from this heterogeneity a slight decrease of fluorescence lifetimes of PLP is observed upon raising the pH. For the interpretation of the polarization experiments (next section) the slight variations in lifetimes have no consequences.

5.4.5. Polarization of PLP

Polarization experiments provide information about the mobility of the part of the protein, that contains the PLP-label. The polarization values (P) are summarized in Fig. 4.

The label in the stable virus particles at pH 5.0 shows a degree of polarization of 0.29, independent of ionic strength or the presence of $MgCl_2$. This value, lower than expected for a virus particle of this size, can only be ex-

Table I Fluorescence lifetimes of PLP determined with single photon counting. Excitation wavelength is 337 nm, emission wavelength 295 nm. The decay function $I(t) = \sum_{i=1}^{n} \alpha_i e^{-t/\tau_i}$ was analyzed in two components. $\langle\tau\rangle$ is the averaged lifetime and χ^2 is a function of the deviation between the measured and the calculated decay curve. A_i is defined as $\alpha_i\tau_i$. For further details see Krüse et al. [7] and Materials and Methods.

condition	A_1	τ_1(ns)	A_2	τ_2(ns)	$\langle\tau\rangle$(ns)	χ^2
pH 5.0	0.26	0.70	0.74	4.20	3.29	8.8
pH 5.0 + 0.01 M $MgCl_2$	0.20	0.51	0.80	3.97	3.29	9.0
pH 7.5	0.25	0.81	0.75	3.19	2.6	2.4
pH 7.5 + 0.01 M $MgCl_2$	0.18	0.50	0.82	3.48	2.95	9.0
pH 7.5 + 1.0 M NaCl	0.19	0.46	0.81	3.24	2.69	5.2

Table II PLP fluorescence lifetimes determined with phase fluorometry. Nucleoprotein solutions (approximately 0.25 mg/ml) were excited at 312 nm, fwhm = 3.2 nm and fluorescence was detected at 425 nm (see M & M). τ_{phase} is the lifetime determined from the phase shift and $\tau_{modulation}$ from changes in depth of modulation.

condition	τ_{phase} (ns)	$\tau_{modulation}$ (ns)
pH 5.0	2.6	3.7
pH 5.0 + 0.01 M $MgCl_2$	2.6	3.6
pH 7.5	2.6	3.4
pH 7.5 + 0.01 M $MgCl_2$	2.2	3.2

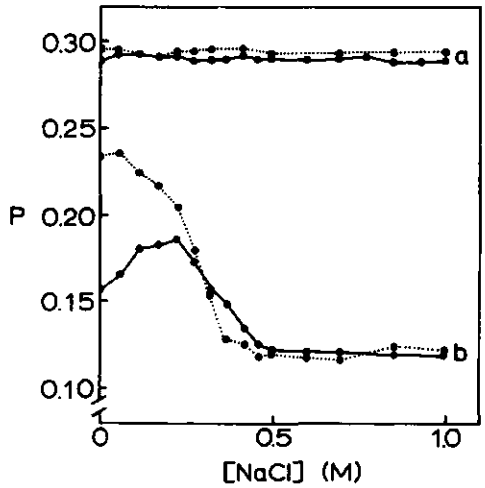

Fig. 4. Polarization of the PLP fluorescence.
The degree of polarization (P) of PLP-CCMV was measured at various ionic strengths in the absence (———) and in the presence of 0.01 M $MgCl_2$ (.....) at pH 5.0 (a) and pH 7.5 (b).

plained, when a local mobility of the labelled part is assumed.

At pH 7.5 and low ionic strength (I < 0.1) where the virus is swollen, P is reduced to 0.16 in the absence and to 0.235 in the presence of 0.01 M $MgCl_2$, when the virus is partially swollen. Upon addition of $MgCl_2$ to a solution without divalent cations the value can be raised to 0.235, indicating that the depolarization process is reversible. Adding 0.2 M NaCl instead of 0.01 M $MgCl_2$ also increases the polarization value, but only to 0.19. Higher NaCl concentrations cause dissociation of the virus and the polarization is lowered to 0.12-0.13.

Empty protein shells (PT) in 1.0 M NaCl at pH 5.0, that were prepared from labelled nucleoprotein particles, showed a degree of polarization of 0.22. This value is lower than that of stable virus particles (0.29) indicating another environment of PLP in PT as compared to stable nucleoprotein particles. A lower value (0.23) was also observed with nucleoprotein particles at pH 5.0, which had previously been swollen at pH 7.5 (0.16).

A solution of pyridoxamine-phosphate in glycerol (v/v > 95%) at 0°C showed a degree of polarization of 0.415 which is in good agreement with the value found by Irwin and Churchich [17]. When the PLP is rigidly bound to the virus particles, this should result in a similar high value of the degree of polarization of the labelled nucleoprotein, as can be determined from the Perrin equation:

$$\left(\frac{1}{P} - \frac{1}{3}\right) = \left(\frac{1}{P_o} - \frac{1}{3}\right)\left(1 - \frac{\tau_{flu}}{\tau_c}\right) \qquad [32]$$

Here P_o and P are the limiting and the actual polarization respectively and τ_{flu} is the fluorescence lifetime. $\tau_c = \frac{\eta V}{kT}$, the rotational correlation time for a spherical particle is determined by the volume of the sphere, the absolute temperature (T) and the viscosity of the solvent (η). At 4^oC, taking a diameter of 28 nm for the nucleoprotein particles, we calculate a value of τ_c = 4710 ns. Taking τ_{flu} = 3 ns, the estimated average lifetime of PLP, an actual polarization of almost 0.415 can be expected. In 1.0 M NaCl, pH 7.5 the virus is dissociated into protein dimers and RNA [10]. The volume and the resulting τ_c of the dimers can be estimated respectively from BMV neutron scattering data (τ_c = 27 ns) [5], from the rough approximation, that V dimer = $\frac{1}{90}$ V virus (τ_c = 52 ns) and from the molecular weight (38,800) and the partial specific volume $\bar{v}$ (0.73) resulting in τ_c = 19.3 ns. This should result in a depolarization from 0.415 (theoretical value for stable virus) to 0.38 ± 0.015 or from 0.29 (experimental value) to 0.265 ± 0.010. The actual measured value for the dimer polarization (0.12) is much lower and this indicates a local mobility of the protein part that contains the PLP-label.

The extent of this internal motion has been investigated, using a method developed by Weber [33]. It has been applied to labeled γ-globulin by Wahl and Weber [34] and to lysozyme by Irwin and Churchich [17]. Weber showed that in the case of a local motion, it is possible to estimate the rotational correlation times, that are associated with the different mobilities. The equation used is:

$$\left(\frac{1}{p} - \frac{1}{3}\right) = \left(\frac{1}{p_o} - \frac{1}{3}\right) \cdot \frac{1}{f}\left(1 - \beta_h T/\eta - \frac{1-f}{1 + f\,\beta_s\, T/\eta}\right)$$

β is related to τ_c in the following way: $\beta . T/\eta = \frac{\tau_{flu}}{\tau_c}$.

Variation of the viscosity (η) by adding sucrose and plotting $\left(\frac{1}{p} - \frac{1}{3}\right)$ vs T/η (Fig. 5) can be used to determine β_h, β_s and f [34]. Following this procedure, we find for the intact nucleoprotein particles at pH 5.0 a long τ_c of 33 ns and a short τ_c of less than 0.1 ns.

For the coat protein dimer solution at pH 7.5 and high ionic strength it is difficult to analyze the plot in more than one rotational correlation time. Here an averaged τ_c of 1.25 ns is calculated.

In principle the observed decrease of the fluorescence lifetime of PLP upon raising pH should result in a higher degree of polarization. However a distinct depolarization was observed upon swelling, which must be explained completely by a higher mobility.

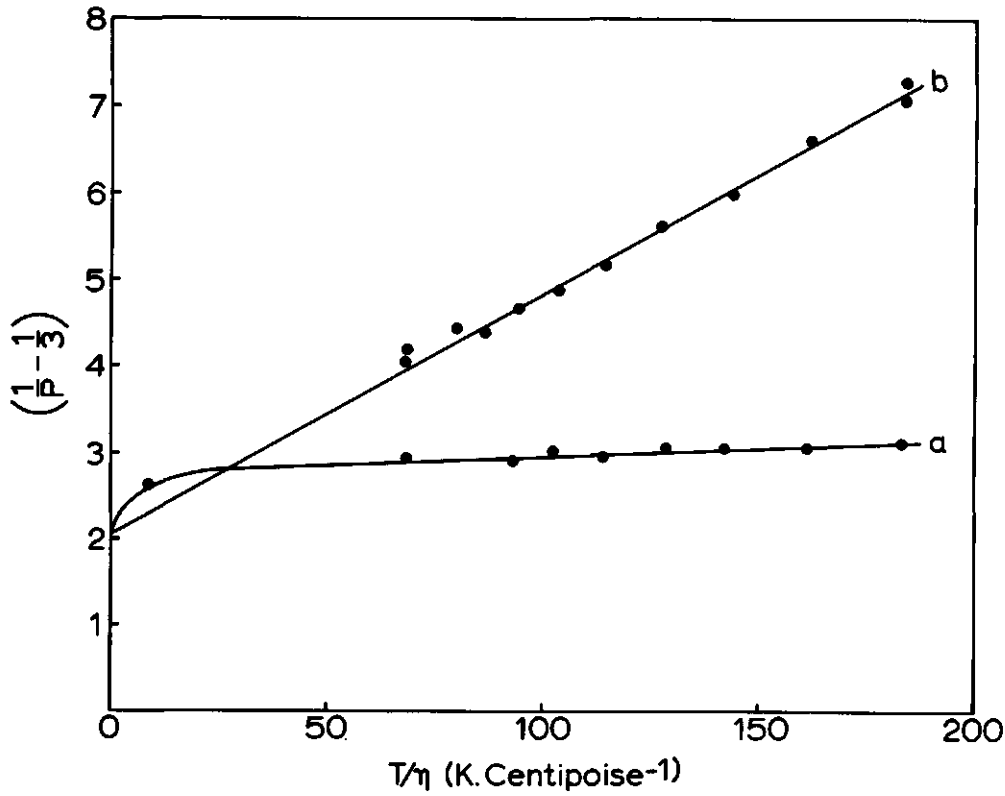

Fig. 5. Variation of the degree of polarization of PLP-CCMV with the viscosity of the solvent.
The viscosity was changed by addition of different amounts of a 60% sucrose solution (w/v).
a) pH 5.0, stable virus particles
b) pH 7.5 + 1.0 M NaCl, dissociated virus

5.5. DISCUSSION

The changes in conformation of the nucleoprotein particles are reflected in the polarization values of the PLP fluorescence and in the protein fluorescence lifetimes of the labelled protein of the virus particles. For an appropriate interpretation of the results obtained with PLP-CCMV, it is necessary to know the maximum number of sites per protein subunit, that can be labelled with PLP. Although 12 lysyl residues are present in a protein subunit, never more than about 1.2 molecules of PLP per protein subunit can be introduced, even

after long incubations with high concentrations of PLP. Accurate determination of the content of PLP in the protein is difficult because of the low extinction of PLP compared to the light scattering and absorption of the nucleoprotein.

CCMV was labelled at pH 5.0 in order to bind PLP to ε-NH_2 groups of lysyl residues [15,35,36], which are presumably not participating in protein-protein and protein-RNA interactions. The position of the PLP in the amino acid sequence of the coat protein has not yet been determined.

The presence of the phosphate group in pyridoxal-5'-phosphate is necessary for the reaction of PLP with CCMV. Attempts to label the protein with pyridoxal were not successful. Variation of the phosphate concentration in the acetate buffer between 0 and 0.1 M keeping the pH at 5.0 did not influence the labelling with PLP or pyridoxal in a detectable way.

When at pH 5.0 the mono- or divalent cation concentrations are changed, no variation in the environment and mobility of the labelled part of the protein is observed. Therefore PLP is not present in that part of the protein molecule, which is involved in protein-nucleic acid interaction. The fluorescence of part of the tryptophanyl residues located in this part increases, when the monovalent cation concentration increased at pH 5.0 [7]. This is interpreted as a contraction of the RNA within the nucleoprotein particle [5,6,37], thereby reducing the protein-RNA interaction. At high ionic strength at pH 5.0 the salt linkages between RNA and the charged amino acid residues are weakened, while the protein-protein interactions, which are at least partly hydrophobic in nature, are stabilized.

In the swollen nucleoprotein particles at pH 7.5 we observe a change in mobility and environment of the PLP label. The effects on PLP that accompany the raise of pH, can partially be prevented by the addition of 10 mM $MgCl_2$ and to a smaller extent by addition of 0.2 M NaCl. Mono- and divalent cations do influence the conformation of RNA within virus particles [38] thereby preventing the action of ribonucleases on RNA within the nucleoprotein particles [12]. Also the conformation of extracted viral RNA is influenced by addition of mono- and divalent cations to the buffer solution [39]. The concentrations needed to induce the latter changes are comparable to the cation concentrations used to influence the fluorescence of PLP-CCMV. The role of RNA therefore appears to be evident. The cations may also bind to the protein or to a binding site formed by phosphate groups of the RNA and one or more negatively charged amino acid residues. In this way charged groups, that cause repulsion and swelling, will be neutralized.

The increase in mobility of PLP exactly parallels the swelling process of the virus particle. This suggests that the PLP molecule is sterically hindered

by the neighbouring protein subunits. This hindering should gradually be abolished, when the protein subunits are shifted to a configuration with a higher radius during the swelling process and when the virus dissociates into protein dimers and RNA. It is also possible that both position and mobility of the PLP is restricted by the presence of the RNA in the nucleoprotein. A change in the orientation of the RNA towards the protein subunits in the swollen particles may induce a change in the conformation of the subunits and thus influence the environment of the PLP. The absence of these effects at pH 5.0 should be a consequence of the compact conformation of the protein coat, which prevents changes in the PLP environment. The increase in protein fluorescence lifetimes of PLP-CCMV upon swelling of the virus can be explained by a lower efficiency of energy transfer from tryptophan and tyrosine to PLP, due to an average increase in distance between these residues and PLP.

The N-terminal region of approximately 25 amino acid residues contains 3 lysine residues and is rapidly cleaved off by the action of trypsin at pH 7.5 [13,40]. From these experiments and from digestion experiments on BMV [14] the conclusion can be drawn that the N-terminus of the coat protein is essential in the maintenance of the nucleoprotein conformation at pH 7.5. However, preliminary experiments to determine the position of the PLP in the protein molecule indicate the absence of PLP in this N-terminal region.

The differences in the PLP-polarization values of stable virus particles and empty protein shells, made of protein isolated from PLP-CCMV, suggest a difference in quaternary structure of the two types of particles. It is known that the surface charge of the pseudo top empty shell is less negative than that of the nucleoprotein particle [12] and that the diameter of the shell is larger than that of the nucleoprotein particle [5]. Based on the latter results, we suggest that for a correct reassembly of the protein and the RNA, it is necessary to bring the protein subunits into the proper conformation. This may be accomplished by binding of RNA to the protein, thus affecting the protein conformation. Also the presence of mono- and divalent cations can influence the conformation of the RNA and as a consequence the protein structure. Because of the absence of the RNA in the formation of the empty protein shell, the protein subunits in the PT will exist in a conformation different from that in the undissociated nucleoprotein particles.

5.6. REFERENCES

1. Bancroft, J.B. (1970) Adv. Vir. Res. 16, 99-134.
2. Lane, L.C. (1974) Adv.Vir.Res. 19, 151-220.
3. Bancroft, J.B. and Flack, I.H. (1972) J.Gen.Virol. 15, 247-251.
4. Finch, J.T. and Bancroft, J.B. (1968) Nature 220, 815-816.
5. Chauvin, C., Pfeiffer, P., Witz, J. and Jacrot, B. (1978) Virology 88, 138-148.
6. Pfeiffer, P. and Hirth, L. (1974) Virology 58, 362-368.
7. Krüse, J., Verduin, B.J.M. and Visser, A.J.W.G. (1979) Eur.J.Biochem. 95, 21-29.
8. Jacrot, B., Pfeiffer, P. and Witz, J. (1976) Phil.Trans.R.Soc.Lond. B 276, 109-112.
9. Pfeiffer, P. and Durham, A.C.H. (1977) Virology 81, 419-432.
10. Adolph, K.W. and Butler, P.J.G. (1977) J.Mol.Biol. 109, 345-357.
11. Verduin, B.J.M. (1974) FEBS Letters 45, 50-54.
12. Bancroft, J.B., Hiebert, E., Rees, M.W. and Markham, R. (1968) Virology 34, 224-239.
13. Tremaine, J.H., Agrawal, H.O. and Chidlow, J. (1972) Virology 48, 245-254.
14. Pfeiffer, P. and Hirth, L. (1975) FEBS Letters 56, 144-148.
15. Means, G.E. and Feeney, R.E. (1971) Chemical Modifications of Proteins, Holden-Day, San Francisco.
16. Churchich, J.E. and Irwin, R. (1970) Biochim.Biophys.Acta 214, 157-167.
17. Irwin, R. and Churchich, J.E. (1971) J.Biol.Chem. 246, 5329-5334.
18. Bancroft, J.B., McLean, G.D., Rees, M.W. and Short, M.N. (1971) Virology 45, 707-715.
19. Verduin, B.J.M. (1978) J.Gen.Virol. 39, 131-147.
20. Schnackerz, K.D. and Noltman, E.A. (1971) Biochemistry 10, 4837-4843.
21. Fischer, E.H. (1964) in Structure and Activity of Enzymes (Goodwin, T.W., Harris, J.I. and Hartley, B.S., eds.) 111-120, Academic Press, New York. N.Y..
22. Forrey, A.W., Olsgaard, R.B., Nolan, C. and Fischer, E.H. (1971) Biochimie 53, 269-281.
23. McKinlee-McKee, J.S., and Morris, D.L. (1972) Eur.J.Biochem. 28, 1-11.
24. Gisin, W. (1972) Anal.Chim.Acta 58, 248.
25. Visser, A.J.W.G., Grande, H.J., Müller, F. and Veeger, C. (1974) Eur.J.Biochem. 45, 99-107.
26. Azumi, T. and McGlynn, S.P. (1962) J.Chem.Phys. 37, 2413-2420.

27. Spencer, R.D. and Weber, G. (1969) Ann. N.Y. Acad.Sci. 158, 361-376.
28. Schürer, K., Ploegaert, P.G.F. and Wennekes, P.G.M. (1976) J.Sci.Instr. 9, 8121-8124.
29. Förster, Th. (1965) in Modern Quantum Chemistry, Istanbul Lectures, Part III (Sinanoglu, O., ed.) 93-137. Academic Press, New York, N.Y..
30. Churchich, J.E. (1965) Biochemistry 4, 1405-1410.
31. Cantor, C.R. and Tao, T. (1971) in Procedures in Nucleic Acid Research 2, 31-93 (Cantoni, G.L. and Davies, D.R., eds.) Harper and Row, N.Y..
32. Perrin, F. (1929) Ann. Phys. (Paris) 12, 169-275.
33. Weber, G. (1952) Biochem.J. 51, 145-154.
34. Wahl, P. and Weber, G. (1967) J.Mol.Biol. 30, 371-382.
35. Pierpoint, W.S. (1974) J.Gen.Virol. 25, 303-312.
36. Pierpoint, W.S. and Carpenter, J.M. (1978) J.Gen.Virol. 38, 505-518.
37. Davidson, J.N. (1972) in The Biochemistry of Nucleic Acids, seventh edition, Chapman and Hall, London.
38. Incardona, N.L., McKee, S. and Flanegan, J.B. (1973) Virology 53, 204-214.
39. Dickerson, P.E. and Trim, A.R. (1978) Nucl. Acids Res. 5, 985-995.
40. Chidlow, J. and Tremaine, J.H. (1971) Virology 43, 267-278.

6. EPR SPECTROSCOPY OF SPIN LABELLED COWPEA CHLOROTIC MOTTLE VIRUS

6.1. SUMMARY

Cowpea chlorotic mottle virus has been labelled with a nitroxide radical, when the nucleoprotein particles were in the swollen state. After the spin labelling reaction the virus was dialyzed to bring the nucleoprotein particles in different conformational states. The mobility of the labelled part of the protein was monitored by EPR spectroscopy and by saturation transfer EPR. Especially the last technique showed sensitivity to conditions that may influence the RNA conformation and the RNA-protein interaction. An increase in ionic strength by addition of 1.0 M NaCl at pH 5.0 or pH 7.5 results in a higher mobility. At pH 7.5 the presence of 0.01 M $MgCl_2$ in the buffer reduces the flexibility of the labelled region. The shape of the EPR and saturation transfer EPR spectra can only be explained by an anisotropic mobility of the spin-labelled viral protein, while an estimate of the rotational correlation times shows that the mobility of the nitroxide radical must be determined by local fluctuations in the labelled nucleoprotein.

6.2. INTRODUCTION

The nucleoprotein particles of cowpea chlorotic mottle virus (CCMV) consist of RNA, encapsulated in a protein coat, that is built from 180 identical protein subunits [1, 2] . Each subunit contains two SH-groups [3]. The virus can be brought into various conformational states by a change in pH, ionic strength or concentration of divalent cations [1]. At pH 7.5 an increase in ionic strength ($I > 0.2$) results in a dissociation of the particles into RNA and protein dimers [1, 4].

In the characterization of CCMV attempts have been made to investigate the mobility and the environment of the SH-groups in the coat protein. Labelling of these groups with fluorescent aromatic maleimide labels did not yield reliable information, because of the precipitation of the labelled nucleoprotein, which may be caused by the apolar character of these labels.

Nitroxide spin labels[5] can be rather easily introduced in the viral coat protein. For high mobilities with rotational correlation times (τ_c) <

0.5 μs, EPR spectroscopy may yield detailed information about the kind of motion and the rotational correlation times [6].

For the slow tumbling motion, expected for CCMV nucleoprotein particles ($\tau_c \sim 5$ μs) the use of saturation transfer (ST) EPR spectroscopy is more appropriate, since this technique has better sensitivity to mobilities with a $\tau_c > 0.5$ μs [6].

In this study we tried to correlate the overall conformational changes in the nucleoprotein with alterations in the vicinity of the modified SH-groups in the protein coat.

6.3. MATERIALS AND METHODS

6.3.1. Preparation of spin labelled CCMV

CCMV was grown and isolated as described previously [7]. The labelling was performed at 0° C in 0.05 M Tris-HCl buffer at pH 7.0, containing 1 mM sodium-EDTA. The nitroxide spin label, 3-maleimido-2,2,5,5-tetramethyl-1-pyrrolidinyloxyl (Fig. 1) was obtained from Synvar (Calif. USA). The spin label was dissolved in aceton and 0.2 ml of this solution was added to the virus solution (2.5 ml of 5 mg/ml) as to give a 5-fold excess of spin label compared with the protein subunit concentration. After 30 minutes non-reacted spin label was removed by extensive dialysis and the virus was dialyzed against 0.05 M Tris-HCl, pH 7.5, or 0.05 M NaAcetate, pH 5.0. The conformation of the nucleoprotein, which depends on the pH, was also influenced by adding 1.0 M NaCl or 0.01 M $MgCl_2$ to the dialysis buffer.

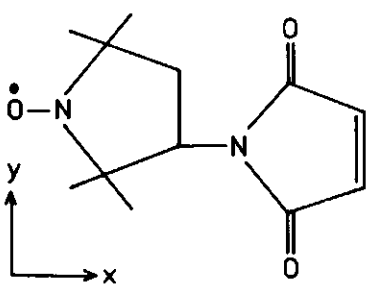

Fig. 1.

The nitroxide spin label, used in the experiments with CCMV

x and y are the axes of the nitroxide group, mentioned in the text. The z-axis is perpendicular to the plane.

The extent of labelling was determined by comparing the EPR spectrum of a known amount of spin label, dissolved in a glycerol-water mixture, with the spectrum of the labelled virus. The spectra which showed comparable mobility were doubly integrated to determine the absorption intensities.

Also by reaction of 5,5'-dithiobis(2-nitrobenzoic acid) (DTNB) with the unlabelled SH-groups in the virus the amount of labelling was calculated [8].

The integrity of the labelled virus was investigated by electron microscopy and gel electrophoresis of protein and RNA as described by Verduin [7].

6.3.2. EPR and ST-EPR

EPR spectra were recorded on a Varian-E3 spectrometer equipped with a Varian Variable Temperature Accessory V-4557 to control the temperature of the solution within 1^{o} C. The experiments were carried out at 4^{o} C. For the ST-EPR measurements the E3 spectrometer was modified as described by De Jager and Hemminga [9]. In this way the second harmonic (200 kHz) out-of-phase signal was recorded. The microwave power setting in the ST-EPR experiments was 100 mW and the modulation amplitude was 5 G. The EPR spectra were recorded, using a microwave power of 10 mW and a modulation amplitude of 4 G.

6.4. RESULTS

6.4.1. Spin labelling

The labelling was carried out on ice during 30 minutes. When the amount of spin label, compared to the protein subunit concentration, is increased above the 5-fold excess or when the labelling time is made longer than 30 minutes, more spin label is incorporated in the protein, but the stability of the nucleoprotein particles decreases. Especially after dialysis against the different buffers, used to change the conformation, precipitation of the virus occurs. In the preparation, used for EPR and ST-EPR spectroscopy a five fold excess of spin label was taken, in which case no denaturation is observed. In this way on the average about 0.2 spin label molecules were introduced per protein subunit. When the degree of modification increases above 0.5 molecules per subunit, part of the virus precipitates. In some experiments we observed that a solution of modified virus, stable at 4^{o} C in buffer at pH 7.5 + 0.01 M $MgCl_2$ becomes opalescent at 20^{o} C.

From gel electrophoresis no differences could be observed between the protein, modified with spin label, and the unmodified protein. The RNA in the labelled nucleoprotein particles showed some degradation. This degradation depends on the conformation of the particles and is least at pH 5.0. The labelling had to be performed at pH 7.0 to introduce a detectable amount of spin label. Under these circumstances the RNA in the swollen nucleoprotein particles is sensitive to RNases. In the electron microscope spherical particles were observed. Except at pH 7.5 in the presence of 1.0 M NaCl, which leads to full dissociation into protein dimers.

6.4.2. EPR measurements

The EPR first derivative absorption spectra were recorded of virus solutions at different pH and ionic strength (Fig. 2). The rotational correlation times were estimated, using the method of Freed *et al.* [10] (Table I). The A_{zz}-values and the shape of the spectra indicate relatively long rotational correlation times ($\tau_c > 10^{-8}$ s). Also in some circumstances at the high field side of the $m_I = 0$ line a peak in the spectrum appears (see arrow in Fig. 2). This could possibly arise from the presence of spin labels in two different environments or from an anisotropic motion of a single spin label. The spectra were compared with those of the used spin label in a mixture of glycerol and water at different degrees of mobility. This learns that it is impossible to fit the virus spectra by adding reference spectra for isotropic motion with different mobilities. Thus it is likely to explain the spectra of the spin labelled nucleoprotein by an anisotropic motion of the spin label.

At pH 5.0 and low ionic strength, where the virus particle is a compact sphere and rather stable, the spectrum is relatively immobile (Fig. 2A). An increase in ionic strength at this pH, causing a reduction of interaction between the protein and the RNA [11], is manifested by an increase in the mobility of the label (see Table I). At pH 7.5 and low ionic strength, where the virus particles are swollen due to a reduction of the protein-protein interaction, the rotational correlation time is slightly longer, when compared with the value at pH 5.0 and high ionic strength. Also it can be seen that the presence of 0.01 M $MgCl_2$ results in an even further increase in rotational correlation time.

At pH 7.5 and high ionic strength the nucleoprotein particles will dissociate into protein dimers and RNA. This is manifested in a shortening of τ_c. For the spin label rigidly attached to the dimer a τ_c of 2.5×10^{-8} s should be expected. (From the Stokes-Einstein relation $\tau_c = \frac{M\bar{v}}{kT}$).

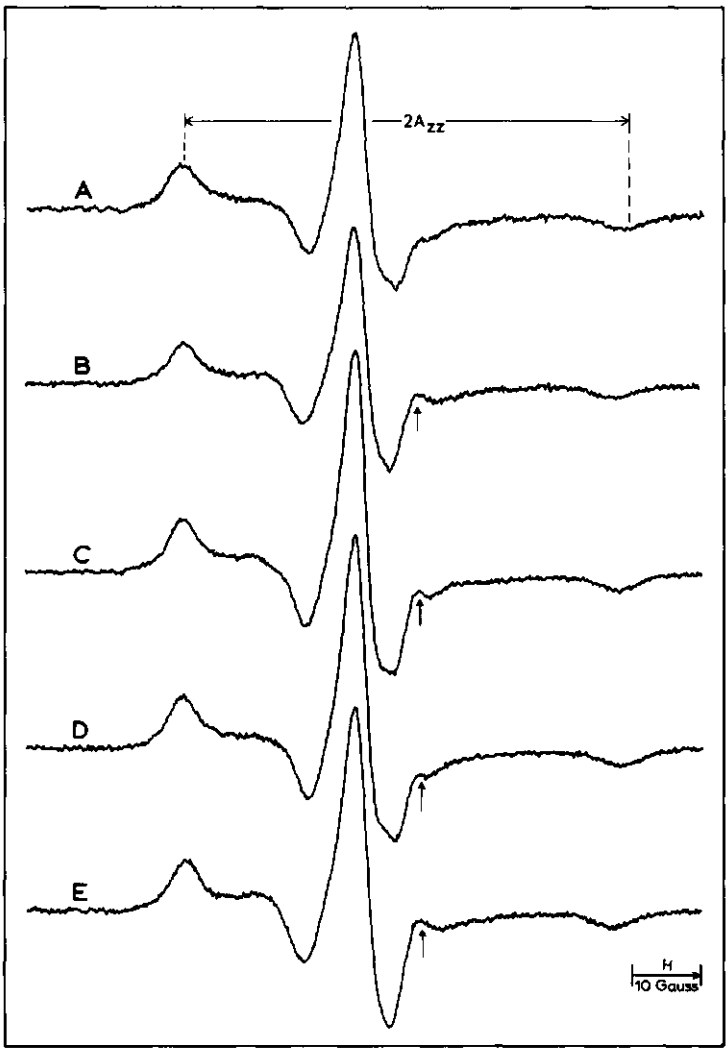

Fig. 2. EPR spectra of spin labelled CCMV

The modulation amplitude was 4 Gauss, the microwave power was 10 mW and the experiments were performed at 4°C in buffer, containing 0.05 M sodium acetate, pH 5.0 or 0.05 M Tris-HCl, pH 7.5.

A. pH 5.0
B. pH 5.0 + 1.0 M NaCl
C. pH 7.5
D. pH 7.5 + 0.01 M $MgCl_2$
E. pH 7.5 + 1.0 M NaCl

The arrows refer to the characteristic peaks, mentioned in the text.

Table I. Rotational correlation times for spin labelled CCMV, obtained from the A_{zz} values, according to the method of Freed 10 : $\tau_c = a(1-R)^b$, where $a = 7.5 \times 10^{-10}$ sec, $b = -1.2$, $R = A_{zz}/A_{zz,0}$.
$2\,A_{zz,0}$ = 73.5 Gauss (determined from frozen solution, t = -40° C)
$2\,A_{zz,0}$ = 67.0 Gauss (resulting in a τ_c for the dissociated virus of 2.5×10^{-8} sec)
The accuracy in the values of $2\,A_{zz}$ is ± 0.2 Gauss.
S is the order parameter for an anisotropic motion within a cone and β is the angle of the cone 12 in S is calculated, assuming $2A_{zz,0}$ = 73.5 Gauss and $A_{xx,0} = A_{yy,0}$ = 5.75 Gauss.

	$2\,A_{zz}$(G)	τ_c (ns)	τ_c (ns)	S	β
		$2A_{zz,0}$ = 67 G	$2A_{zz,0}$ = 73.5 G		
pH 5.0	65.1	53.9	10.1	0.935	22.0
pH 5.0 + 1.0 M NaCl	63.6	26.8	8.3	0.898	21.5
pH 7.5	64.6	40.7	9.5	0.923	18.7
pH 7.5 + 0.01 M $MgCl_2$	65.0	50.7	10.0	0.932	22.0
pH 7.5 + 1.0 M NaCl	63.4	25.0	8.1	0.893	17.4

The changes, observed here on swelling and dissociation are small (Table I). However a distinct feature in the spectra is the intensity of the peak at the high field side of $m_I = 0$ (Fig. 2). This is increased at high ionic strength, both at pH 5.0 and pH 7.5. The method of Freed [10] is based on isotropic motion. As outlined before this is probably not the case. An anisotropic motion can quantitatively be described by calculating an order parameter (S) according to equation 20 of reference 12. If the spin label is assumed to perform a random motion within a cone of angle β, then this angle can be calculated from S through equation 19 of reference 20. The results of these calculations are given in Table I.

6.4.3. ST-EPR

The differences, shown in the EPR spectra, are confirmed and more clearly manifested in the ST-EPR spectra (Fig. 3). The features of the spectra are tabulated as described by Thomas *et al* [13] in Table II. From the ratio of the

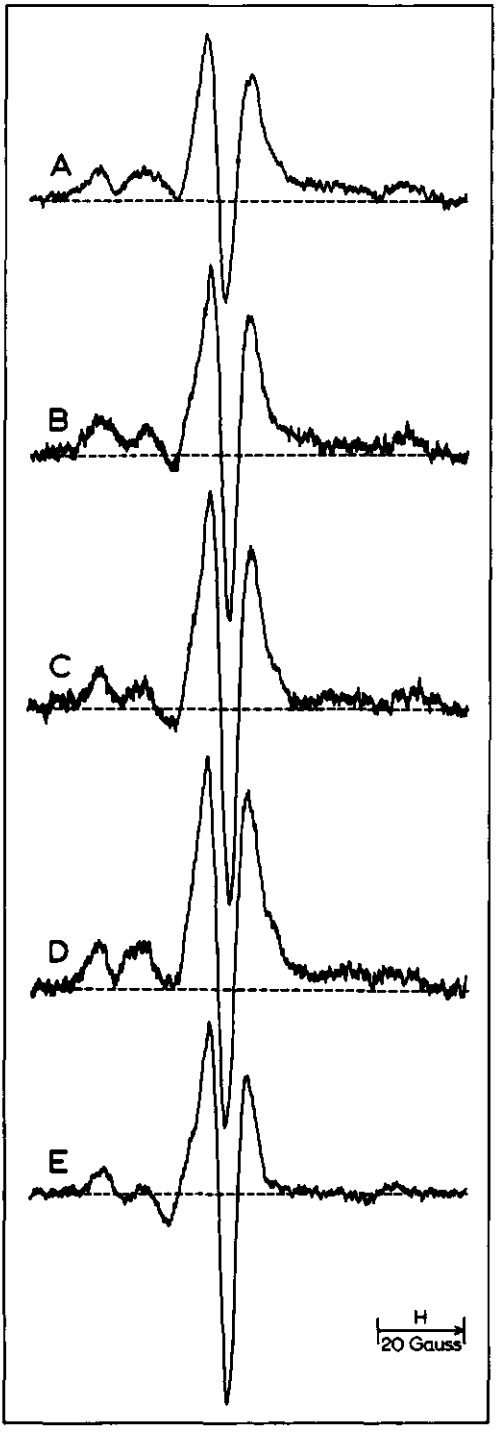

Fig. 3. Saturation transfer EPR spectra of spin labelled CCMV

A to E refer to the situations given in the legend of Fig. 2. The experiments were carried out under similar conditions to those used in EPR measurements. The microwave power setting was at 100 mW and a peak to peak modulation amplitude of 5 Gauss was used. The modulation frequency was 100 kHz and the signal detected was the second harmonic out of phase.

intensities (H''/H, L''/L and C'/C) the rotational correlation times were estimated. Because the τ_c values, derived from H''/H, L''/L and C'/C are different (Table II), the ST-EPR spectra (Fig. 3A-D) must be ascribed to an anisotropic motion [14]. For example the virus at pH 5.0 + 1.0 M NaCl shows for the three ratios τ_c of 2×10^{-5}, 5×10^{-5} and 2×10^{-7} s, respectively. The correlation times, derived from the ST-EPR spectra differ considerably from those derived from the EPR spectra (Table I). However, because of the anisotropy of the motion, the real meaning of the τ_c values from ST-EPR is questionable. At pH 7.5 + 1.0 M NaCl (Fig. 3E) the ST-EPR spectrum reflects a more isotropic motion (Table II).

Table II. Parameters and estimated rotational correlation times from saturation-transfer spectra of CCMV. The parameters are defined by Thomas *et al* [13] . The correlation times are estimated from comparison with experiments on spin labelled hemoglobin [13]. However in our experiments the field modulation was 100 kHz, while the experiments with hemoglobin are performed with 50 kHz modulation.

	H''/H	τ_c (s)	L''/L	τ_c (s)	C'/C	τ_c (s)
pH 5.0	0.94	5×10^{-3}	0.93	1×10^{-4}	0.61	5×10^{-7}
pH 5.0 + 1.0 M NaCl	0.42	2×10^{-5}	0.80	5×10^{-5}	0.90	2×10^{-7}
pH 7.5	0.69	1×10^{-4}	0.66	2×10^{-5}	0.90	2×10^{-7}
pH 7.5 + 0.01 M $MgCl_2$	1.3	1×10^{-3}	1.0	1×10^{-4}	0.58	5×10^{-7}
pH 7.5 + 1.0 M NaCl	<0.1	$<1 \times 10^{-6}$	0.24	5×10^{-8}	1.25	8×10^{-8}

The general conclusions from the ST-EPR spectra of different conformational states are in good agreement with those from the conventional EPR spectra. The influence of $MgCl_2$ in the buffer at pH 7.5, which is difficult to observe in the EPR spectra can be clearly observed in the ST-EPR spectra. This is a consequence of the greater sensitivity of ST-EPR to relatively slow motions of the spin label. Addition of $MgCl_2$ to the buffer immobilizes the nitroxide label and the spectrum becomes more similar to the situation, observed at pH 5.0 and low ionic strength (Fig. 3).

6.5. DISCUSSION

In the experiments described here we have observed EPR and ST-EPR spectra, which differ considerably from spectra for particles that perform an isotropic motion. As noticed before the spectra probably reflect an anisotropic motion. This type of motion has been thoroughly investigated for lipid spin labels embedded in lipid model membranes. These labels generally perform a fast motion around the axis through the fatty acid chain, in a cone with a small angle around this axis. The two extreme situations, motion around the y-axis in the plane of the nitroxide moiety and motion around the z-axis perpendicular to the plane of the nitroxide moiety (Fig. 1), are described by Israelachvili *et al.* for a cholestan spin label (motion predominantly around the y-axis) [15] and the (12,3) stearic acid spin label (motion around the z-axis) [12]. The EPR spectra of spin labelled CCMV are very similar to those observed for the (12,3) stearic acid spin label [12] in a model membrane. Thus the label is probably rotating within a cone predominantly around the z-axis. Also the ST-EPR spectra of the (12,3) stearic acid spin label in model membranes are in accordance with the ST-EPR spectra of CCMV (Fig. 3A-D) indicating motion around the z-axis [14].

When the spin label is thought to be a stretched molecule, positioned in a cleft of the protein molecule and performing a rapid motion around its simple bonds, a motion predominantly around the N-O bond can be expected. It can therefore be concluded that in the case of CCMV the motion around the z-axis probably reflects an anisotropic motion of the whole protein or part of the protein subunit in the protein core of the virus particles. The ST-EPR spectrum of the dissociated virus particles (Fig. 3E) reflects a more isotropic motion with a correlation time expected for a protein dimer (Table II). From the EPR and ST-EPR spectra it can be concluded that in the other conformations a more anisotropic motion is present. When the spectra of the different conformational states are compared, it can be seen, that an apparent increase in mobility can also be caused by an increase of the angle (β) of the cone in which the rapid motion of the label takes place (Table I).

One observation, which is not yet clearly understood, is the large value of τ_c, estimated from the H''/H and L''/L values. In the ST-EPR experiments on CCMV a modulation frequency of 100 kHz was used instead of a frequency of 50 kHz for the experiments of Thomas *et al.* [13] on which the estimation of the τ_c values is based. Perkins *et al.* [16] showed that this change in frequency results in a change of the ST-EPR spectra in such a direction, that this might

at least partly explain the discrepancy from the theoretical maximum value of $\tau_c \sim 5 \times 10^{-6}$s expected for CCMV.

Another effect, which influences the ST-EPR spectra, is mentioned by Kirino *et al.* [17]. They argue, that in the case of rotation around the z-axis of the nitroxide label the experimentally obtained apparent rotational correlation time from a ST-EPR spectrum is generally longer than the true correlation time for the axial rotation. Here by a factor 1/ sin α, in which α is the angle between the axis of rotation and the nitrogen $2p_z$-orbital.

A possible aggregation of the nucleoprotein particles into larger aggregates could explain the long rotational correlation times, but this is not very likely, since no aggregation was observed in the samples used in the ST-EPR experiments. The electron microscope pictures of the nucleoprotein solutions show spheres, similar to those of the unlabeled virus, while aggregates of about 1000 spheres should be needed to explain the τ_c values, calculated from the ST-EPR spectrum.

From a comparison of the EPR and ST-EPR spectra recorded for the different conformational states of the virus, it can be concluded that the mobility of the spin labelled protein is changed, especially when the RNA-protein interaction is reduced (at high ionic strength) or when the conformation of the RNA is influenced by the presence of mono- or divalent cations. The mobility of the spin labelled protein is less affected by a change in pH, which determines the interaction between the protein subunits. Thus the protein mobility is sensitive to the protein-RNA interaction. In contrast to our observations with CCMV modified with pyridoxal-5'-phosphate (PLP) (Chapter 5), where no influence of the ionic strength at pH 5.0 on the mobility was observed, here a strong influence of the NaCl concentration on the mobility of the spin labelled protein could be shown. This indicates a distinctly different site of the spin label compared to that of the fluorescent PLP label. It is suggested that there is another conformation after swelling and recontraction of the nucleoprotein particles. This is based on the experiments of Powell *et al.* [18] , where spin labelled poly-A was encapsulated by the coat protein of CCMV. It could be shown that the resulting particles clearly differed from native CCMV by their sensitivity to RNase.

In future studies labelling experiments can be carried out with spin labels of different chain lengths. This may provide more information about the environment of the label in the nucleoprotein and the type of motion carried out by the spin label. A variation in the conditions of labelling (temperature, pH and buffer composition, reaction time and concentration of the spin label) and a

further characterization of the products can help in the understanding of the nature and environment of the SH groups in the protein subunits and their role in the stability of the virus particles. In addition to the experiments on nucleoprotein particles protein dimers, labelled at neutral pH and reassociated into pseudo top component, may yield specific information about protein--protein interaction.

A change in the modulation frequency of the magnetic field to 50 kHz, will yield results that can be more easily correlated with ST-EPR spectra in literature.

6.6. REFERENCES

1. Bancroft, J.B. (1970) Adv. Vir. Res. 16, 99-134.
2. Lane, L.C. (1974) Adv. Vir. Res. 19, 151-220.
3. Bancroft, J.B., Rees, M.W. and Short, M.N. (1971) Virology 45, 707-715.
4. Adolph, K.W. and Butler, P.J.G. (1977) J. Mol. Biol. 109, 345-357.
5. Berliner, L.J. (1976) Spin Labeling, Theory and Applications, Academic Press, New York.
6. Hyde, J.S. (1978) Meth. in Enzymol. XLIX, 480-511.
7. Verduin, B.J.M. (1978) J. Gen. Virol. 39, 131-147.
8. Means, G.E. and Feeney, R.E. (1971) Chemical Modifications of Proteins, p. 220, Holden-Day, San Francisco.
9. De Jager, P.A. and Hemminga, M.A. (1978) J. Magn. Res. 31, 491-496.
10. Freed, J.H. in ref. 1, pp. 53-132.
11. Krüse, J., Verduin, B.J.M. and Visser, A.J.W.G. (1979) Eur. J. Biochem. 95, 21-29.
12. Israelachvili, J., Sjösten, J., Eriksson, L.E.G., Ehrström, M., Gräslund, A. and Ehrenberg, A. (1974) Biochim. Biophys. Acta 339, 164-172.
13. Thomas, D.D., Daltin, L.R. and Hyde, J.S. (1976) J. Chem. Phys. 65, 3006-3024.
14. Marsh, D. (1979) Molecular Motion in Phospholipid Bilayers in the Gel Phase-Long Axis Rotation, to be published.
15. Israelachvili, J., Sjösten, J., Eriksson, L.E.G., Ehrström, M., Gräslund, A. and Ehrenberg, A. (1975) Biochim. Biophys. Acta 382, 125-141.
16. Perkins, R.C., Lionel, T., Robinson, B.H., Dalton, L.A. and Dalton, L.R. (1976) Chem. Phys. 16, 393-404.
17. Kirino, Y., Ohkuma, T. and Shimiza, H. (1978) J. Biochem. 84, 111-115.
18. Powell, A.T., Gordon, M.P., Caspary, W.J., Greene, J.J. and Ts'o, P.O.P. (1978) Nucleic Acid Res. 5, 3977-3992.

7. BINDING OF Mn^{2+} TO BROMOVIRUSES AS STUDIED BY EPR SPECTROSCOPY

7.1. SUMMARY

The binding of manganese-ions to cowpea chlorotic mottle virus, brome mosaic virus and broad bean mottle virus has been studied, using the technique of electron paramagnetic resonance (EPR) for the detection of the unbound Mn^{2+}-ions. When the virus in its swollen state at pH 7.5 is titrated with Mn^{2+}-ions, two to three ions per protein subunit are bound. At pH 5.0 approximately one Mn^{2+}-ion per subunit is bound.

The binding constant of the formed complexes at the different pH values is in the order of 10^4 M^{-1}. The different aggregation states of the virus have a slightly different affinity for manganese-ions.

Using competitive binding between the mono- and divalent cations and Mn^{2+} the binding properties of Mg^{2+}, Ca^{2+}, Ba^{2+}, Li^+, Na^+, K^+ and Cs^+ were determined.

The results of these experiments are discussed in terms of both negative cooperativity and site heterogeneity of the binding of cations. The interpretation was assisted by comparing the results with simulated binding curves.

7.2. INTRODUCTION

The assembly of the bromoviruses is dependent on the presence of divalent cations, like Mg^{2+} and Ca^{2+}, which stabilize the structure of the nucleo-protein particles [1,2]. The conformation of the bromoviruses [3,4] at neutral pH can be influenced by varying the divalent cation concentration [5,6].
A raise in pH from 5.0 to 7.5 increases the hydrodynamic volume of the nucleo-protein particles (swelling). This effect can partly be prevented by the presence of 0.01 M $MgCl_2$.

Incardona *et al.* [5] studied the swelling of BMV and showed that this process is temperature dependent, and partly irreversible. However, in the presence of 5 mM $MgCl_2$ this temperature dependence is eliminated and the swelling process becomes completely reversible. From their results it was concluded that the effect of Mg^{2+}-ions resides mainly on the RNA, preserving its conformation during the swelling process.

From proton titration experiments on BMV, Pfeiffer and Durham [7] concluded that the positively charged ions neutralize the charges on both protein and RNA, by binding to the protein subunits, the RNA or the interface between the protein and the RNA in the nucleoprotein particles. In this way the repulsion between the RNA-phosphates and the negatively charged amino acid residues is reduced, resulting in a reduction of the swelling.

In this paper the binding of Mn^{2+} to nucleoprotein, free RNA and free protein subunits at various conditions of pH and ionic strength was studied. The binding was monitored by observing the unbound Mn^{2+} with EPR spectroscopy. The degree of binding of other cations was estimated by conducting competition experiments with a constant amount of Mn^{2+} or competing ions present in the equilibrium mixture.

For a better understanding of the role of metal ions in the process of swelling, dissociation and assembly of the virus, it is important to know not only the optimum concentration of those ions for the observed effects, but also the binding constants and the number of binding sites.

7.3. MATERIALS AND METHODS

7.3.1. Purification of virus, RNA and protein

Bromoviruses were grown and isolated according to the procedures described by Verduin [9]. Protein was prepared according to the $CaCl_2$-method [10] and RNA was obtained by phenol extraction from the virus particles [9]. Virus was kept in a 100 mM sodium acetate buffer, pH 5.0 containing 1 mM sodium azide and 1 mM sodium EDTA. Before performing binding experiments, the nucleoprotein was dialyzed for 18 hours against a 500-fold excess of 0.05 M Tris-HCl buffer of the desired pH.

7.3.2. Determination of the Mn^{2+} concentration

In the binding studies Mn^{2+} was added to freshly dialyzed solutions. For each binding experiment two titrations were performed: one with the virus solution and another with the dialysis buffer. The 6-line-Mn^{2+}-EPR spectra were recorded with a Varian E-3 spectrometer operating at 8.875 GHz (X-band). As illustrated by Reed and Cohn only the Mn^{2+}-aquo complex, free in solution, gives rise to an EPR signal under the experimental conditions [8]. The modulation amplitude was 8 G and the microwave power was 50 mW for all spectra.

The temperature was kept at 4° C with a Varian Variable Temperature Accessory V-4557.

For the determination of the free Mn^{2+}-concentration a capillary (inner diameter 0.8 mm) was filled with the solution by suction and the capillary was placed in a fixed position in the thermostated cavity. Reproducibility was checked frequently. By comparing the titrations of the virus and the buffer solutions, the amount of bound Mn^{2+} could be determined.

7.3.3. Binding of other cations

The binding properties of other cations were determined in titration experiments, where other ions competer with Mn^{2+} for binding. To investigate the influence of time dependence and the possibility of irreversible binding of ions, two types of titrations were carried out.

1. A normal titration with Mn^{2+} was performed. After addition of a certain amount of Mn^{2+} to the solution, part of the bound Mn^{2+} was displaced from the nucleoprotein by adding other cations.
2. Before the titration with Mn^{2+}, the nucleoprotein was dialyzed against a large excess of buffer, containing a known concentration of cations different from Mn^{2+}.

7.3.4. Analysis of the binding properties

For the determination of the binding constants and the number of binding sites per protein subunit, the results of the titration experiments are given in the form of a Scatchard plot [11-13].

a) The equation used:

$$\frac{\bar{\upsilon}}{[Mn^{2+}]_{free}} = K.\ (n-\bar{\upsilon}) \qquad (1)$$

is for one class of n identical binding sites. $\bar{\upsilon}$ is the ratio of bound Mn^{2+} to the total concentration of protein subunits, and n is the number of manganese-ions that can be found per protein subunit. K is the binding constant, defined as:

$$K = \frac{[Mn\ Prot]}{[Prot].[Mn^{2+}]_{free}} \qquad (2)$$

From the intercepts and the slope the number of binding sites and the binding constant can be calculated.

b) For two different classes of binding sites the Scatchard equation takes the following form [12, 14] :

$$\frac{\bar{\upsilon}}{[Mn^{2+}]_{free}} = \tfrac{1}{2}\left[K_1 (n_1 - \bar{\upsilon}) + K_2 (n_2 - \bar{\upsilon}) + \sqrt{\{K_1 (n_1 - \bar{\upsilon}) - K_2 (n_2 - \bar{\upsilon})\}^2 + 4K_1K_2n_1n_2}\right] \quad (3)$$

The analysis can be performed according to the method described by Klotz and Hunston [15], using the limiting slopes of a Scatchard plot and their intercepts. Here K_i and n_i are the binding constant and stoichiometry of class i, respectively.

c) When in addition to Mn^{2+} another kind of cation, competing with Mn^{2+} for the same binding class, is present in the buffer solution, the equation becomes:

$$\frac{\bar{\upsilon}}{[Mn^{2+}]_{free}} = \frac{K}{2K^*} \cdot \left[-\frac{1}{[prot]} - K^* (\bar{\upsilon} + c - n) + \sqrt{\{\frac{1}{[prot]} - K^* (\bar{\upsilon} + c - n)\}^2 + 4\,K^*.c}\right] \quad (4)$$

K^* is the binding constant of the competing ligand, [prot] is here the total concentration of protein subunits and c is the total amount of competing ligand in the solution divided by the protein subunit concentration.

The determination of binding constants and stoichiometry in the case of two or more binding classes and more than one type of ligand can be solved with aid of a computer program, as described by Feldman [14]. A subroutine of this program was modified to generate plots of the calculated curves [16].

d) In the case of more than one class of independant binding sites, the Scatchard plot is concave upward. However, this shape is also observed, when negative cooperativity of binding exists [17]. For cooperative binding the empirical Hill equation [18] can be converted into a Scatchard like formula:

$$\frac{\bar{\upsilon}}{[Mn^{2+}]_{free}} = \sqrt[N]{K.\ \bar{\upsilon}^{N-1}(n-\bar{\upsilon})} \quad (5)$$

where N is the empirical Hill coefficient [18].

Positive and negative cooperativity exists for N>1 and N<1, respectively.

7.4. RESULTS

7.4.1. Simulation of binding curves

For a better understanding of the effects of site heterogeneity and the presence of competing ions on the binding properties, we simulated Scatchard curves, which may be representative for the binding properties of the investigated nucleoprotein solutions. In Fig. 1 the situation is shown for two binding classes, with binding constants for Mn^{2+}, which differ by a factor 100 (Fig. 1A and B) and by a factor 10 (Fig. 1C and D).

Fig. 1A and 1C, in which $K/K^{*} = 100$ (K^{*} is the binding constant of the competing ion) represents the situation, expected for monovalent ions, competing with Mn^{2+}. In Fig. 1B and 1D, where $K=K^{*}$, we show the situation expected for divalent cations. The curves in Fig. 1, denoted with an (a) represent the Scatchard plots in the absence of competing ions, while curves b to g show the plots in the presence of increasing concentrations of competing ions. We can see that the effect of site heterogeneity is difficult to observe in the presence of relatively high concentrations of competing ions. Small concentrations of competing ions will result in much lower values of the apparent binding constants, when compared with the values in the absence of competing ions. The presence of rather small concentrations of competing ions will considerably reduce an accurate estimate of the binding properties of the manganese ions.

The points of intersection of curves b to g with curve i or k are the titration points, observed when Mn^{2+} is displaced by increasing amounts of competing ions.

The concave Scatchard plots in the absence of competing ions are caused by site heterogeneity, but can also be fitted reasonably well, assuming negative cooperativity. Using equation (5), we obtain for Fig. 1Aa:
$K = 2311$, $N = 0.87$ and $n = 2.2$ and for Fig 1.Ca:
$K = 3188$, $N = 0.91$ and $n = 2.2$.

7.4.2. Binding of Mn^{2+} to CCMV

Cowpea chlorotic mottle virus at pH 5.0, 6.5 and 7.5 was titrated with increasing concentrations of $MnCl_2$. The parameters describing the binding properties, which are obtained from a Scatchard analyses (Fig. 2), are summarized

Fig. 1. Simulation of binding and displacement of Mn^{2+}-ions

The protein subunit concentration is 150 μM.
For A and B : $K_1 = 6.\ 10^5\ M^{-1}$, $K_2 = 6.10^3\ M^{-1}$ $n_1 = 0.2$ $n_2 = 2.0$
For C and D : $K_1 = 6.10^4\ M^{-1}$, $K_2 = 6.10^3\ M^{-1}$ $n_1 = 0.2$ $n_2 = 2.0$

A) $K_1^* = 6.10^3\ M^{-1}$ $K_2^* = 6.10^1\ M^{-1}$
in the presence of competing ion in a total concentration of:
a), 0 M; e), 10^{-2} M;
b), 5.10^{-4} M; f), 5.10^{-2} M;
c), 10^{-3} M; g), 10^{-1} M;
d), 5.10^{-3} M.

B) $K_1^* = 6.10^5\ M^{-1}$ $K_2^* + 6.10^3\ M^{-1}$
in the presence of:
a), 0 M; d), 10^{-4} M;
b), 10^{-5} M; e), 5.10^{-4} M;
c), 5.10^{-5} M; f), 10^{-3} M.

C) $K_1^* = 6.10^2\ M^{-1}$ $K_2^* = 6.10^1\ M^{-1}$
concentrations of competing ions are the same as in A.

D) $K_1^* = 6.10^4\ M^{-1}$ $K_2^* = 6.10^3\ M^{-1}$
concentrations of competing ions are the same as in B.

For A, B, C and D:
curve i: total added concentration of Mn^{2+} = 1.5×10^{-4} M
curve k: total added concentration of Mn^{2+} = 5×10^{-4} M

in Table I. The Tris-HCl concentration was kept at 0.05 M.
At pH 5.0 only one Mn^{2+}-ion is bound per protein subunit. At pH 6.5 and pH 7.5 the Scatchard curves are concave upward (Fig. 2B and C), indicating the presence of more than one class of binding sites. At both pH's about two Mn^{2+}-ions are bound per protein subunit with a log K of 4.0 ± 0.1. In addition to this binding at pH 7.5 about 0.1 Mn^{2+}-ion per protein subunit is strongly bound with a log K of approximately 6.

When the virus solutions were dialyzed against 0.005 M Tris-HCl, the resulting Scatchard curves are located higher, especially at pH 7.5 (Fig. 3C) In this case at pH 5.0 and 6.5 only one Mn^{2+}-ion is bound per protein subunit, whereas at pH 7.5 three to four ions can be found (Table II).

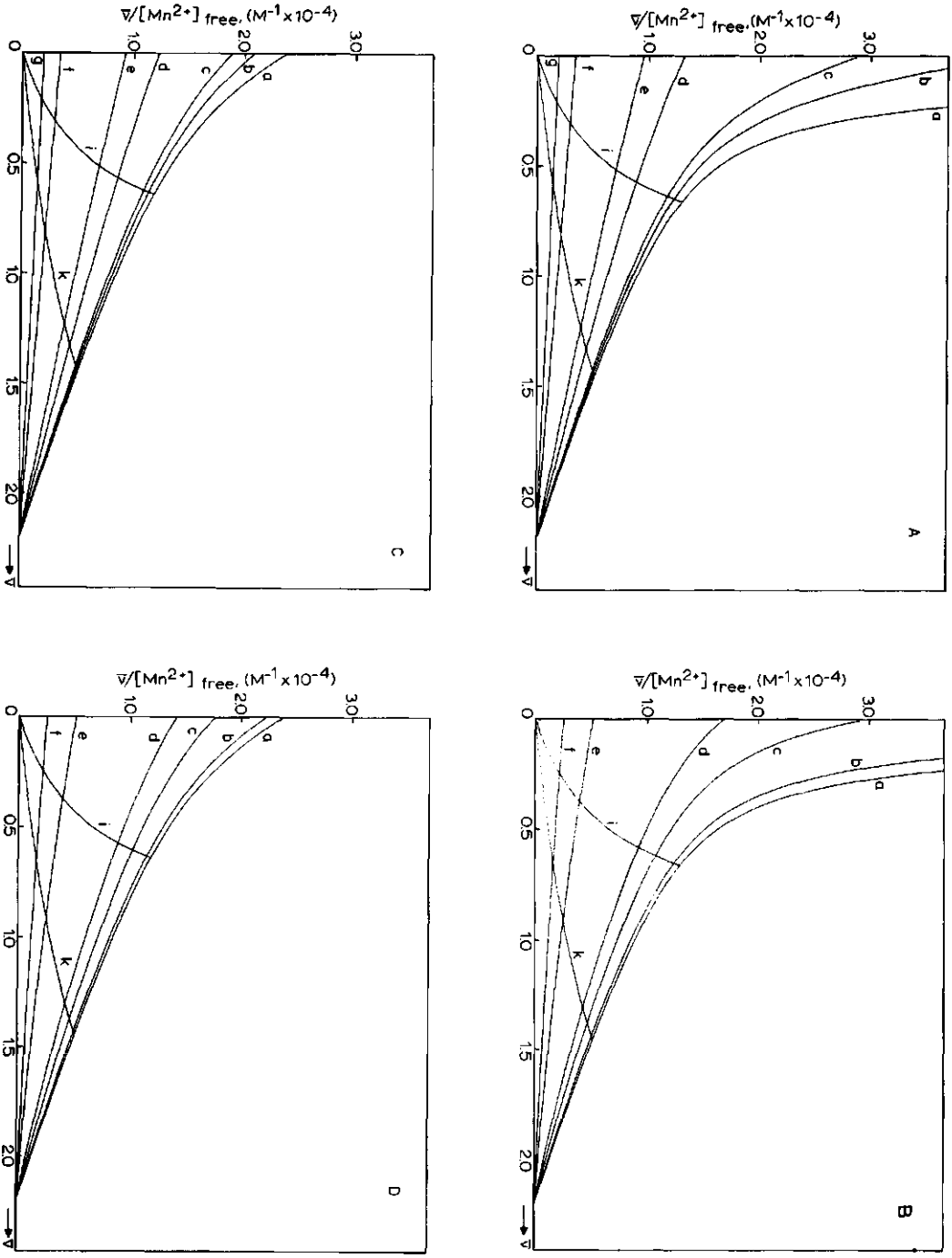
ν/[Mn2+] free, (M-1x10-4)
0
10
20
30
0.5
1.0
1.5
2.0
ν
a
b
c
d
e
f
g
i
k
A
B
C
D

are not stable at low ionic strength ($I < 0.1$), the absence of binding in the protein could not be investigated further.

The binding properties of Mn^{2+} for isolated RNA are expressed in sites per nucleotide (n) (Table III). From the composition of the RNA [19] and the average molecular weight of the RNA in the nucleoprotein particles, we calculate that about 18 nucleotides are present per protein subunit. At pH 7.5 about one Mn^{2+}-ion is bound per three nucleotides (equivalent with 6 per subunit). Thus when RNA is free in solution, more ions are bound compared to nucleoprotein solutions with an equal concentration of RNA. The observed binding constant and the stoichiometry are in good agreement with the results of Schreier and Schimmel [20] , obtained for binding of manganese ions to synthetic polynucleotides.

Table III. The binding of cations to free RNA as determined from direct titrations (Mn^{2+}) and competition experiments (Mg^{2+} and K^{+}). The number of binding sites is expressed in sites per nucleotide (n) and sites per protein subunit (n^{*}).

	K (M^{-1})	n	n^{*}
CCMV-RNA 0.05 M Tris-HCl, pH 7.5			
Mn^{2+}	9.5×10^{3}	0.33	6
Mg^{2+}	6×10^{3}		
K^{+}	3×10^{1}		
BMV-RNA 0.05 M Tris-HCl, pH 7.5			
Mn^{2+}	1.1×10^{4}	0.25	5
Mg^{2+}	3×10^{3}		
K^{+}	4×10^{1}		

7.4.3. Competition for binding between Mn^{2+} and other cations

From the influence of other cations on the binding of Mn^{2+}-ions to the the nucleoprotein, the binding constants of these ions were estimated. The expected effects on the Scatchard curves in this case have been illustrated in Fig. 1 for a number of different situations. It can be noticed that this indirect way of determining binding constants is much less accurate than the method, used for Mn^{2+}-ions alone. The variation of the stability

of the strong binding site (K_1) by a factor 10, has no large effects on the course of the Scatchard curves, provided that $\bar{\upsilon}$ is not too small.

Competition experiments for CCMV at pH 7.5 were done for a number of mono- and divalent cations and the results of a Scatchard analysis are summarized in Table IV. The accuracy of the data makes it difficult to draw firm conclusions from the differences in the binding constants of the different cations. The data were also analyzed, assuming only one class of binding sites

Table IV. The binding of cations to CCMV at pH 7.5, as determined from the competition between Mn^{2+} and other cations. The concentration of protein subunits was 1.61×10^{-4} M. $K_1 = 6.21 \times 10^4\ M^{-1}$, $K_2 = 5.26 \times 10^3\ M^{-1}$, $n_1 = 0.25$ $n_2 = 2.14$ (equation 3). The Tris-HCl concentration was 0.05 M, K^{*}, K_1^{*} and K_2^{*} are the binding constants of the competing ions.

competing ion	Mn^{2+} added (M)	K_1^{*} (M^{-1})	K_2^{*} (M^{-1})	K^{*} (M^{-1}) ⊛
Mg^{2+}	1.5×10^{-4}	1.7×10^{14}	1.6×10^3	7.0×10^3
Mg^{2+}	5×10^{-4}	1.3×10^5	5.9×10^5	1.3×10^3
Mg^{2+} ⊛⊛	variable			1.6×10^3
Ca^{2+}	5×10^{-4}	5.0×10^5	1.2×10^3	2.5×10^3
Ba^{2+}	5×10^{-4}	1.0×10^5	1.4×10^3	2.7×10^3
Na^{+}	5×10^{-4}	1.1×10.3	1.7×10^1	3.2×10^1
Na^{+} ⊛⊛	variable			3.7×10^1
K^{+}	5×10^{-4}	2.1×10^3	2.1×10^1	4.2×10^1
Li^{+}	5×10^{-4}	3.4×10^3	1.3×10^1	2.8×10^1
Cs^{+}	5×10^{-4}	1.4×10^3	1.4×10^1	3.0×10^1

⊛ K^{*} is calculated, assuming only one type of binding sites with $K = 8.314 \times 10^3$ and $n = 2.165$

⊛⊛ In these experiments the virus was dialyzed against buffer containing 0.1 M NaCl or 0.001 M $MgCl_2$. Here $K = 7.82 \times 10^3$ and $n = 2.75$ (fig. 4).

(Table IV). In Fig. 4 an example is given of a competition experiment, in which the competing ion was added before the titration with Mn^{2+}.

From the data of the competition experiments the following statements can be made. The competing cations show a lower binding constant than Mn^{2+}. When the competition is performed at a lower concentration of Mn^{2+}, this results in a higher value of the binding constant of the competing ions. This was observed for Mg^{2+}.

Mn^{2+}-ions can be replaced by monovalent cations, showing that these ions are competing with Mn^{2+} for the same binding sites. The binding sites of monovalent cations are approximately two orders smaller than the constants, found for divalent cations.

In the competition experiments no large differences are observed, when the competing ions are added before or after titration with Mn^{2+}. Thus the possibility of irreversible binding or time dependent effects, disturbing the results of the competition experiments, can be excluded.

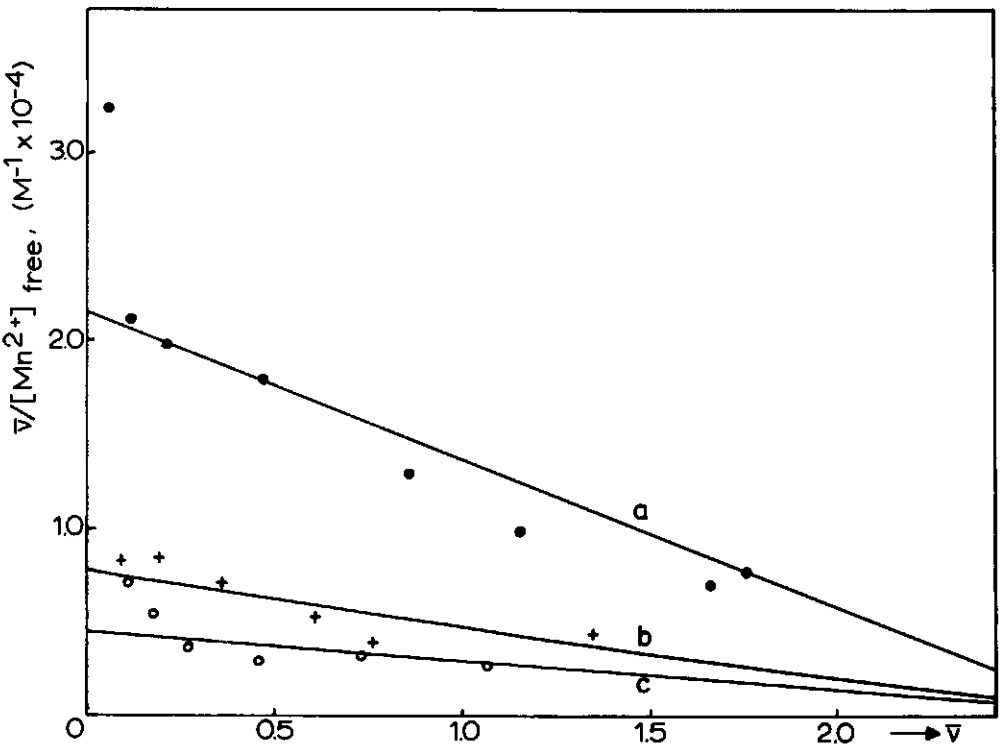

Fig. 4. Influence of other cations on Mn^{2+} binding to CCMV

The Tris-HCl concentration was 0.05 M.
a), without other cation;
b), with 0.001 M $MgCl_2$;
c), with 0.1 M NaCl.
The concentration of cations was reached by dialysis against a large excess of buffer, containing 0.001 M $MgCl_2$ and 0.1 M NaCl, respectively.

Table V. The binding of Mn^{2+} to BMV and BBMV nucleoprotein at different pH values in the presence of 0.05 M Tris-HCl. n is expressed in binding sites per protein subunit.

	K_1 (M^{-1})	K_2 (M^{-1})	n_1	n_2
BMV 4°C 0.05 M Tris-HCl				
pH 5.0	8.6×10^3		1.3	
pH 6.5	2.9×10^4	3.4×10^3	0.6	1.8
pH 7.5	3.7×10^4	1.8×10^3	0.8	3.1
BBMV 4°C 0.05 M Tris-HCl				
pH 5.0	5.0×10^3		1.5	
pH 7.5	6.6×10^4	3.4×10^3	0.1	3.0

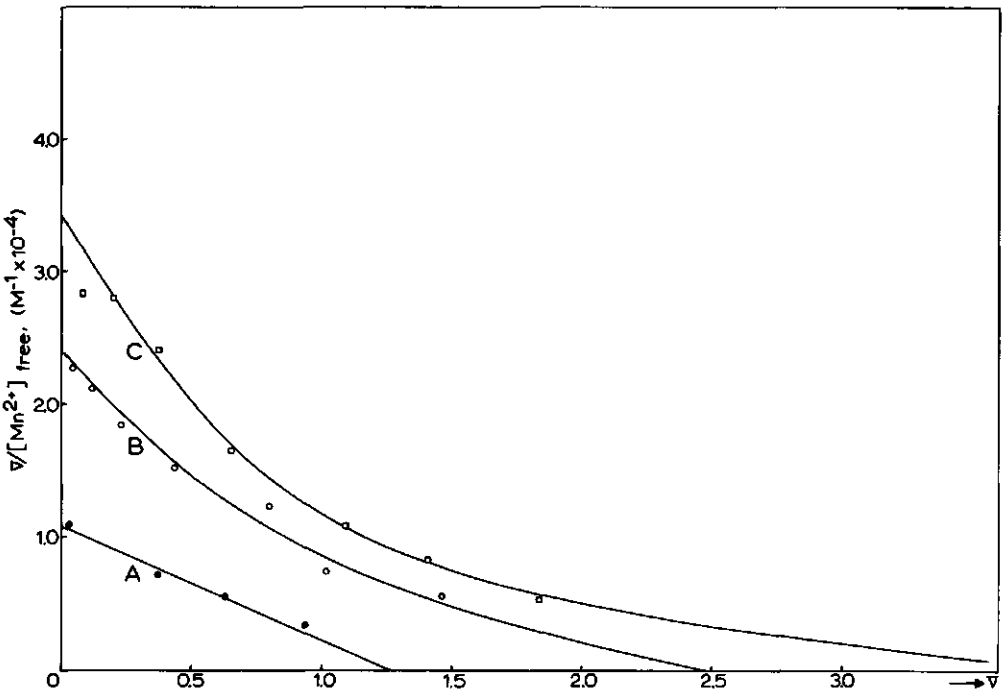

Fig. 5. Binding of Mn^{2+} to BMV in the presence of 0.05 M Tris-HCL

A), pH 5.0;
B), pH 6.5;
C), pH 7.5. See also Table V

7.4.4. *Binding of Mn^{2+} to brome mosaic virus and broad bean mottle virus*

The binding of Mn^{2+} to nucleoprotein particles was also investigated for BMV and BBMV (Figs. 5 and 6). The binding properties are summarized in Table V. At pH 7.5 slightly more manganese ions are bound as compared with CCMV. The results of binding of different cations to BMV-RNA are given in Table III. No great differences between BMV and CCMV-RNA can be noticed. The binding properties of the three bromoviruses appeared to be very much the same although some differences in binding occurred.

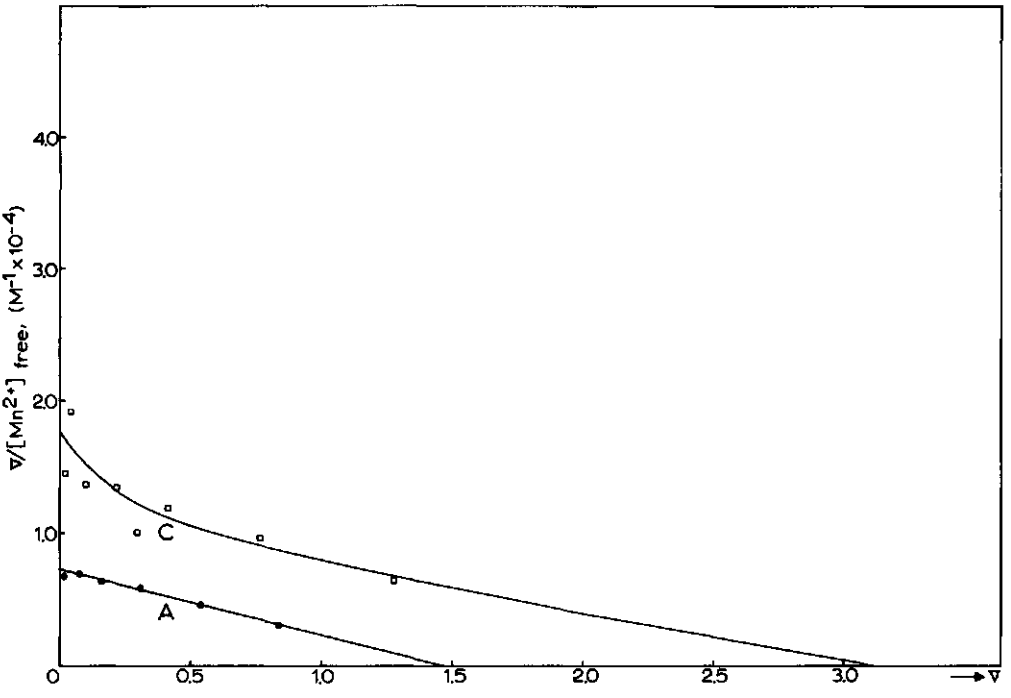

Fig. 6. Binding of Mn^{2+} to BBMV in the presence of 0.05 M Tris-HCl

A), pH 5.0;
C), pH 7.5. See also Table V

7.5. DISCUSSION

In the protein titration experiments of Pfeiffer and Durham [7] the binding constants and the stoichiometry for the binding of Ca^{2+} and Mg^{2+} to the nucleoprotein particles of BMV, were estimated in an indirect way, by measuring the number of protons that were displaced, upon addition of cations. However in our experiments the binding properties of Mn^{2+} to the nucleoprotein, the protein and the free RNA were directly monitored. The binding properties of the monovalent cations and some other divalent cations were investigated in an indirect way by means of competition experiments between Mn^{2+} and those ions. The indirect method is clearly much less reliable.

The binding properties, summarized in this article are expressed in binding sites per protein subunit, and for free RNA also in sites per nucleotide. However in an icosahedral particle with a triangulation number of three, the protein subunits are normally clustered into 12 pentamers and 20 hexamers. The protein subunits in these two types of cluster may show different binding properties, which would result in one third of the subunits, belonging to one class and two thirds belonging to another ($n = 0.33$ and $n = 0.66$). Distortion of the hexamer-pentamer clustering can result into dimer or even trimer clustering [21] . Thus the appearance of a stoichiometry of $n = 0.33$ or $n = 0.5$ may also be an indication of these effects. In the rest of the discussion we did not consider this possibility. Such an effect is clearly possible in view of the data at low Tris-HCl concentration at pH 5.0, where the asymptotes of the Scatchard curve indicates a stoichiometry of 0.33 and 0.5 per subunit (Table II, Fig. 3a).

From our studies it is observed that for the bromoviruses at pH 5.0 about one binding site per protein subunit exists with a log K of about 4. At pH 6.5 and 7.5 in addition to this site at least one other binding place appears with a log K in the same order. It can be deduced that the binding of cations depends on the pH in the following way:

$$\frac{\bar{\upsilon}}{[Mn^{2+}]_{free}} = \frac{K}{1 + \frac{[H^+]}{K_a}} \cdot (n - \bar{\upsilon}) = K_{app} \cdot (n - \bar{\upsilon}) \qquad (6)$$

where K_a is the proton dissociation constant of the binding group. For $pH < pK_a$ the apparant binding constant: K_{app} will become small and the binding of

metalions to this group will disappear. From our results it can be concluded that in the binding of Mn^{2+}-ions one site is involved with a pK_a between 5.5 and 6.0 and another with a $pK_a < 5.0$. However the posibility that a binding group, buried at low pH, will become exposed to the solvent at low pH, cannot be excluded as a possible explanation.

In the case of binding cations to free RNA more ions are bound than in the case of an equivalent amount of nucleoprotein at pH 7.5. The binding to the nucleoprotein may thus originate completely from the RNA. The reduced number of sites in the nucleoprotein can be caused by a shielding of some sites by the protein or by the occupation of these sites by positively charged groups of the protein.

From the competition experiments we calculate binding constants for other divalent cations with a log K that is approximately 0.5 lower than the value for Mn^{2+} (Table III). No clear correlation could be observed between the values of the binding constants and the ionic radii or the electronegativity of the different divalent cations [22]. The differences between the binding constants of the mono- and divalent cations is in good agreement with the values observed for binding to model compounds [23]. The relatively low values of the binding constants and the absence of a correlation between ionic radii and these constants makes it unlikely that the binding site has the form of a cage of a certain dimension, in which more than one carboxyl- and phosphate group are cooperating.

The stability constants for complexes, involving Mn^{2+}-ions are generally higher than the constants for Ca^{2+} and Mg^{2+} with model compounds [23]. This is in good agreement with the relatively low values, we observed for Ca^{2+}, Ba^{2+} and Mg^{2+} in the competition experiments. Another explanation of the low value of these binding constants may be found in the assumption, that instead of heterogeneity in the binding sites, the shape of the Scatchard curve must be attributed to negative cooperativity [17]. The Scatchard equation (5) in the case of cooperative binding can also be written in the following form:

$$\frac{\bar{\upsilon}}{[M_n^{2+}]_{free}} = K.\,[M_n^{2+}]_{free}^{N-1}.\,(n-\bar{\upsilon}) = K'_{app}.\,(n-\bar{\upsilon}) \qquad (7)$$

From this equation it can be noted that the apparent binding constant, K'_{app}, depends on the concentration of the unbound ligand. In the case of negative cooperativity ($N<1$), the K'_{app} becomes smaller at higher concentration of unbound ligand. Since the competition experiments were performed in the presence of both Mn^{2+} and other cations, this may explain the lower value of

the binding constants observed for other cations. Also the observation, that K_{Mg} is higher in the presence of 1.5×10^{-4} N Mn^{2+}, than in the presence of 5×10^{-4} M Mn^{2+} agrees with the concept of negative cooperativity. The negative cooperativity is in good agreement with the observed change in the conformation of the virus (reduction of swelling), that occurs upon binding of Mg^{2+} [24].

In some experiments with nucleoproteins a rather strong binding site of 0.05 to 0.2 ions per subunit was detected. Apart from the possibility of artefacts, such as the low accuracy for small values of $\bar{\upsilon}$, and impurities in the solution, the observation can be explained by binding of one Mn^{2+}-ion to a small number of nucleotides or to a group of protein subunits in the nucleoprotein. Because of the quarternary structure of the protein coat, (20 hexamers and 12 pentamers of protein subunits) this could mean a binding of one ion per 180/32 protein subunits or 0.18 ions per subunit, when the site is located in or near the hexamers and pentamers.

The changed binding properties in the presence of 0.005 M Tris-HCl instead of 0.05 M Tris-HCl can be caused by a destabilization of the nucleoprotein structure at extremely low ionic strength. Pfeiffer and Durham [7] performed their proton titration experiments in the presence of at least 50 mM KCl and then found still improper folding after dissociation and reassembly. Apart from the possibility of increased binding, caused by structural changes, the effect of decreased binding of metal ions at higher Tris concentrations might also be explained by a competition between the Tris and metal ions.

The binding of the different mono- and divalent cations may take place to the same sites, but the effects of bound ions can depend on the nature of these ions. Therefore it is not only important to know binding constants of the different cations, but also the concentration of the different cations in the cytoplasm. The possible role of calcium ions in virus infection has been discussed by Durham [2]. The gain in free energy, that occurs, when the virus particles penetrate the cell, is supplied by the release of calcium-ions in the cytoplasm. This is due to the much lower concentration of calcium-ions in the cytoplasm, compared with the medium outside the cell. When calcium ions are not bound specifically to the nucleoprotein, they can be replaced by other cations, that reduce the swelling and stabilize the particles. In our study no evidence has been found for a specific binding site for calcium. However in turnip rosette virus one Ca^{2+}-ion binds specifically per protein subunit [25].

For a better understanding of the role of calcium ions in virus disassembly binding studies on the bromoviruses have to be performed in which calcium ions are detected directly by using calcium indicators or by using ^{45}Ca. The method of analyzing the binding results, as described here, may be helpful in understanding the binding properties and the specificity of Ca^{2+}.

7.6. REFERENCES

1. Durham, A.C.H., Hendry, D.A. and Von Wechmar, M.B. (1977) Virology 77, 524-533.
2. Durham, A.C.H. (1978) Biomedicine 28, 307-314.
3. Bancroft, J.B. (1970) Adv. Vir. Res. 16, 99-134.
4. Lane, L.C. (1974) Adv. Vir. Res. 19, 151-220.
5. Incardona, N.L., McKee, S. and Flanegan, J.B. (1973) Virology 53, 204-214.
6. Zulauf, M. (1977) J. Mol. Biol. 114, 259-266.
7. Pfeiffer, P. and Durham, A.C.H. (1977) Virology 81, 419-432.
8. Reed, G.H. and Cohn, M. (1970) J. Biol. Chem. 245, 662-664.
9. Verduin, B.J.M. (1978) J. Gen. Virol. 39, 134-147.
10. Verduin, B.J.M. (1974) FEBS Letters 45, 50-54.
11. Scatchard, G. (1949) Ann. N.Y. Acad. Sci. 51, 660-672.
12. Scatchard, G., Scheinberg, I.H. and Armstrong, S.H. (1950) J. Am. Chem. Soc. 72, 535.
13. Scatchard, G., Coleman, J.S. and Shen, A.L. (1957) J. Am. Chem. Soc. 79, 12-20.
14. Feldman, H.A. (1972) Anal. Biochem. 48, 317-338.
15. Klotz, I.M. and Hunston, D.L. (1971) Biochemistry 10, 3065-3069.
16. Feldman, H., Rodbard, D. and Levine, D. (1972) Anal. Biochem. 45. 530-556.
17. Dahlquist, F.W. (1978) Meth. in Enzymol. XLVIII, 270-299.
18. Hill, A.V. (1910) J. Physiol. (London) IV-VII.
19. Bancroft, J.B., Hiebert, E., Rees, M.W. and Markham, R. (1968) Virology 34, 224-239.
20. Schreier, A.A. and Schimmel, P.R. (1974) J. Mol. Biol. 86, 601-620.
21. Kaper, J.M. in The Chemical Basis of Virus Structure, Dissociation and Reassembly, Oxford (1975) 42-49.
22. Handbook of Chemistry and Physics, 55th edition (1974), CRC Press, Cleveland, U.S.A., E-81, F-198.

23. Dawson, R.M. and Elliot, D.C. in Data for Biochemical Research, Oxford (1969) 423-434.
24. Koshland, D.E., Némethy, G. and Filmer, D. (1966) Biochemistry 5, 365.
25. Hull, R. (1978) Virology 89, 418-422.

8. SUMMARY AND DISCUSSION

This thesis describes the characterization of cowpea chlorotic mottle virus (CCMV) by using spectroscopic techniques. In chapter one and two the main properties of CCMV, which belongs to the bromoviruses [1,2], are summarized. The application of spectroscopic techniques in the study of other viruses is reviewed in chapter two.

The changes in the nucleoprotein particles, induced by variation of the pH, the ionic strength or the divalent cation concentration, may be important in the process of infection of the plant [3]. After the penetration of the virus particles into the cell, the RNA must be released from its protective protein coat (dissociation) to be transcribed, to start the production of protein and to influence the metabolism of the cell. Subsequently coat protein subunits and RNA are assembled to form new spherical nucleoprotein particles, that can be transported to other parts of the plant for new infection.

Dissociation and assembly can be induced *in vitro* by changing the composition of the buffer solution. The accompanying changes in the structure of the coat protein subunits and in the interaction between the different constituents of the nucleoprotein particles were investigated by using a number of different spectroscopic techniques to be described subsequently.

With fluorescence and phosphorescence spectroscopy, the characteristics of tryptophanyl and tyrosyl residues in the protein subunits were observed. From fluorescence quantum yield and lifetime measurements (chapter 3) it can be concluded that the presence of RNA in the protein particles results in a static quenching of part of the tryptophanyl residues. These residues become fluorescent and exposed to the solvent, when the interaction between protein and RNA is diminished by an increase in ionic strength or is completely absent as in empty protein shells or in dissociated virus at pH 7.5 and high ionic strength. A rise in pH from 5.0 to 7.5 results in a similar effect on the fluorescence, probably because of a different location of the RNA in the swollen particles, compared to the stable virus particles at pH 5.0.

Because the phosphorescence spectra of proteins show more fine structure than the fluorescence spectra, the effects of conformation on the phosphorescence properties of the virus particles at 77 K were investigated. In contrast to the expectations, no influence of the conformational changes on the position of the phosphorescence maxima was observed (chapter 4). Contrary to the interpretation obtained from fluorescence experiments, the location of the peaks in the phosphorescence spectra (413 and 440 nm) is more representative for tryptophanyl residues buried in the interior of the protein subunits [4,5].

A more refined characterization of the phosphorescent triplet state is made by the determination at 1.2 K of the zero field splitting parameters, using optical detection of magnetic resonance [6]. The observed $|D| - |E|$ and $2|E|$ transitions of the tryptophan moieties showed a large bandwidth in the virus, but no fine structure. The large bandwidth must be ascribed to statistical and structural heterogeneity in the environment of the tryptophanyl residues of the coat protein subunits. It also masks the possible shifts in the zero field transitions, when the protein-RNA interaction is reduced. From the slight changes in the ODMR parameters one can conclude that a decrease in the protein-RNA interactions causes an increase in the exposure of some of the tryptophanyl residues.

At this stage a quantitative interpretation of the fluorescence and phosphorescence data cannot be given. However in contrast to what has been observed with BMV [7], the intrinsic spectroscopic properties of CCMV can very well be applied to a qualitative study of the assembly of this virus and it can be utilized to check the correct encapsulation of the RNA in the protein coat. In this respect the application of techniques like optical rotatory dispersion (ORD), circular dichroism (CD) and light absorption does lead to a more complex interpretation because of the large contribution of RNA to these spectra. For rodshaped viruses like TMV with an RNA content of 5% in contrast to the 24% of CCMV, ORD and CD are more useful techniques. In experiments on TMV these techniques were applied very successfully to obtain information about the involvement of tryptophanyl residues in protein-RNA interactions [8].

It is difficult to relate the observations of the tryptophan fluorescence in CCMV directly to specific residues in each of the protein subunits in the nucleoprotein particles. This is a consequence of the differences in location of the subunits in the nucleoprotein particles. The protein subunits of CCMV are arranged quasi-symmetrically in the coat of the virus particles. As shown by Caspar and Klug [9] the interactions between the subunits may differ in the vicinity of a quasi sixfold and of a fivefold symmetry axis of the protein subunit arrangement. In addition, it is not very likely that the interactions between the

nucleotides and each of the protein subunits are identical. Thus instead of three classes of tryptophanyl residues in the nucleoprotein particles of CCMV, this number is possibly higher. The heterogeneity may be caused by structural differences within the subunits. This effect is observed in tomato bushy stunt virus, where two different conformations for the protein subunits are present in the virus particle [10].

In the case of TMV one major source of heterogeneity, the interaction between the subunits, is absent, when the 1.5% of the protein subunits on the ends of the rod is neglected. It is also observed that the contact between RNA and each of the TMV subunits in the rod is very similar [11].

Apart from the probes that are already present in the protein molecules, like tryptophan and tyrosine, fluorescent and paramagnetic probes that can be attached covalently to the protein have been employed. These labels provide data about the mobility of certain regions in the protein subunits, about the role of RNA-protein interactions in this process and about the influence of small concentrations of mono- and divalent cations.

As a fluorescent probe pyridoxal-5'-phosphate (PLP) was used (chapter 5). The advantage of this label is that it can be introduced into the stable virus particles at pH 5.0. The mobility of the labelled part was estimated from fluorescence polarization studies. Changes in ionic strength or divalent cation concentration at pH 5.0 had no effect on the mobility of the label. Upon swelling of the particles the label became more mobile. Immobilization occurred in the presence of divalent cations and to a smaller extent when monovalent cations were present. Measurements of radiationless energy transfer from tryptophanyl and from tyrosyl residues to the label indicated distinct changes in transfer efficiency when the conditions were varied.

A second type of label used in the study of CCMV is a paramagnetic nitroxide spin label (chapter 6). By using electron paramagnetic resonance (EPR) the mobility of the spin label could be monitored from the shape of the EPR spectra. The application of the recently developed technique of saturation transfer EPR (ST-EPR) allows the determination of the slow motions of the virus particles. From the spin label experiments, it was observed that the mobility of the label is sensitive to conditions that influence the protein-RNA interactions and the RNA conformation. The mobility of the spin label at pH 5.0 is increased markedly upon raising the ionic strength. Also a swelling of the particles enhances the mobility, while addition of $MgCl_2$, which reduces the swelling, lowers the flexibility of the labelled region of the protein.

The effect of ionic strength on the mobility of the spin label at pH 5.0 is in contrast to the results obtained for PLP-modified virus. However a principal difference between the two probes attached to CCMV is formed by the labelling conditions. PLP is attached to the virus under conditions, that keep the particles in a stable conformation. The spin label is bound to CCMV, when it is in the swollen state and where the RNA is sensitive to ribonuclease. Attempts to perform the labelling reaction at pH 5.0 were unsuccessful. Apart from the different sites that are labelled, the differences at pH 5.0 may reflect the incomplete reversibility of the swelling or the incorrect refolding of CCMV after the labelling at pH 7.0.

It is likely that the observed local flexibility in the protein subunits, when the nucleoprotein particles are in the swollen or dissociated form, plays an important role in the mechanism of assembly and dissociation. For TMV it has been noticed, that a change in the quarternary structure is accompanied by an increase in the flexibility of a certain section in the protein subunits. This was concluded from the disappearance of a detailed X-ray structure in parts of the double disc of TMV [12], while this structure could clearly be observed in the case of TMV nucleoprotein particles [11]. The flexibility within the TMV protein subunits was confirmed by NMR spectroscopy by De Wit *et al.* [13-15] and by Jardetzky *et al.* [16].

In tomato bushy stunt virus (TBSV) it was not possible to observe a considerable number of amino acid residues at the N-terminus in the X-ray analysis. It is not yet understood, whether this must be explained by a local mobility of the N-terminal arms or by an irregular folding of these arms [10].

The effect of mono- and divalent cations on the conformation of CCMV, which was also noticed in the experiments with labelled virus, was investigated quantitatively in titration experiments. Mn^{2+}-ions were used as a paramagnetic probe and the binding of these ions was detected by means of EPR spectrscopy. Competition for binding with Mn^{2+}-ions made it possible to determine the binding properties of other cations. In the bromoviruses approximately two to three ions are bound per protein subunit at pH $\geq$ 6.5, while at pH 5.0 approximately one binding site was observed. In isolated RNA relatively more binding sites were detected. Since protein without RNA is not stable at low ionic strength no meaningful binding data could be obtained in this case.

The binding properties were also considerably influenced by changes in the concentration of Tris-HCl. The binding of Mn^{2+} to the nucleoprotein might reflect

a negative cooperative behaviour or non-identical sites. Monovalent cations can effectively displace the divalent manganese ion from the nucleoprotein, whereby the binding constant was approximately a factor 100 smaller than found for divalent cations. Pfeiffer and Durham [17] determined the binding of Ca^{2+} and Mg^{2+} to BMV by measuring the displacement of protons from the nucleoprotein after addition of certain amounts of Ca^{2+} and Mg^{2+}. This method can only be applied at pH values below the pK of the titrating group. However the binding of metal ions to the virus is especially important at pH values above the pK of the titrating group. The more direct method described in this thesis, is more appropriate in this respect. In this way from our binding studies it could be observed that at pH 5.0 one binding site was present, while at pH 7.5 between two and three binding sites were observed. At pH 7.5 the binding of cations is more important in controlling the swelling of the nucleoprotein.

In the interpretation of the binding properties similar problems may arise as mentioned for the classification of the tryptophan fluorescence properties. In the investigation of specific binding sites, formed by a protein subunit and the RNA, it seems reasonable to express the binding stoichiometry in sites per subunit. However, since the environments of the subunits in the protein coat are not identical, the observed binding may be an average value from the different sites. Especially for the binding properties, it can be imagined that the stoichiometry is less determined by the individual subunits and more by the clustering of the subunits in hexamers and pentamers. From the binding experiments it can be concluded that RNA is important in the formation of the cation binding sites. The arrangement of RNA between the protein subunits can results in values of stoichiometry not related directly to a single subunit.

When the binding of cations is seen in terms of neutralizing charges [17] on the nucleoprotein particles, it will be more important to know the concentration dependence of the binding, which should not necessarily be specific, than the specific binding constants and the stoichiometry. Apart from the direct determination of the binding, it is also possible to observe indirect effects of mono- and divalent cations on native and modified nucleoprotein particles. The presence of these cations can be manifested in structural effects, like flexibility of certain regions in the protein. These effects can be employed to follow the binding. In CCMV modified with PLP (chapter 5) the addition of Mg^{2+} and Na^{+} to the solution influences the mobility of the fluorescent label. A more detailed study in which also other cations are used and their concentration dependence on the mobility of the label is followed, may be a useful means in the interpretation of these effects.

In this thesis the characterization of CCMV, its assembly and dissociation is described, using a number of spectroscopic techniques. In this way information was obtained about the virus conformation and its dynamic behaviour. The application of fluorescence and phosphorescence of intrinsic probes is restricted to tryptophanyl and to a smaller extent to tyrosyl residues. The interpretation of the spectral properties is often very complicated, because of the character of the residues and the large number of environmental aspects, that play a role. Labelling with fluorescent or paramagnetic probes can yield useful information about intramolecular distances, mobility and hydrophobicity in the virus particles. One should however be careful to use only modified nucleoprotein in the investigation of the structureal transitions in the virus particles. Firstly, it is difficult to estimate to what extent the effects on the label reflect the intrinsic effects and secondly, it is uncertain what the contribution is, due to the modification.

When information is available about the amino acid sequence and the X-ray structure, the application of spectral techniques becomes more useful. For this reason and because of the use of several mutants, rather detailed information is obtained on tryptophan and tyrosine in the subunits of tobacco mosaic virus. For the study of protein association and virus assembly, this knowledge may yield good perspectives.

In recent years the technique of laser-Raman-scattering has become a powerfull technique in the characterization of protein structure [18,19]. The studies are facilitated by extensive knowledge about the interpretation of Raman spectra of biomolecules. This method also seems to be very promising for the investigation of virus structure [20-22]. It provides information about several amino acid residues, the folding of the backbone and the structure of the RNA. Also information about the RNA-protein interaction may be deduced from the spectra.

The role of membranes in virus assembly and dissociation [3] can be investigated by monitoring the spectroscopic behaviour of viral protein, when nucleoprotein particles and artificial membranes are brought together. By the study of the hydrophobicity of the probes and their mobility in the protein upon penetration in the membrane it is possible to obtain information on this process. The sensitivity of fluorescence to protein-RNA interactions can be used to follow the possible dissociation of the nucleoprotein particles, when they cross the membranes.

REFERENCES

1. Bancroft, J.B. (1970) Adv.Vir.res. 16, 99-134.
2. Lane, L.C. (1974) Adv.Vir.Res. 19, 151-220.
3. Durham, A.C.H. (1978) Biomedicine 28, 307-314.
4. Longworth, J.W. (1971) in: Excited states of Proteins and Nucleic Acids, (Steiner, R.F. and Weinryb, I. eds.) Plenum Press, New York.
5. Purkey, R.M. and Galley, W.C. (1970) Biochemistry 9, 3569-3575.
6. Maki, A.H. and Zuclich, J.A. (1975) Topics in Current Chemistry 54, 115-163.
7. Herzog, M., Gerard, D., Hirth, L. and Laustriat, G. (1977) Biochim.Biophys. Acta 493, 167-177.
8. Dobrov, E.N., Kust, S.V., Yakovleva, O.A. and Tikchonenko, T.I. (1977) Biochim.Biophys.Acta 475, 623-637.
9. Caspar, D.L.D. and Klug, A. (1962) Cold Spring Harb.Symp.Quant.Biol. 27, 1-24.
10. Harrison, S.C., Olson, A.J., Schutt, C.E., Winkler, F.K. and Bricogne, G. (1978) Nature (Lond.) 276, 368-373.
11. Stubbs, G., Warren, S. and Holmes, K. (1977) Nature (Lond.) 267, 216-221.
12. Bloomer, A.C., Champners, J.N., Bricogne, G., Staden, R. and Klug, A. (1978) Nature (Lond.) 276, 362-368.
13. De Wit, J.L. (1978) NMR of TMV, Thesis of the Agricultural University, Wageningen, The Netherlands.
14. De Wit, J.L., Hemminga, M.A. and Schaafsma, T.J. (1978) J.Magn.Res. 31, 97-107.
15. De Wit, J.L. and Schaafsma, T.J. (1978) FEBS Lett. 92, 273-277.
16. Jardetzky, O., Akasaka, K., Vogel, D., Morris, S. and Holmes, K.C. (1978) Nature (Lond.) 273, 564-566.
17. Pfeiffer, P. and Durham, A.C.H. (1977) Virology 81, 419-432.
18. Yu, N.T. (1977) Crit.Rev.Bioch. 4,229-280.
19. Spiro, T.G. and Gaber, B.P. (1977) Ann.Rev.Biochem. 46, 553-572.
20. Thomas, G.J. Jr, Prescott, B., McDonald-Ordzie, P.E. and Hartman, K.A. (1976) J.Mol.Biol. 102, 103-124.
21. Hartman, K.A., McDonald-Ordzie, P.E., Kaper, J.M., Prescott, B. and Thomas, G.J. Jr. (1978) Biochemistry 17, 2118-2123.
22. Shie, M., Dobrov, E.N. and Tikchonenko, T.I. (1978) Biochem.Biophys.Res. Comm. 81, 907-914.

SAMENVATTING

Dit proefschrift beschrijft de karakterisering van cowpea chlorotic mottle virus (CCMV) met behulp van spectroscopische technieken. Speciaal de veranderingen die optreden bij overgangen in de quarternaire structuur van de nucleoproteinedeeltjes kunnen worden gevolgd en geanalyseerd met behulp van deze technieken.

Het onderzochte virus, CCMV, is een bolvormig plantevirus, waarin ribonucleinezuur (RNA) omgeven is door een beschermende eiwitmantel, die gevormd wordt door 180 identieke eiwitmoleculen. De vorm van dit RNA-eiwit complex in oplossing kan worden gevarieerd door de zuurgraad (pH), de ionensterkte, of the concentratie van divalente kationen te veranderen. Onder invloed hiervan kunnen de virusdeeltjes een toename in diameter vertonen (zwelling) en uiteenvallen in eiwitdimeren en vrij RNA (dissociatie). De beide componenten kunnen ook weer worden samengevoegd tot deeltjes die gelijkenis vertonen met het oorspronkelijke virus (assemblage). Ook kunnen eiwitmoleculen zonder RNA worden samengevoegd tot bolvormige polymeren, die een met het virusdeeltje overeenkomende structuur vertonen.

In dit proefschrift zijn een aantal experimenten beschreven, waarin met behulp van diverse spectroscopische technieken de hiervoor geschetste processen werden onderzocht. Speciaal werd de aandacht gericht op de veranderingen die hierbij binnen de eiwitmantel optreden. Ook werd onderzocht wat de invloed was van de veranderingen in wisselwerking tussen de eiwitmoleculen onderling en met het RNA op de spectrale eigenschappen.

In de eerste plaats werden de intrinsieke spectroscopische eigenschappen van het manteleiwit in de verschillende aggregatietoestanden onderzocht. Uit fluorescentiegegevens kon worden geconcludeerd, dat de tryptofaangroepen in het manteleiwit in contact staan met het oplosmiddel. De interacties tussen de eiwitsubeenheden lijken de omgeving van deze groepen niet te beïnvloeden. Aangezien het kleinste oligomeer van de eiwitsubeenheden waarschijnlijk een dimeer is, kon niet precies worden nagegaan of de tryptofaangroepen een rol spelen bij de interactie tussen twee subeenheden. Bij zwelling en dissociatie van de nucleoproteinedeeltjes treedt een aanzienlijke toename van de quantumopbrengst van de fluorescentie op. Het maximum van de tryptofaanemissie verschuift daarbij naar hogere

golflengte. De verandering in fluorescentielevensduur was echter veel kleiner dan verwacht. Deze aspecten wijzen op een aanzienlijke invloed van de RNA-eiwit interactie op de omgeving van een deel van de in het eiwit aanwezige trytofaangroepen.

Enkele conformatietoestanden van het virus en het manteleiwit werden bij 77 K onderzocht met behulp van fosforescentie en bij 1.2 K door het bepalen van de nulveldovergangen in de triplettoestand met behulp van optische detectie van magnetische resonantie. Fosforescentiemaxima werden waargenomen bij 413 en 440 nm. De positie van de maxima hing niet af van de conformatie van de virusdeeltjes. De nulveldovergangen bij ongeveer 1,65 en 2,70 GHz werden gekenmerkt door een grote lijnbreedte en het ontbreken van een fijnstructuur. Bij het verbreken van de interactie tussen het eiwit en het RNA lijkt een verschuiving in de positie van de nulveldovergangen op te treden. De met deze methoden verkregen informatie lijkt voor een deel in tegenspraak met de fluorescentie resultaten. Een dergelijk paradox is echter ook voor andere eiwitten geconstateerd. Dit wijst erop, dat de classificatie van tryptofaangroepen aan de hand van spectroscopische parameters vaak een te eenvoudige voorstelling van de werkelijke toestand geeft en de gecompliceerde omgevingseffecten op deze groepen binnen een eiwitmolecuul niet juist weergeven.

Naast de informatieverschaffende groepen die van nature aanwezig zijn in de eiwitmoleculen, zoals trytofaan en tyrosine, werd voor het verkrijgen van aanvullende informatie gebruik gemaakt van fluorescente (fluorescentie label) en paramagnetische "reporter" moleculen (spin label) die covalent aan het eiwit kunnen worden gebonden. De plaats en de beweeglijkheid van de fluorescente moleculen werd gevolgd met behulp van fluorescentietechnieken (polarisatie en levensduur). Met behulp van electron spin resonantie (ESR) kon de beweeglijkheid van spin labels worden bepaald. De toepassing van de recent ontwikkelde techniek van "saturation-transfer" ESR maakte het mogelijk de trage bewegingen van het deeltje te detecteren.

Het fluorescente pyridoxal-5'-fosfaat (PLP) kon covalent worden gebonden aan een lysine residu in het manteleiwit. Het gelabelde deel vertoonde een zekere beweeglijkheid ten opzichte van het nucleoproteinedeeltje. De beweeglijkheid en de positie van het PLP werden bij het gezwollen virus beinvloed door de aanwezigheid van mono- en divalente cationen.

De paramagnetische moleculen konden covalent worden gebonden aan de SH-groepen in het virus. De reactie verliep alleen bij pH 7,0, waar het virus zich in een gezwollen conformatie bevond. Het label bleek een anisotrope beweging te

beschrijven, die kon worden beinvloed door de toevoeging van mono- en divalente kationen aan de buffer. In tegenstelling tot PLP was het spinlabel in CCMV ook bij pH 5,0 gevoelig voor de aanwezigheid van deze ionen.

De beïnvloeding van de conformatie van de virusdeeltjes, die volgt uit de resultaten van de fluorescentie en spinlabel experimenten, is in overeenstemming met de waarnemingen aan de bromovirussen gedaan met behulp van ultracentrifugatie, intensiteits fluctuatie spectroscopie en neutronenverstrooiing.

Het bindingsgedrag van mono- en divalente kationen aan virus, geïsoleerd RNA en eiwit werd bepaald door gebruik te maken van paramagnetische mangaanionen, en ESR als detectiemethode toe te passen. Bij verhoging van de zuurgraad nam het aantal bindingsplaatsen per subeenheid in de nucleoproteinedeeltjes toe van één bij pH 5,0 tot twee à drie bij pH 7,5. Verschillen in de concentratie van Tris-ionen bleken het gedrag sterk te beïnvloeden. De bindingsresultaten kunnen zowel op negatieve coöperativiteit als op heterogeniteit in de bindingsplaatsen wijzen. Ook bleek uit de experimenten dat het moeilijk is de binding aan eiwit zonder RNA te bepalen.

CURRICULUM VITAE

Jacob Krüse is geboren op 19 oktober 1951 te Zunderdorp. In 1969 behaalde hij het H.B.S.-B diploma aan de Scholengemeenschap Noord te Amsterdam. In datzelfde jaar begon hij zijn studie in de scheikunde aan de Universiteit van Amsterdam. In juni 1972 werd het kandidaatsexamen S3 behaald, en in september 1975 het doctoraalexamen, cum laude (hoofdvak fysische chemie, bijvak chemische fysica, speciale richting mathematische statistiek)

Op 1 september 1975 trad hij als promotie-assistent in dienst van de Landbouwhogeschool te Wageningen bij de vakgroep Virologie. Tot 10 oktober 1978 werd in het kader van de werkgroep "Assemblage van bolvormige plantevirussen" onderzoek verricht op het Laboratorium voor Biochemie van de Landbouwhogeschool.

Sinds 1 augustus 1979 verricht hij, daartoe in staat gesteld door een beurs van de European Molecular Biology Organization, fysisch-chemisch onderzoek aan plantevirussen op het Institut de Biologie Moléculaire et Cellulaire du C.N.R.S. te Straatsburg, Frankrijk.